AD-A091 755 GENERAL ELECTRIC CO LYNN MA AIRCRAFT ENGINE GROUP F/G 21/5
REGENERATIVE ENGINE ANALYSIS.(U)
OCT 80 R P TAMEO, P W VINSON, R E NEITZEL DAAK51-79-C-0055
UNCLASSIFIED R80AEG049 USAAVRADCOM-TR-80-D-18 NL

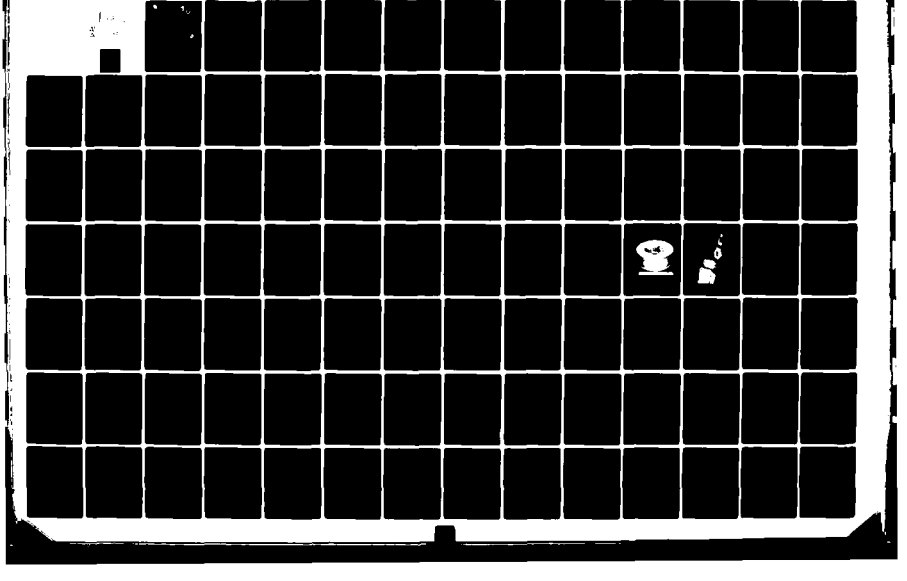

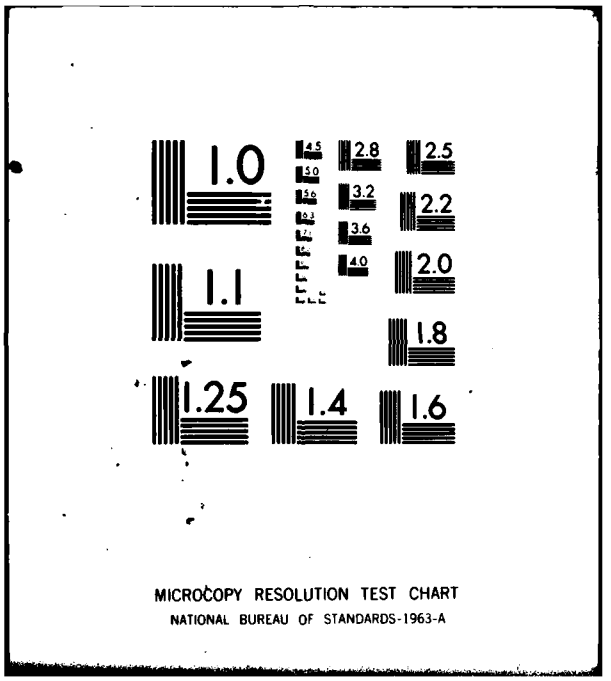
1.0
1.1
1.25
1.4
1.6
1.8
2.0
2.2
2.5
2.8
3.2
3.6
4.0
4.5
5.0
5.6
6.3
7.1
8.0
9.0
MICROCOPY RESOLUTION TEST CHART
NATIONAL BUREAU OF STANDARDS-1963-A

USAAVRADCOM-TR-80-D-18

LEVEL II

REGENERATIVE ENGINE ANALYSIS

AD A091755

R. W. Tameo, P. W. Vinson, R. E. Neitzel
GENERAL ELECTRIC COMPANY
Aircraft Engine Group
Lynn, Mass. 01910

October 1980

Final Report

Prepared for

APPLIED TECHNOLOGY LABORATORY
U. S. ARMY RESEARCH AND TECHNOLOGY LABORATORIES (AVRADCOM)
Fort Eustis, Va. 23604

APPLIED TECHNOLOGY LABORATORY POSITION STATEMENT

The results of previous regenerative engine technology programs have become somewhat obsolete by intervening technology development. In 1980, the Army supported several engine design investigations to update regenerative cycle engine data for helicopter application. Results of this effort will be used in conjunction with parallel efforts at other engine companies, and in-house, to formalize future efforts directly related to small fuel efficient gas turbine engines.

Mr. Albert E. Easterling of the Propulsion Technical Area, Aeronautical Technology Division served as project engineer for this effort.

Unclassified

SECURITY CLASSIFICATION OF THIS PAGE (When Data Entered)

REPORT DOCUMENTATION PAGE

READ INSTRUCTIONS BEFORE COMPLETING FORM

1. REPORT NUMBER (19) USAAVRADCOM TR-80-D-18	2. GOVT ACCESSION NO. AD-A091
3. RECIPIENT'S CATALOG NUMBER 755	
4. TITLE (and Subtitle) (6) REGENERATIVE ENGINE ANALYSIS	5. TYPE OF REPORT & PERIOD COVERED (9) Final Report
6. PERFORMING ORG. REPORT NUMBER (14) R80AEG049	
7. AUTHOR(s) (10) R.P. Tameo, P.W. Vinson, R.E. Neitzel	8. CONTRACT OR GRANT NUMBER(s) (15) DAAK51-79-C-0055
9. PERFORMING ORGANIZATION NAME AND ADDRESS General Electric Company, Aircraft Engine Group, Lynn, Massachusetts 01910	10. PROGRAM ELEMENT, PROJECT, TASK AREA & WORK UNIT NUMBERS (16) 1L162209AH76, (17) 00 304 EK
11. CONTROLLING OFFICE NAME AND ADDRESS Applied Technology Laboratory, U.S. Army Research and Technology Laboratories (AVRADCOM), Fort Eustis, Virginia 23604	12. REPORT DATE (11) October 1980
	13. NUMBER OF PAGES 137
14. MONITORING AGENCY NAME & ADDRESS (if different from Controlling Office) (12) 140	15. SECURITY CLASS. (of this report) Unclassified
	15a. DECLASSIFICATION/DOWNGRADING SCHEDULE

16. DISTRIBUTION STATEMENT (of this Report)

Approved for public release; distribution unlimited.

17. DISTRIBUTION STATEMENT (of the abstract entered in Block 20, if different from Report)

18. SUPPLEMENTARY NOTES

19. KEY WORDS (Continue on reverse side if necessary and identify by block number)

Regenerator/Recuperator Turboshaft Engines
Turboshaft Cycle Analysis
Reduction in Specific Fuel Consumption
Recuperator/Regenerator Design

20. ABSTRACT (Continue on reverse side if necessary and identify by block number)

This report summarizes the results of a regenerative turboshaft study. The work was performed in two tasks. Task I was a 4-month parametric study of cycle and recuperator design parameters leading to the selection of those parameters providing minimum fuel consumption and life-cycle cost. Task II consisted of a 2-month preliminary design of a selected regenerative engine cycle.

The AiResearch Manufacturing Co., Heat transfer and Cryogenics Systems

DD FORM 1 JAN 73 1473 EDITION OF 1 NOV 65 IS OBSOLETE

Unclassified

SECURITY CLASSIFICATION OF THIS PAGE (When Data Entered)

403389

20. ABSTRACT - (Continued)

Division, provided recuperator design support under subcontract to General Electric.

A parametric cycle study was performed to identify cycle and recuperator design parameters appropriate to a 500 shp class regenerative turboshaft engine with the objective of obtaining minimum specific fuel consumption (SFC) at cruise (40 to 60% of Intermediate Rated Power - IRP) and minimum engine weight compatible with helicopter applications. The overall engine configuration was restricted to a front drive, free output shaft operated at 20,000 rpm from flight idle to IRP. The level of component technology chosen is consistent with that which could be incorporated in a demonstrator engine program.

Twenty-seven regenerative engine cycles were evaluated parametrically to determine the proper combination of variables for minimum fuel consumption and weight in a typical lightweight twin-engine military helicopter mission. The study identified a cycle pressure ratio in the range of 8 to 10 and a cycle temperature of 2400°F as the best choices for a regenerative engine from the fuel consumption standpoint. Recuperator design parameters of 70% effectiveness and 7-1/2% total pressure drop were identified as providing a reasonable balance between fuel consumption and life-cycle cost. A variable area turbine nozzle (VATN) was shown to be beneficial from the fuel consumption standpoint.

A preliminary aeromechanical design of a 500 shp class regenerative turboshaft engine with a cycle pressure ratio of 8.6 and turbine temperature of 2250°F was performed to integrate the heat exchanger with the other engine components and to define the overall engine envelope. Performance, weight, acquisition cost, and maintenance costs were estimated and compared to a nonregenerative engine based on consistent technology but with a higher cycle pressure ratio of 12:1.

Finally, a mission evaluation was performed to assess the potential fuel savings and life-cycle cost impact of the regenerative turboshaft engine relative to the nonregenerative engine. The regenerative cycle benefits to a lightweight twin-engine military helicopter were evaluated as a 20% reduction in fuel consumption but with a 12% life-cycle cost penalty for fuel costs of $1/gallon. The life-cycle cost penalty is shown to be strongly dependent upon fuel costs. At a typical helicopter use of 300 hours per year, the regenerative engine life-cycle cost penalty would equal that of the conventional engine at a fuel cost of $4/gallon.

PREFACE

This report was prepared by the Aircraft Engine Group of the General Electric Company, Lynn, Mass. to document the results of a regenerative turboshaft engine study conducted to identify appropriate cycle parameters, and to perform a preliminary engine design of a selected regenerative turboshaft cycle. Mr. A. E. Easterling, Applied Technology Laboratory, U.S. Army Research and Technology Laboratories (AVRADCOM) was Program Manager.

The authors wish to acknowledge the valuable contribution made to this program by Mr. William Miller of AiResearch Manufacturing Company, Heat Transfer and Cryogenic Systems Division in performing the heat exchanger parametric study and preliminary design under subcontract to the General Electric Company.

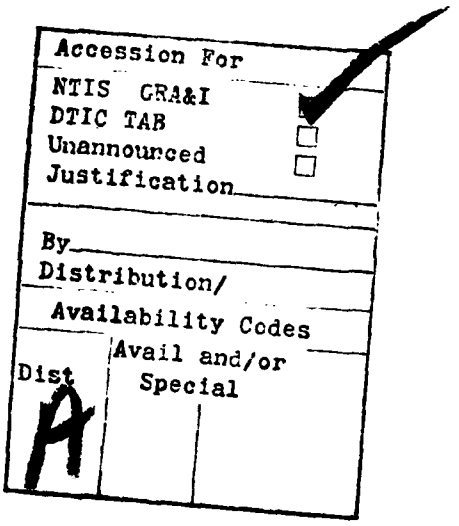

TABLE OF CONTENTS

LIST OF ILLUSTRATIONS

LIST OF ILLUSTRATIONS - Continued

LIST OF ILLUSTRATIONS - Continued

LIST OF TABLES

LIST OF TABLES - continued

INTRODUCTION

The idea of improvement of gas turbine engine fuel consumption through waste heat recovery is not new. The regenerative gas turbine engine is well established in the areas of stationary and vehicular power. The U.S. Army for instance, has with the XM1 tank and the Lycoming AGT 1500 engine, made a major commitment to the development of regenerative gas turbines. The application of regeneratve engines to aircraft, either fixed or rotary wing, presents a more difficult challenge for the regenerative engine than ground based applications. The penalty for the incremental weight (compared to simple cycle engines) of the heat exchanger (plus associated hardware such as headers, ducting, etc.) opposes fuel weight benefits and the generality has been that for aircraft applications, extremely long missions were required to show a payload-range payoff for regeneration. In addition, over the past several decades, the simple cycle engine typified by the General Electric T700 and the Allison and Lycoming 800 shp Advanced Technology Demonstrator Engines has evolved into a thermodynamically more sophisticated machine through increases in cycle pressure ratio, cycle temperature, and component efficiency improvements so that the performance edge of the regenerative engine over the simple cycle engine has narrowed.

Therefore, in spite of such success as the U.S. Army Aviation Materials Laboratories program of the 1960's in which a T63 engine with regenerator was flown in a light observation helicopter, the penetration of regeneration into aircraft propulsion has been essentially zero to date.

World events of recent years which have resulted in a dramatic increase in fuel costs and raised the spector of fuel shortages make it appropriate to re-examine the regenerative engine. It remains to be seen whether the case can be made for helicopter applications of the regenerative turboshaft engine. Critical to this question is the assessment of the impact of modern high temperature technology plus manufacturing process and materials developments in heat exchangers. The final assessment will depend on a realistic accounting of the life-cycle cost implications of such a power plant including research, development, testing, and evaluation, acquisition, operation and support cost trades relative to a simple cycle engine.

Table 1 outlines the scope of the regenerative turboshaft study described herein. The study was divided into two tasks. Task I consisted of a parametric analysis of cycle and heat exchanger design parameters to evaluate their effect on engine performance, weight, and cost. Current technology component levels were utilized for the parametric study and a 10-year projection of the performance level of the most promising cycle was made.

In Task II, an engine aeromechanical preliminary design was performed to refine the component performance levels, to integrate the heat exchanger with the other engine components, and to define the overall engine

envelope. Engine performance, weight, acquisition cost, and maintenance costs were determined and compared to a nonregenerative engine.

Regenerative engine payoff was evaluated by comparison of helicopter takeoff gross weight, fuel burned and life-cycle costs with those of a conventionally powered vehicle where both vehicles were sized to perform identical missions.

TABLE 1. REGENERATIVE TURBOSHAFT STUDY PROGRAM SCOPE

TASK I - ENGINE AND HEAT EXCHANGER PARAMETRIC ANALYSIS

Current Technology

Performance

Weight

Cost

Ten-Year Performance Projection

TASK II - REGENERATIVE ENGINE PRELIMINARY DESIGN

Refine Most Promising Cycle

Define Envelope

Refine Weight Cost Estimates

TASK I - CYCLE PARAMETRIC STUDY

The parametric study was structured to separately evaluate the effects of:

	Range Investigated
Cycle Temperature, T_{41}	2100° to 2400°F
Cycle Pressure Ratio, P_3/P_2	6 to 12:1
Recuperator Effectiveness, ϵ	50 to 80%
Recuperator Total Pressure Loss, $\Delta P/P$	5 to 15%
Tubular vs Plate-Fin Recuperator Type	
Fixed Power Turbine Geometry vs. Variable Geometry on regenerative engine performance.	

Table 2 summarizes the 27 regenerative engine cycles evaluated in the parametric study.

Engine 1 of the parametric family is the baseline for the study. Figure 1 shows the nominal flowpath configuration for the baseline engine. It is a front drive with a free power turbine output shaft and includes an integral inlet particle separator. Compressor discharge air is diverted to the heat exchanger through a collector scroll and returned to the combustor in a return scroll. Power turbine exhaust air is ducted to the inside of the heat exchanger core, passes radially through the core, and is collected by an exhaust scroll and discharged through an exhaust nozzle at a right angle to the engine centerline.

Both tubular and plate-fin heat exchangers were evaluated in the study. Only fixed geometry, stationary heat exchangers were evaluated. Rotary heat exchangers were not considered since the additional weight of the rotating mechanism would be prohibitive for a flight vehicle. Furthermore, leakage and carryover losses of a rotary heat exchanger tend to restrict their suitability to low cycle pressure ratios.

The tubular heat exchanger is an annular cross-counter flow-type with ring-dimpled tubes as shown in Figure 2. Compressor discharge air is routed to the outer portion of the tube bundle through an annular scroll, flows axially through the tubes and is returned through the inner portion of the tube bundle. The hot exhaust gases flow radially outward over the tubes.

The plate-fin heat exchanger arrangement is also shown in Figure 2. Since the plate-fin configuration does not lend itself to a full annular design, four modules were arranged in an annular ring. Compressor discharge air is piped to the inlet port of each module and flows inward to the return ports. Low pressure turbine exhaust gas enters the inner face of each module and flows outward in pure counter flow to the cold gases.

Engine Cycle 19 includes heat exchanger bypass valves in both the cold and hot gas streams to bypass the heat exchanger at high power settings. The bypass arrangement is shown schematically in Figure 3.

TABLE 2. TASK I - PARAMETRIC CYCLES

	Parametric Cycle									
Engine 1	1	2	3	4	5	6	7	8	9	10
T_{41}°F	2100	2100	2100	2400	2400	2400	2100	2100	2100	2100
P/P	8.6	6	12	6	8.6	12	6	8.6	12	6
Regenerator										
ϵ %	75	75	75	75	75	75	70	70	70	80
$\Delta P/P$%	5	5	5	5	5	5	5	5	5	5
VATN	yes	yes	yes	yes	yes	yes	yes	yes	yes	yes

	Parametric Cycle									
Engine 1	11	12	13	14	15	16	17	18	19	20
T_{41}°	2100	2100	2100	2100	2100	2100	2100	2400	2100	2100
P/P	8.6	12	8.6	8.6	6	8.6	12	8.6	8.6	8.6
Regenerator										
ϵ %	80	80	75	75	75	75	75	75	75	75
$\Delta P/P$%	5	5	10	15	5	5	5	5	5	5
VATN	yes	yes	yes	yes	no	no	no	no	yes	yes

	Parametric Cycle								
Engine 1	21	22	23	24	25	26	27	53	57
T_{41}°	2100	2100	2100	2100	2250	2400	2100	2100	2400
P/P	8.6	8.6	8.6	8.6	8.6	8.6	8.6	12	12
Regenerator									
ϵ %	75	75	70	80	75	50	50	*	*
$\Delta P/P$%	5	5	5	5	5	5	5	*	*
VATN	yes	yes	yes	yes	yes	yes	yes	*	*

NOTES: Engine Cycle 19 bypasses recuperator At MC AND IRP.

Engine Cycles 20 and 21 are alternate flowpath configurations.

Engine Cycles 22, 23, and 24 have plate-fin recuperators, others have tubular recuperators.

*Nonregenerator cycles.

At low power settings, both of the bypass valves are closed and all of the air passes through the heat exchanger matrix. At high power settings (maximum continuous to IRP), both of the bypass valves open to divert a portion of the cold and hot flow streams around the heat exchanger. Bypassing approximately 49% of the cold side flow and 62% of the hot gas flow reduces the pressure losses from 2% to 0.5% and from 3% to 1.0% respectively, while the overall heat exchanger effectiveness (including dilution of the cold side bypass flow) is reduced from 75% to 68%.

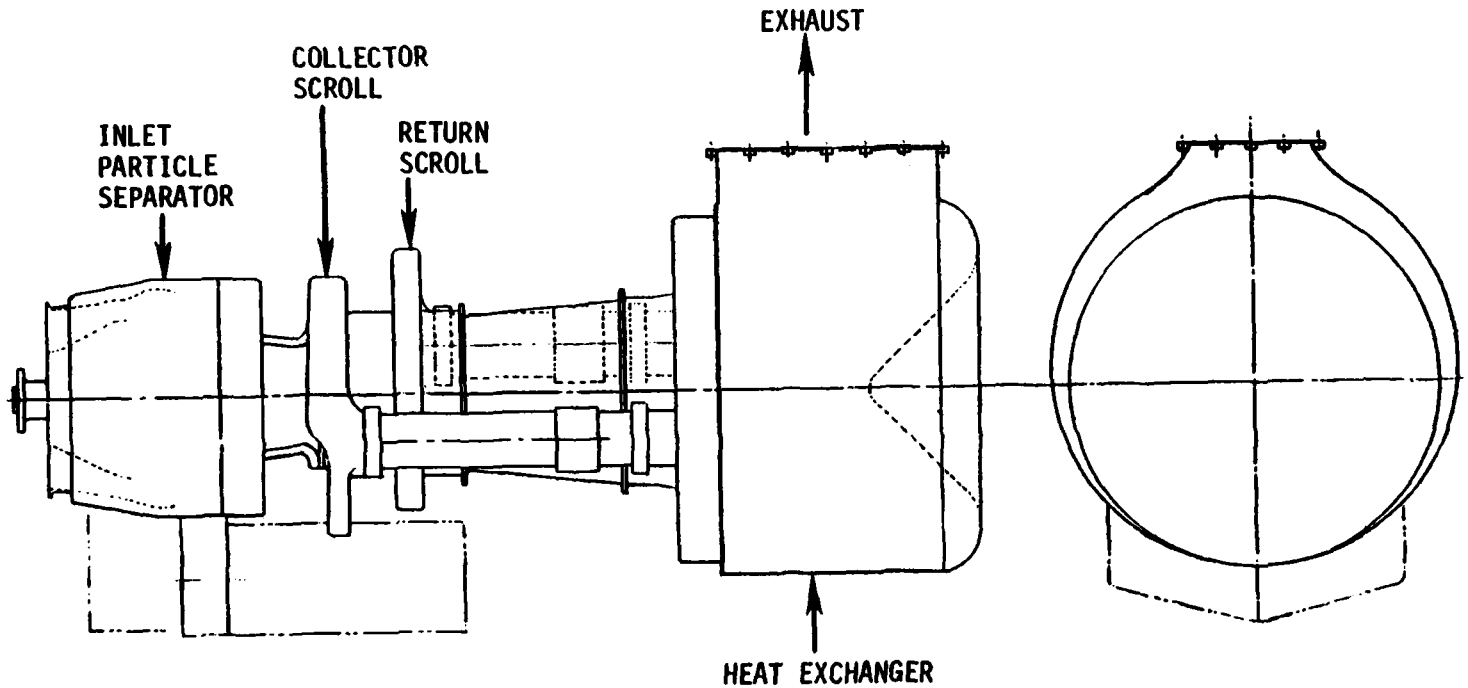

Figure 1. Nominal Flowpath Configuration.

Two alternate flowpath configurations were evaluated as shown in Figures 4 and 5. Engine Cycle 20 incorporates a rectangular heat exchanger tube bundle side-mounted on the exhaust pipe. Engine exhaust gases are collected from the power turbine annulus, directed through the heat exchanger and discharged to ambient. Suitable manifolds provide for compressor discharge air supply and return. The principal advantage envisioned for this arrangement is the simpler rectangular heat exchanger matrix.

Engine Cycle 21 evaluated a single can combustor configuration located in the heat exchanger return pipe. With this arrangement, the combustor is more accessible for maintainance and repair.

BASELINE CYCLE DEFINITION

The components of the baseline cycle (Engine 1) are summarized in Table 3. The component performance levels shown represent current technology levels in the 500 shp engine size. An integral inlet particle separator with 14% scavange flow is included. An axicentrifugal compressor configuration provides a corrected flow of 3.5 lb/sec at an overall total-to-total pressure ratio of 8.6. The combustor is an annular, axial through-flow design with a discharge temperature (turbine rotor inlet) of 2100°F.

The compressor is driven by a single-stage moderately loaded axial flow high-pressure turbine. Output power is supplied by a three-stage axial flow, shrouded power turbine. The power turbine counter-rotates with the high-pressure spool to take advantage of the high-pressure turbine residual swirl and is sized for an overall loading* of 1.0 at IRP. The nominal heat exchanger was sized for 75% effectiveness** and a total pressure drop (cold plus hot side) of 5%. Ducting losses were accounted for separately.

Cycle parasitic flows were estimated to be consistent with the configuration, cycle temperature, and materials

---

* TURBINE LOADING, $\psi_p = \frac{gJ\Delta H^2}{2U_p}$

** EFFECTIVENESS, $\epsilon = \frac{\Delta T_{\text{COLDSIDE}}}{T_{\text{HOT IN}} - T_{\text{COLD IN}}}$

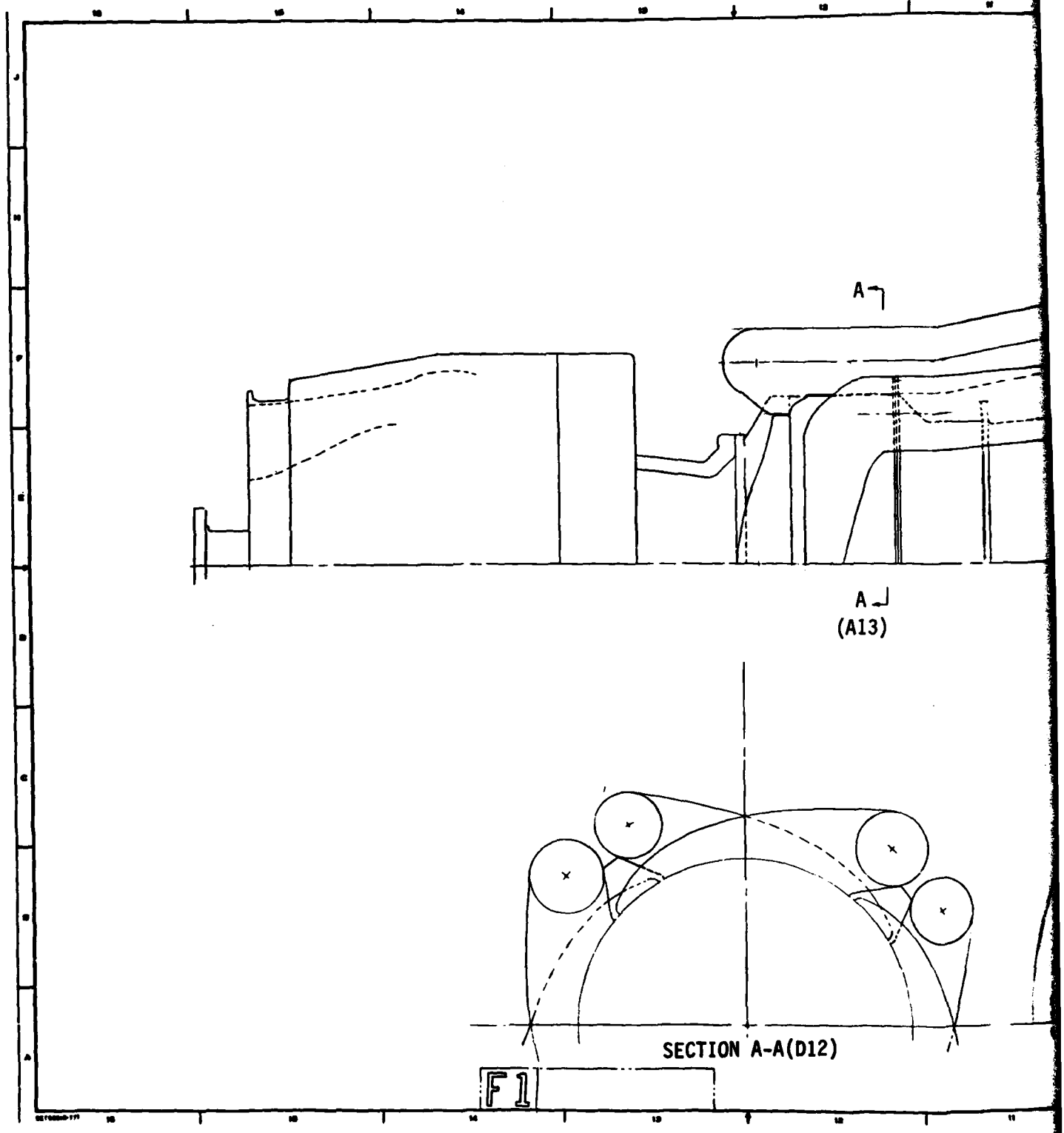

Figure 2. Heat Exchanger Arrangement.

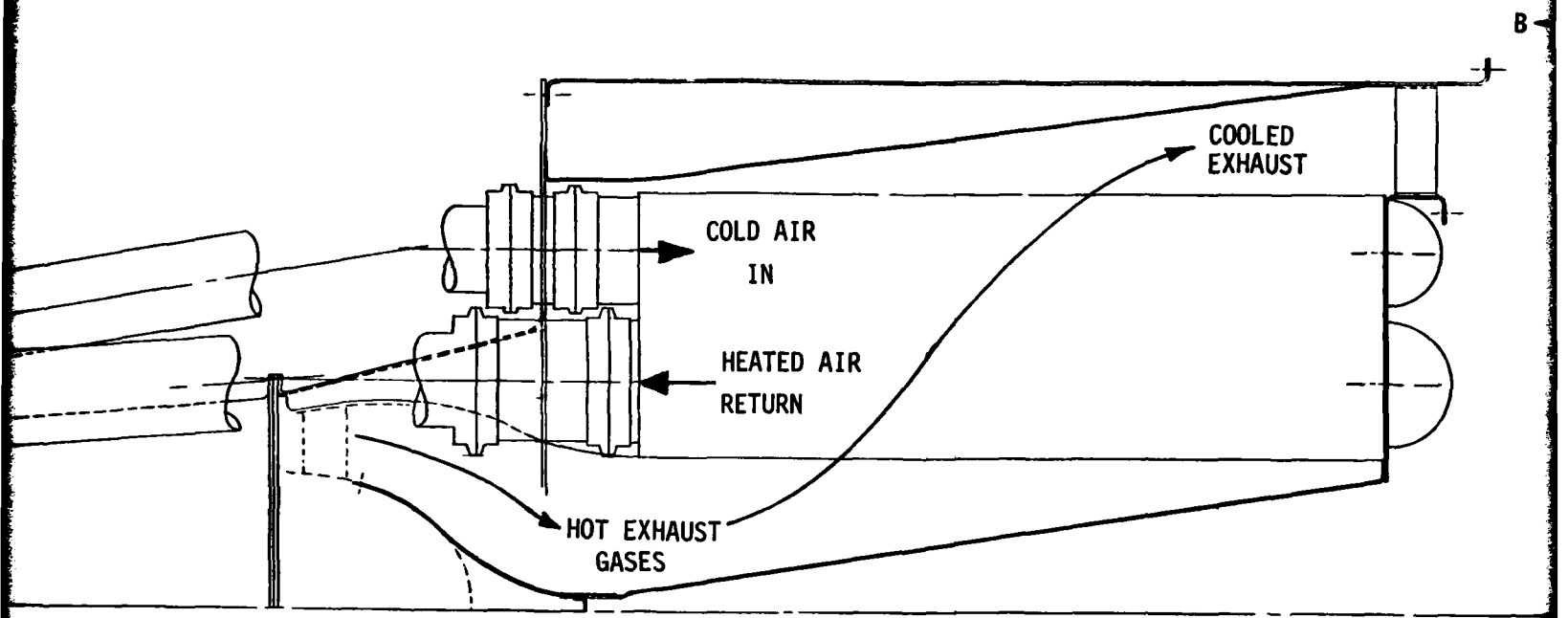
B
COOLED
EXHAUST
COLD AIR
IN
HEATED AIR
RETURN
HOT EXHAUST
GASES

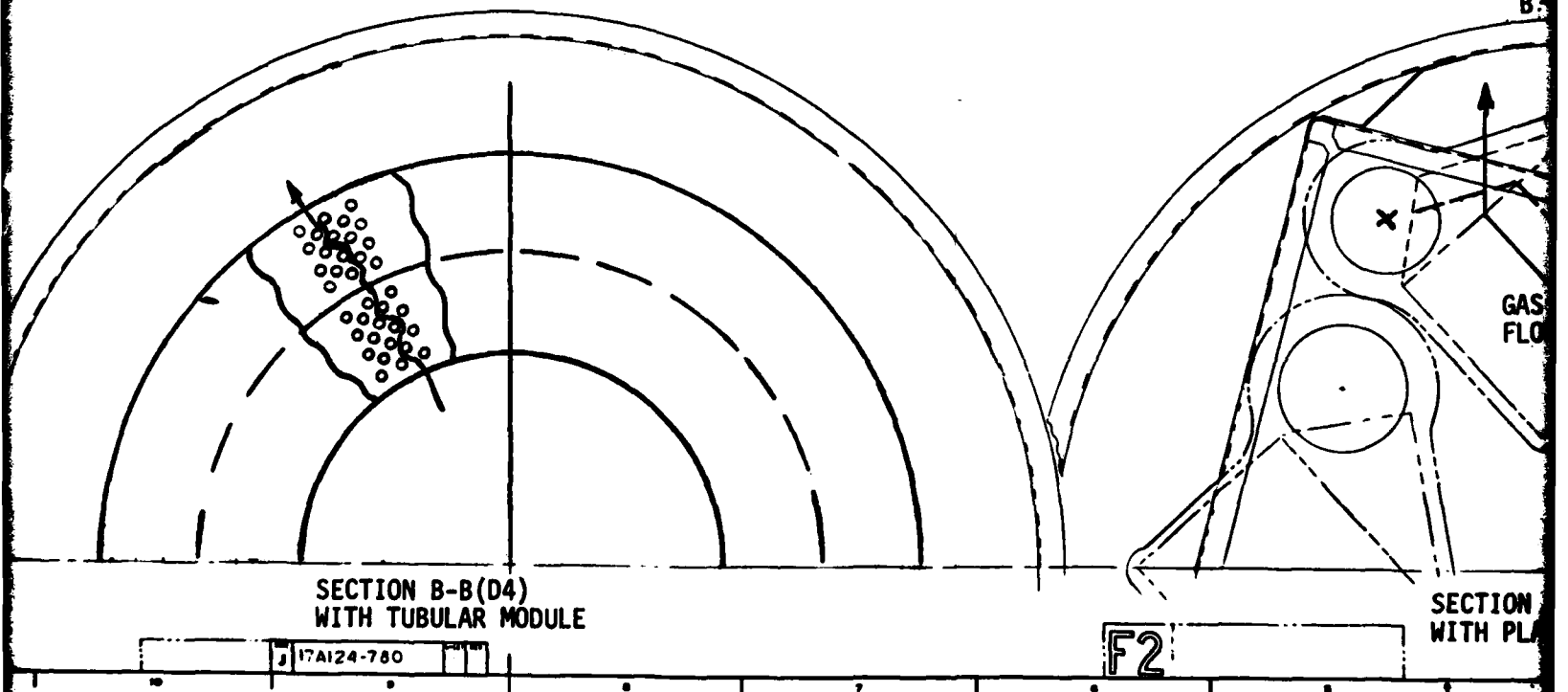
B
GAS
FLO
SECTION B-B(D4)
WITH TUBULAR MODULE
SECTION
WITH PL
17A124-780
F2

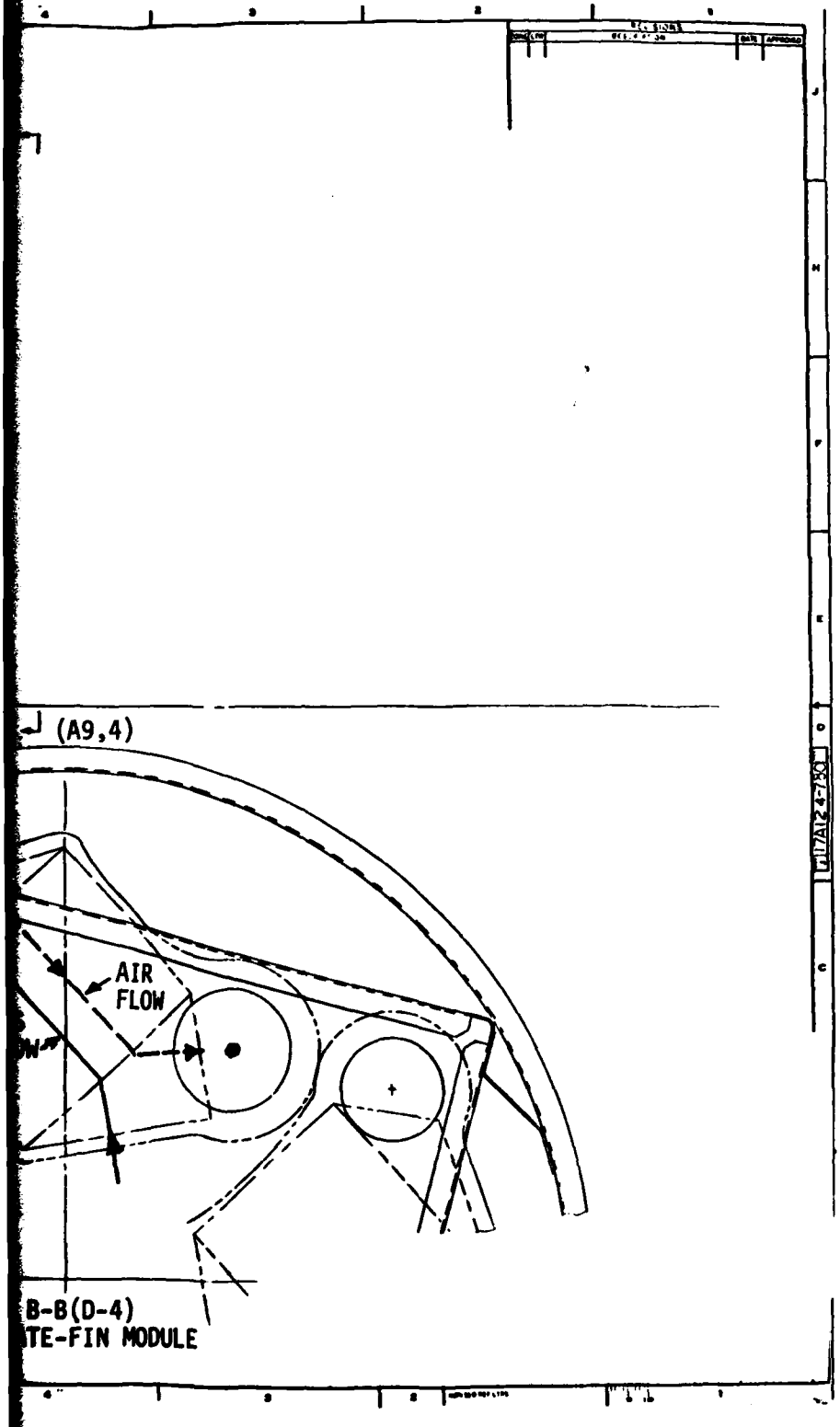

3

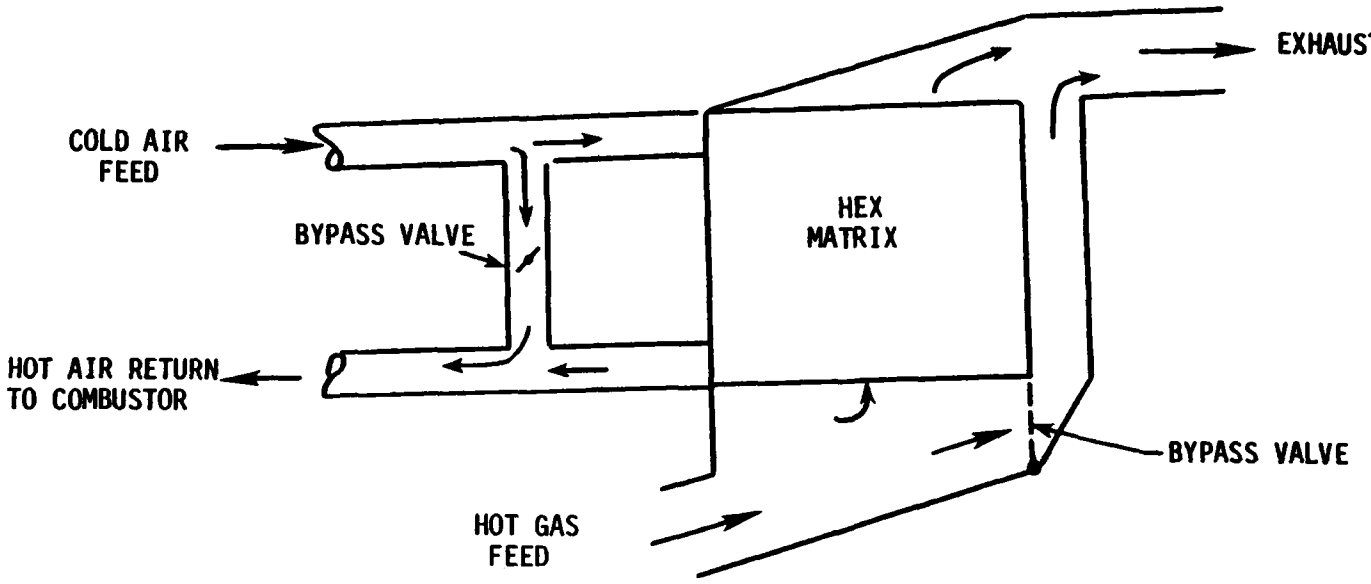

PART POWER

- BOTH BYPASS VALVES CLOSED
- $\Delta P/P$ = 2% COLD SIDE
  $\Delta P/P$ = 3% HOT SIDE
- ϵ = 75% @ 300 SHP

HIGH POWER

- BOTH BYPASS VALVES OPEN
- $\Delta P/P$ = 0.5% COLD SIDE
  $\Delta P/P$ = 1.0% HOT SIDE
- EFFECTIVENESS = 68%
- BYPASS 49% COLD SIDE FLOW
- BYPASS 62% HOT SIDE FLOW

Figure 3. Schematic of Bypass Valving for Engine Cycle 19.

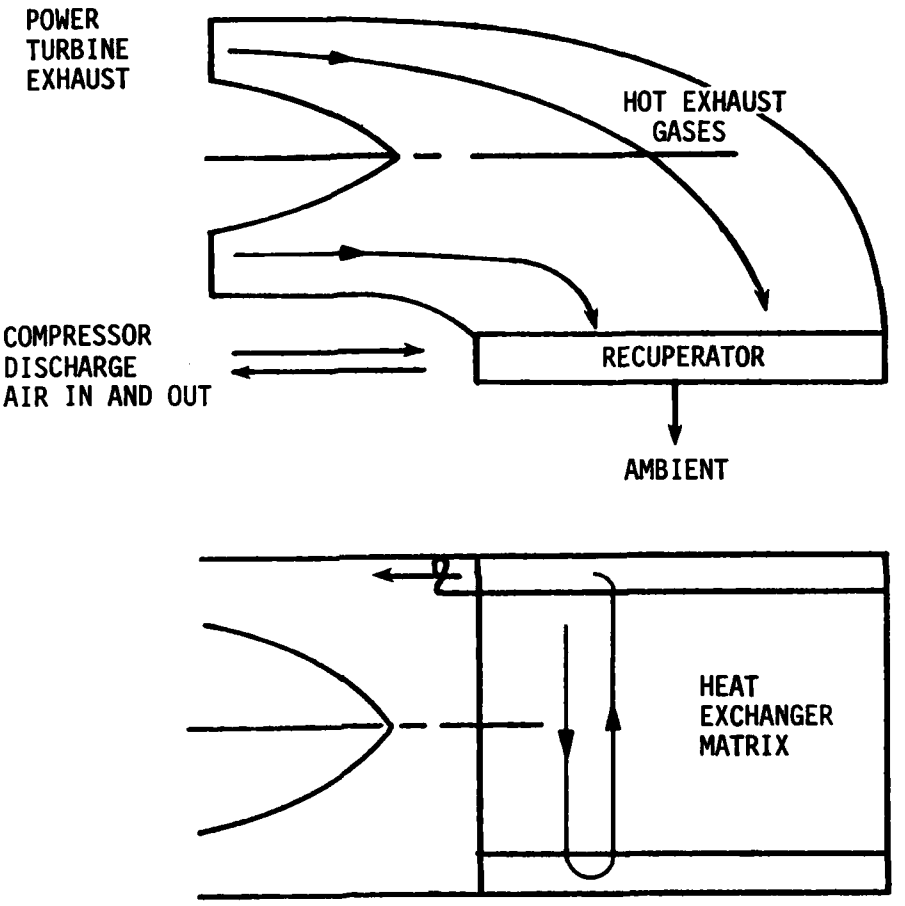

Figure 4. Alternate Flow Path Configuration for Engine Cycle 20.

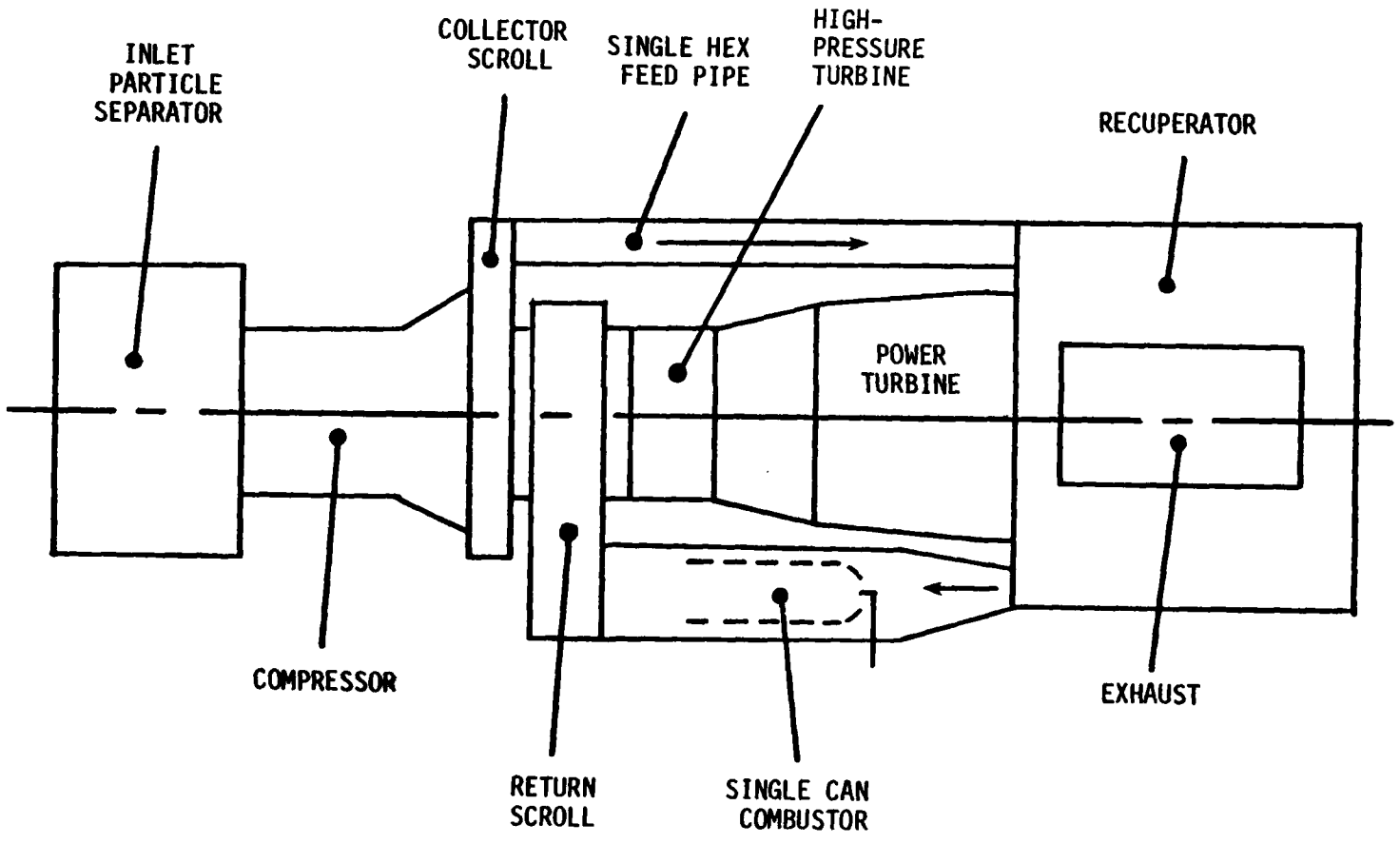

Figure 5. Alternate Flowpath Configuration for Engine Cycle 21.

TABLE 3. REFERENCE CYCLE (ENGINE 1) AT 500 SHP

INLET PARTICLE SEPARATOR
- 14% Bleed
- 2.34% $\Delta P/P$

COMPRESSOR
- 2- + 1-Stage* (58,000 rpm)
- 3.5 $W_2\sqrt{\theta}/\delta$
- 8.6 P/P
- 81.5% η

COMBUSTOR
- 2100°F T_{41}
- 99.5% η
- 4.15% $\Delta P/P$

HIGH PRESSURE TURBINE
- Single Stage
- 86.6% η
- 20° Swirl
- 0.76 Loading

INTERTURBINE DUCT
- 0.5% $\Delta P/P$

Power Turbine
- 3 Stages (20,000 rpm)
- 89% η
- 25° Swirl
- 1.0 Loading at IRP
- Counter Rotates With Core

EXHAUST
- 3.2% $\Delta P/P$

RECUPERATOR
- 75% Effectiveness
- 5% Total $\Delta P/P$
- 0.1% Piping $\Delta P/P$

TAILPIPE
- 1.0% $\Delta P/P$
- 1.03 P_8/P_0

PARASITICS
- 0.9% Windage Horsepower
- 0.5% Blower Horsepower
- 8.5% Nonchargeable Cooling
- 4.5% Chargeable Compressor Discharge Pressure
- 0.13% Mid Stage (Sumps)

*Two axial stages and one centrifugal stage.

PERFORMANCE TRENDS

Since the range of cycle parameters covered involves a significant variation in airflow to maintain the desired 500 shp rating, size effects are an important consideration in evaluating the relative performance of the parametric cycles.

Table 4 summarizes the factors considered in adjusting the component efficiency levels of each of the parametric cycles relative to the nominal baseline cycle (Engine 1). The compressor staging was varied with cycle pressure ratio as indicated, while the turbine staging was held constant (single stage high-pressure turbine and 3 stage power turbine) and the diameters were adjusted to maintain loading.

Figure 6 shows the compressor efficiency trends with pressure ratio and flow size. The efficiency trend with pressure ratio represents a constant level of technology with varying staging (but constant flow size), while the size effect includes Reynolds number effects (Reynolds number based on inlet flow conditions), clearances, and blade thickness effects which do not scale directly with size.

The high-pressure turbine performance variation with cycle parameters is shown in Figure 7. In addition to the size related variations, a variation in efficiency with pressure ratio was also used.

The primary size related variation in power turbine efficiency is due to Reynolds number as shown in Figure 8. VATN (variable area turbine nozzle) effects were modeled by modifying a basic power turbine map with an efficiency adder as a function of the VATN setting. The power turbine efficiency level with a VATN was reduced by 0.5 point relative to a non-VATN configuration to account for leakage effects in the variable nozzle. The VATN for the power turbine was sized to provide peak efficiency at a 90% VATN setting (typical of cruise conditions) with a reduction in performance at VATN settings above and below the 90% design value. At the IRP engine sizing point, the VATN is at 100% and the power turbine efficiency is 1 point lower than it is without a VATN.

TABLE 4. TURBOMACHINERY SCALING FOR PARAMETRIC CYCLES

COMPRESSOR

Pressure Ratio = 8.6
(Base Configuration)
- 2- + 1-Stage* Configuration
- Scaled for Airflow
- Size Correction to η

Pressure Ratio = 6
- 1- + 1-Stage* Configuration
- Scaled for Airflow
- Size Correction to η

Pressure Ratio = 12
- 3- + 1-Stage* Configuration
- Scaled for Airflow
- Size Correction to η

HIGH-PRESSURE TURBINE

Base Configuration
- ψ_P = 0.76, L = 0.62
- C_L/L = 1.8

For Parametric Cycles:
- Constant Vane and Blade Chords
- Flowpath Resized ψ_P = .76
- Pressure Ratio Correction to η
- C_L/L Correction to η
- AR (Aspect Ratio) Correction to η
- RNI Correction to η
- Cooling Correction to η

COOLING FLOWS

Function of:
- RPM, Annulus Area
- T_3
- T_{41}
- Materials

POWER TURBINE

Base Configuration
- ψ_P = 1.0 at IRP, 20,000 rpm

For Parametric Cycles:
- ψ_P = 1.0 at IRP
- (3 Stages, 20,000 rpm)
- RNI Correction to η
- VATN Correction to η

*Axial and centrifugal stages respectively

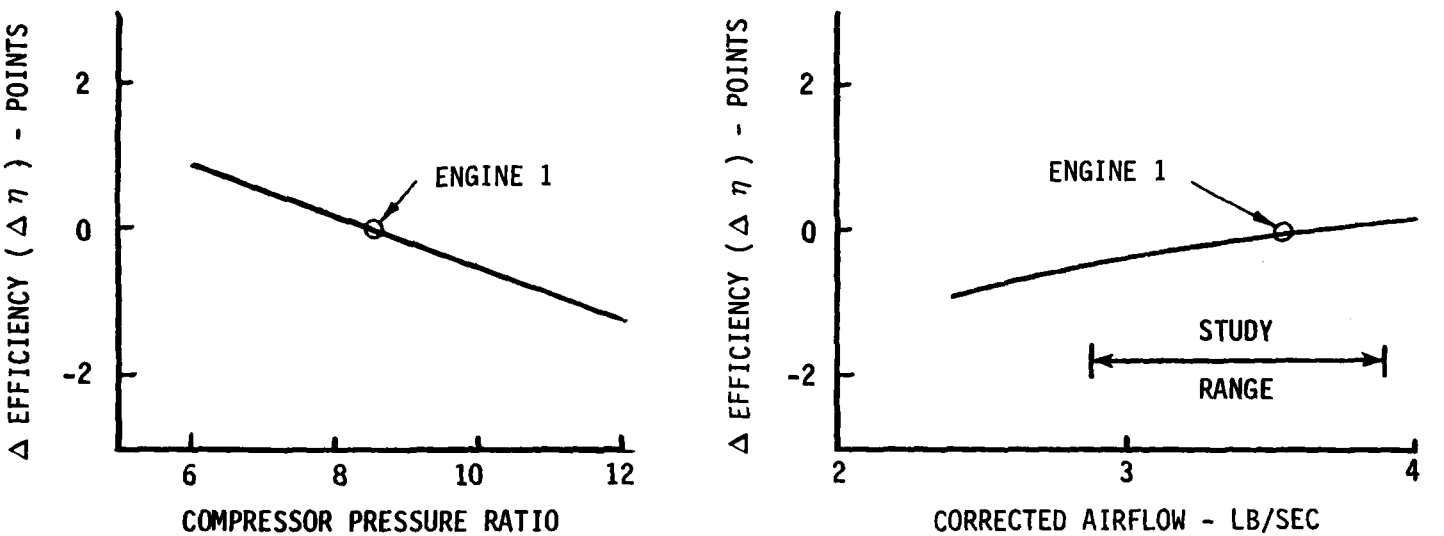

Figure 6. Compressor Efficiency Trends.

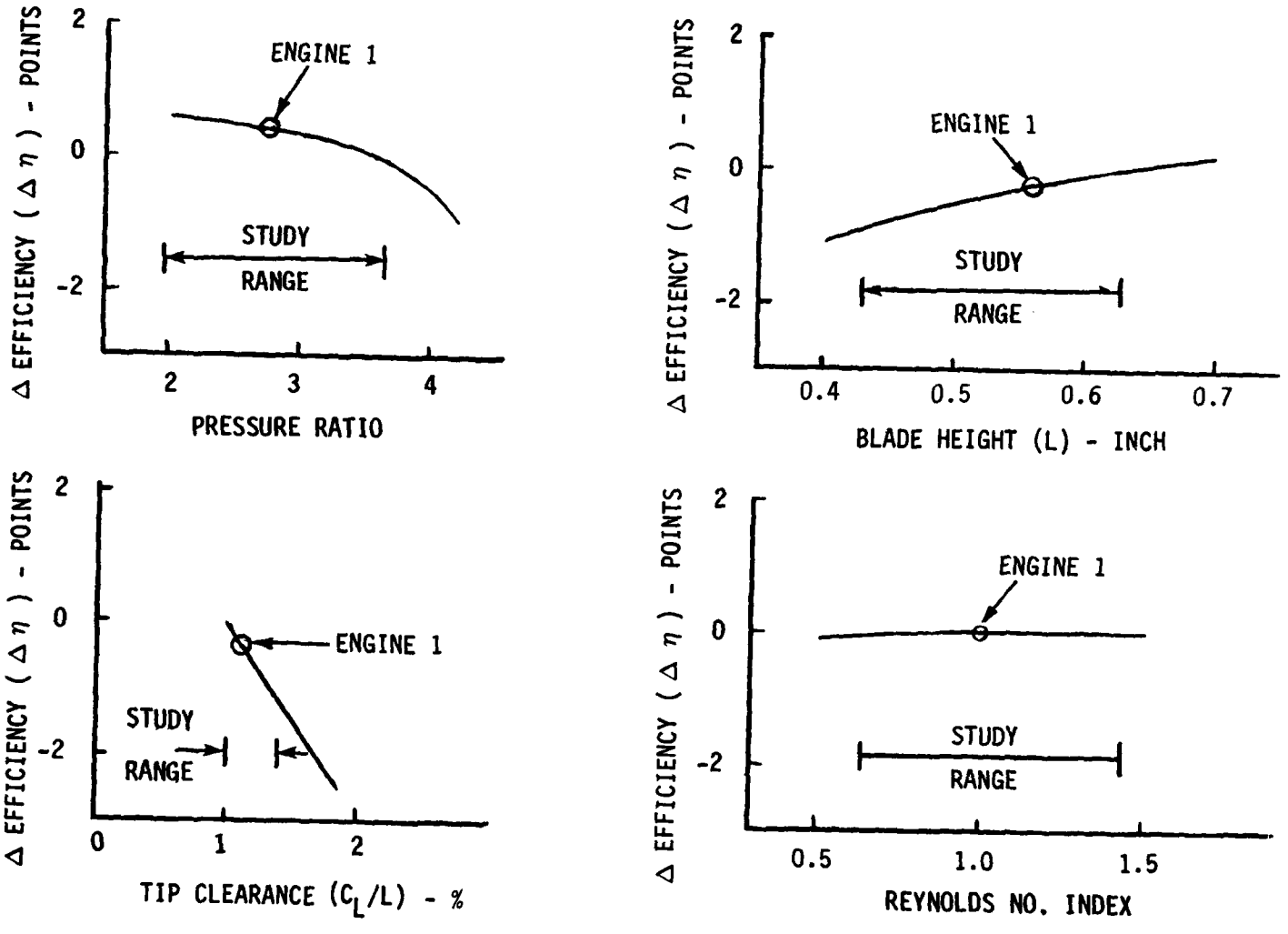

Figure 7. High-Pressure Turbine Efficiency Trends.

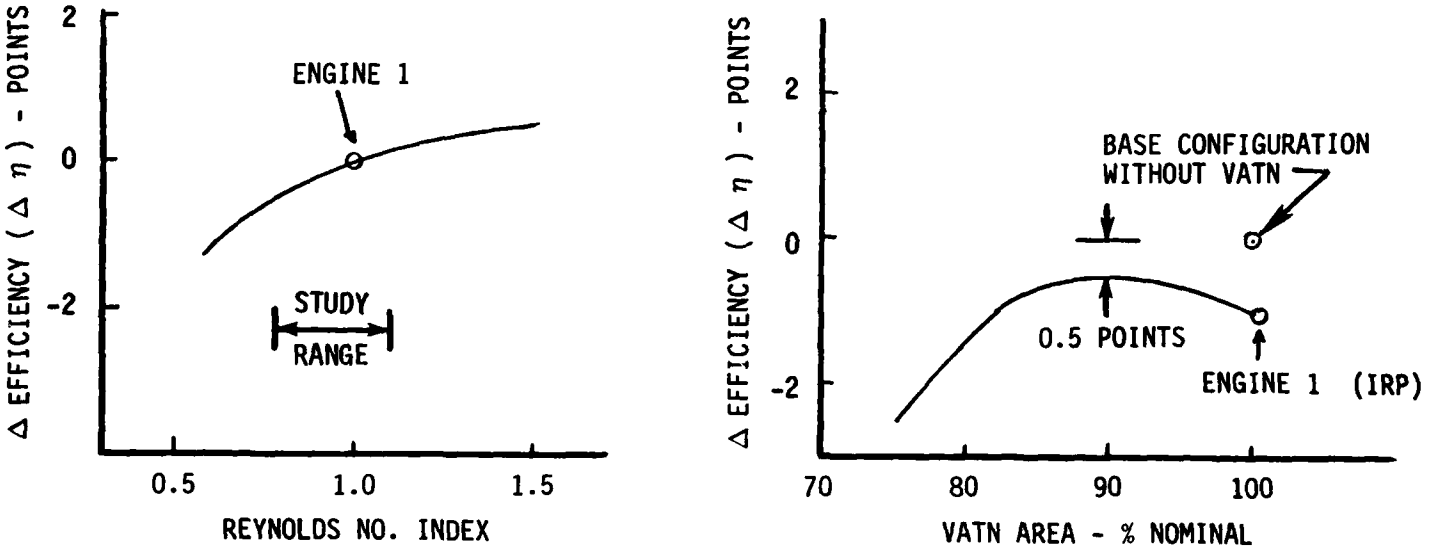

Figure 8. Power Turbine Efficiency Trends.

Parasitic flow variations with cycle pressure ratio and cycle temperature (T41) are shown in Figure 9. These variations were estimated to maintain constant hot parts life (750 hours at rated temperature, 5000 hours total life) with the variation in coolant and gas temperatures for the parametric cycles. Currently available production materials were used in the analysis. The turbine blades were assumed to be made of Rene' 125 for all of the parametric cycles. Material X40 was assumed for the high-pressure turbine nozzles at 2100°F cycle temperature while MA754 material was assumed for the 2400°F cycles in order to keep the cooling flows at reasonable levels.

The high-pressure turbine nozzle allowable temperature was set at 1490°F for X40 material and 1640°F for MA754. The high-pressure blade allowable temperature was varied with the stress parameter (AN^2) as shown in Figure 10.

While the power turbine rotor is uncooled for all the parametric cycles, centrifugal impeller tip bleed of 2% was utilized to cool the interturbine frame and power turbine first stage nozzle.

Since the component performance levels are size dependent and the flow size is affected by the assumed levels (at constant shaft horsepower) an iterative procedure was used in the definition of each of the parametric cycles. As shown in Figure 11, sizing cycle data were generated with assumed component levels. The sizing data were then used to check the assumed levels, and the sizing cycle calculations were repeated with revised component levels. This iteration process was repeated until the revised levels agreed with the previous pass values.

Recuperation off-design effectiveness and pressure loss characteristics as supplied by AiResearch are shown in Figures 12 and 13 respectively. The tubular recuperators were designed for a cold air and hot gas pressure loss split of 40/60%, while the plate-fin recuperators were designed for a 20/80% pressure loss split. These choices were made as the result of parametric studies conducted by AiResearch which indicated that they provided minimum weight.

In generating off-design performance data for the variable area power turbine cycles, the VATN was scheduled to obtain the maximum SFC benefit within constraints of not exceeding the high-pressure turbine maximum continuous temperature rating (IRP minus 100°) or the power turbine IRP inlet temperature. In addition the VATN closure was restricted to maintain acceptable compressor stall margin as discussed below.

VATN schedules were investigated for the nominal regenerative cycle (Engine 1) as shown in Figure 14. As indicated, continued SFC improvements at part power were obtained with VATN settings as low as 80%. However, as shown in Figure 14 turbine temperature limits were encountered at VATN settings slightly greater than 80%. In order to

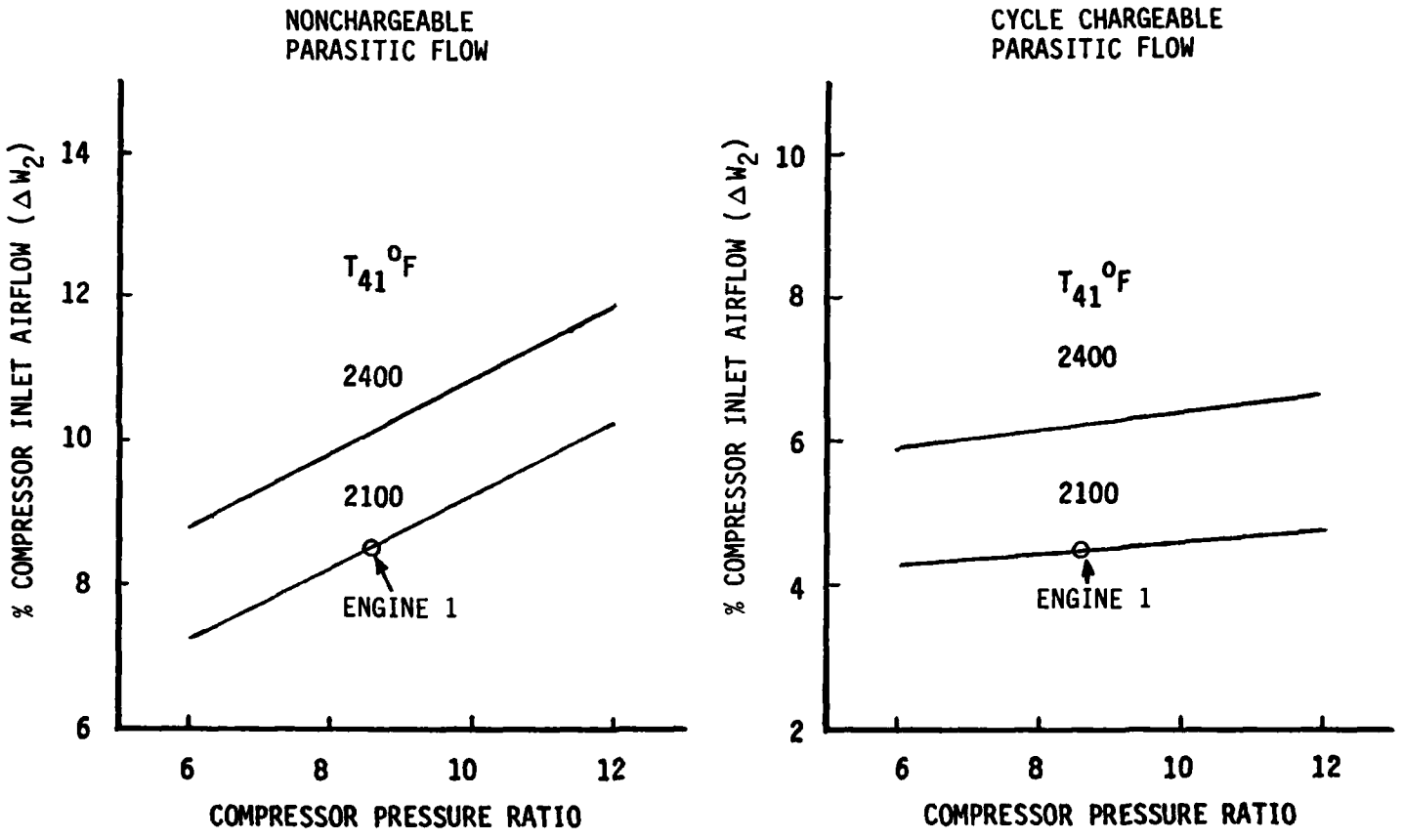

Figure 9. Parasitic Flow Trends.

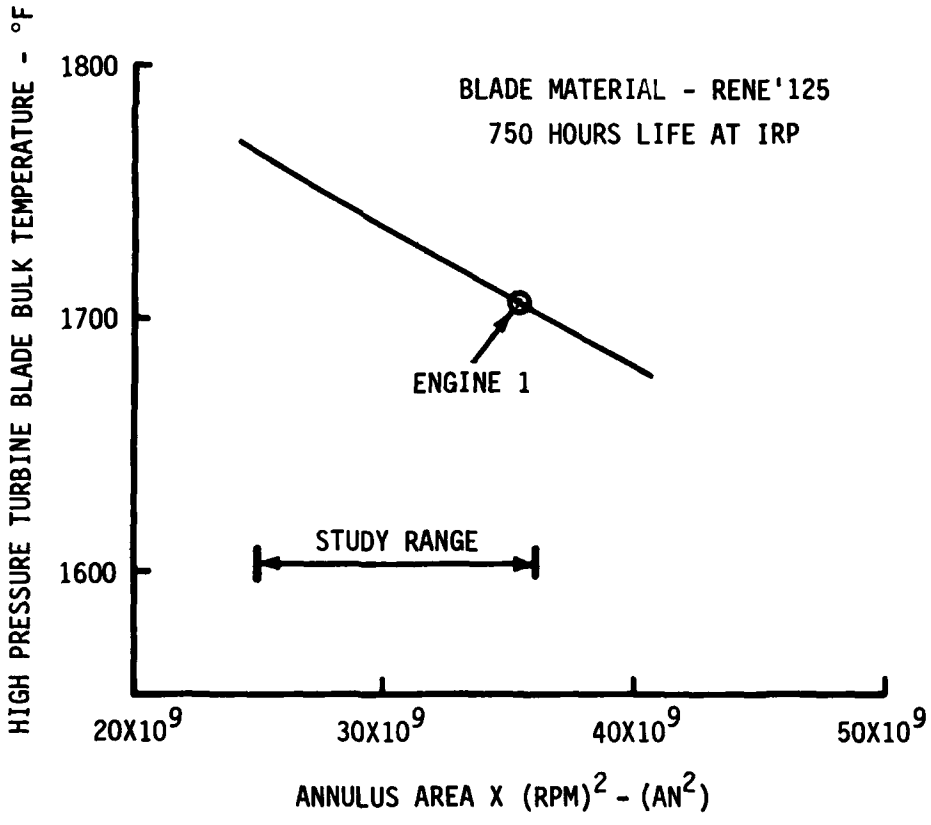

Figure 10. High-Pressure Turbine Allowable Blade Temperature.

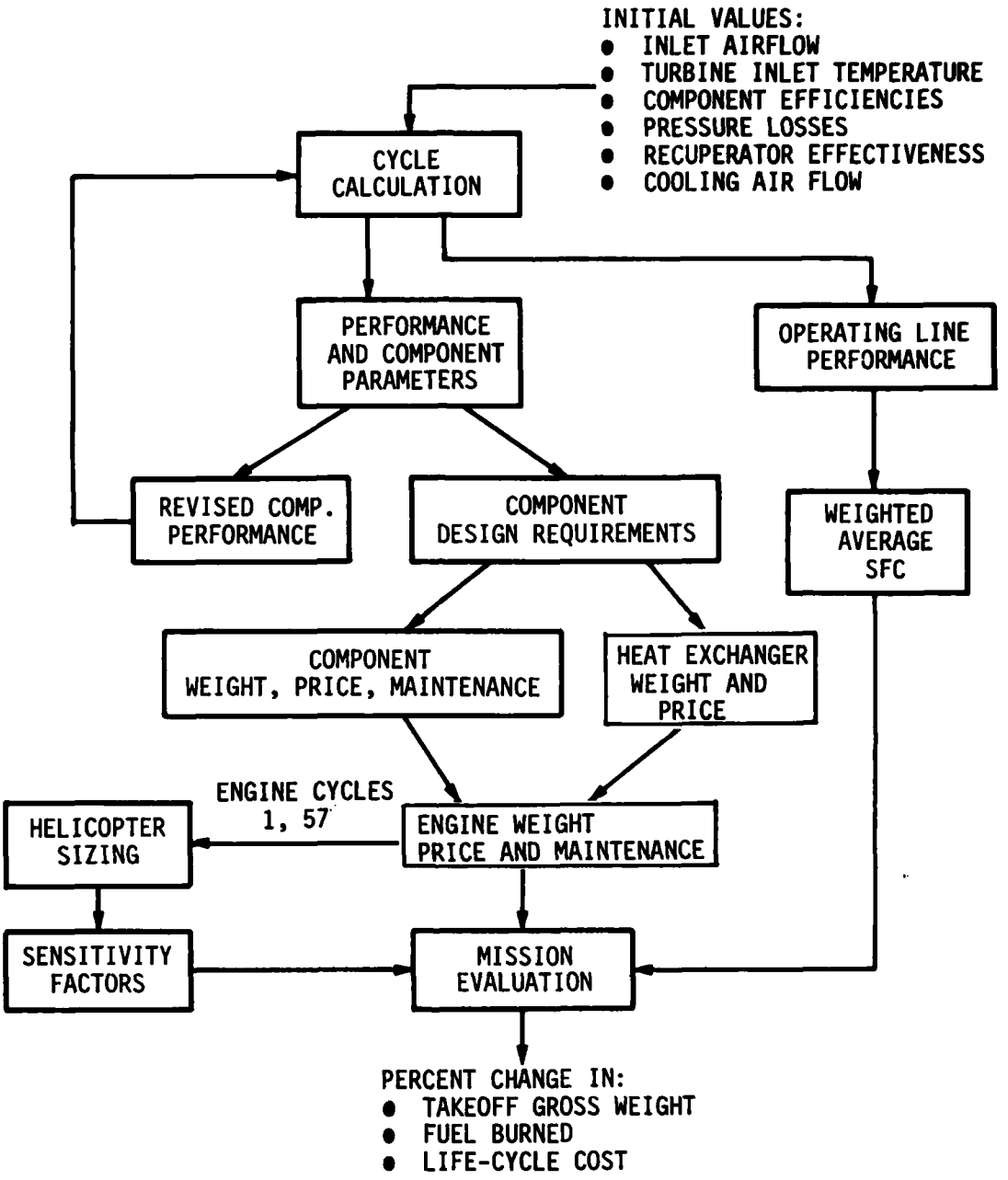

Figure 11. Task I Parametric Flow Chart.

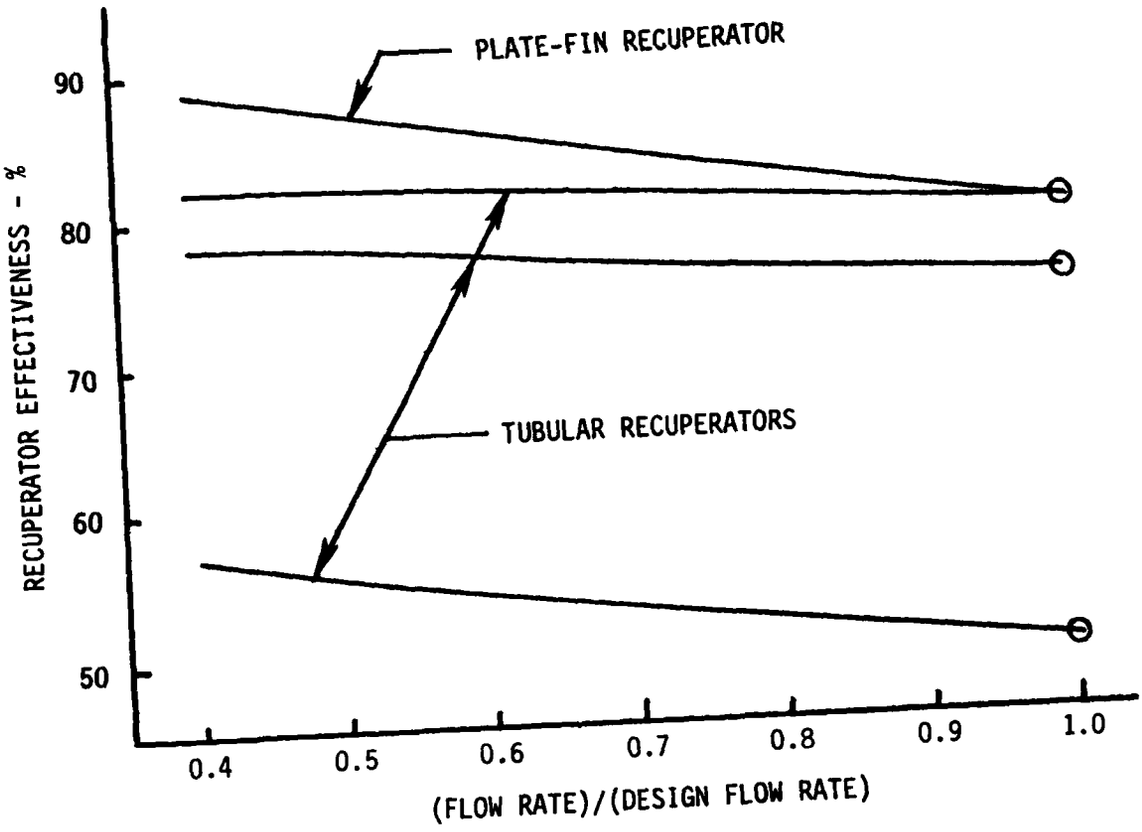

Figure 12. Recuperator Effectiveness Characteristics.

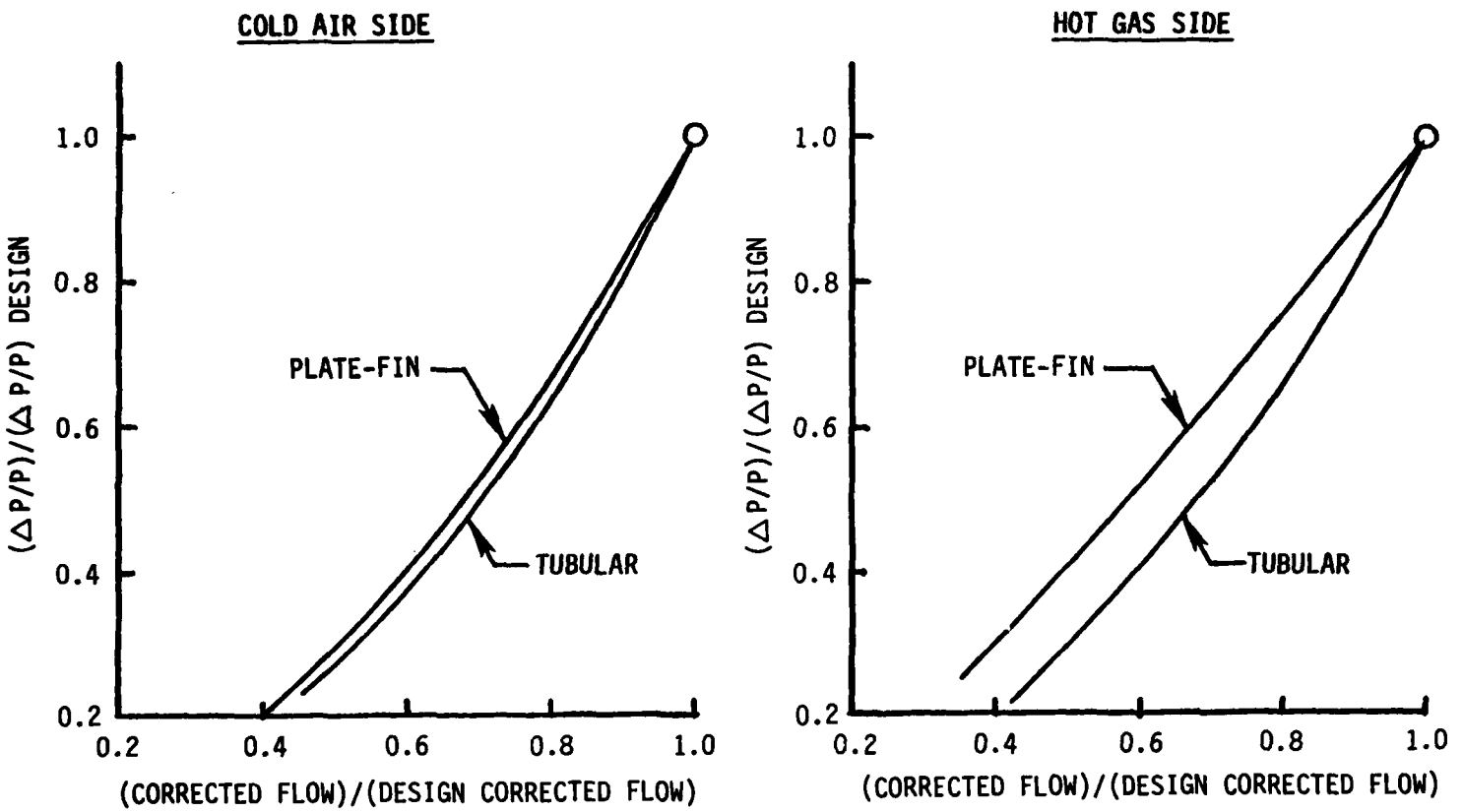

Figure 13. Recuperator Pressure Loss Characteristics.

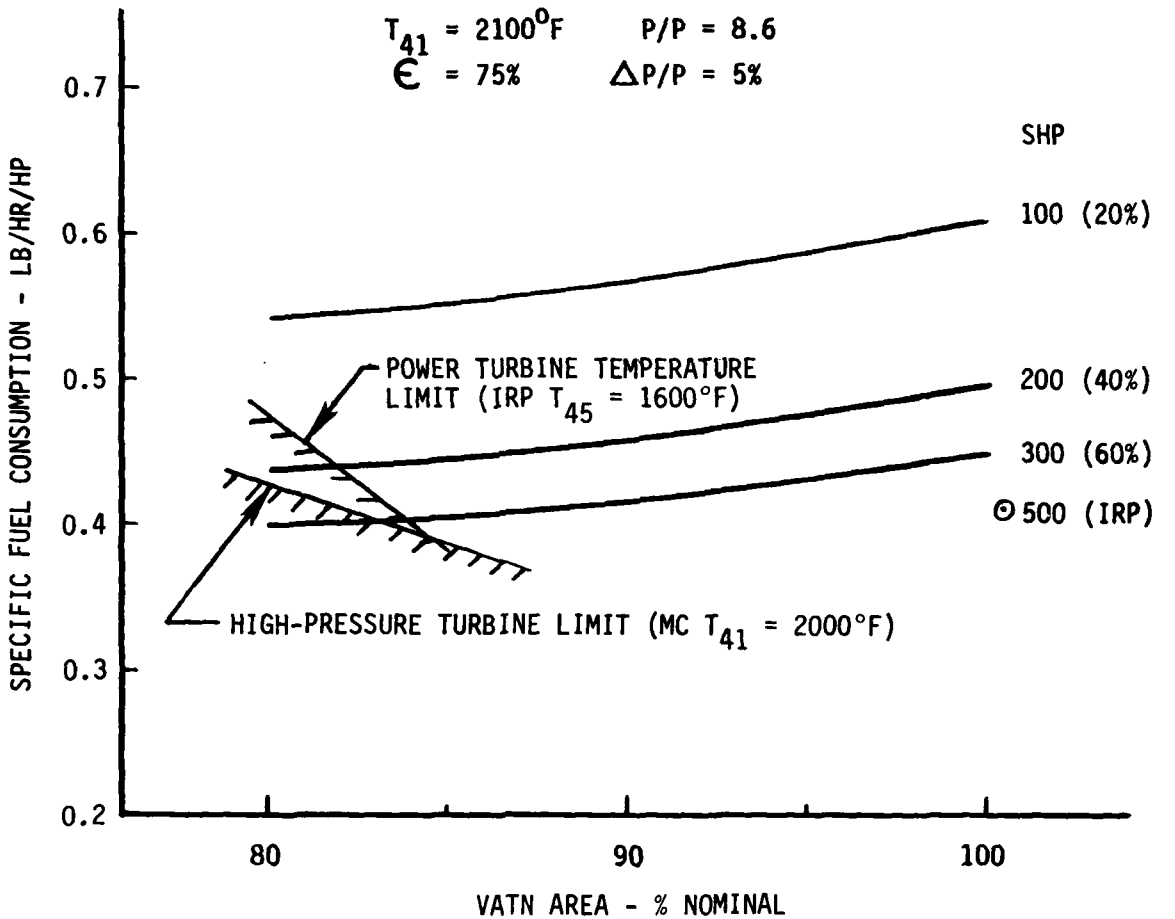

Figure 14. Variable Area Turbine Nozzle Effects at Constant Shaft Horsepower - Engine 1.

maintain hot parts life with cooling flows consistent with IRP power requirements, the VATN closure was restricted to stay within the high-pressure turbine MC T_{41} level and the power turbine IRP T_{45} level. Application of this defined VATN scheduling as a function of cycle pressure ratio is shown in Figure 15.

Figure 16 illustrates the importance of scheduling the VATN to maintain the highest permissible cycle temperatures at part power. In spite of the loss in compressor and high-pressure turbine efficiency with VATN closure in the 100 to 300 shp regime, the part power SFC is improved. Thus the cycle benefit of higher temperatures (and pressure ratio) at part power is greater than the effect of the component efficiency losses for a net SFC benefit.

Another aspect of VATN closure at part power that must be considered is the effect on the compressor operating line. Figure 17 illustrates the effect of VATN closure on operating line migration. For a fixed geometry operating line, the part power stall margin is typically greater than at the IRP sizing point. The part power stall margin is reduced with VATN closure, but within the cycle temperature limit constraints the remaining stall margin is still in excess of the IRP value and is adequate for steady-state operation.

Transient (accelerations) stall margin requirements can be met by using a digital electronic control to differentiate between steady state and transient operation and by scheduling the VATN to be open (towards or even beyond fixed geometry operating line) during accelerations.

Sea level static operating line performance characteristics were generated for each engine cycle using the component performance characteristics and VATN schedules noted above.

Regenerative engine operating line performance characteristics with the selected VATN schedules are shown in Figures 18 through 23.

Figure 18 illustrates the effect of cycle pressure ratio and compares the operating line performance characteristics with a 12:1 P/P nonregenerative cycle (engine Cycle 53). The increasing SFC benefits of the regenerative cycles at part power (relative to the nonregenerative cycle are due to VATN effects and to the increase in recuperator effectiveness at reduced airflow. Figure 19 compares the regenerative engine characteristics to a nonregenerative engine at increased cycle temperature (T_{41} = 2400°F).

Figure 20 compares the operating line SFC characteristics variation with T_{41}. Note the SFC continuously improves with increased T_{41}.
VATN effects on regenerative engine operating line performance characteristics are shown in Figure 21. While engine Cycle 16 (without

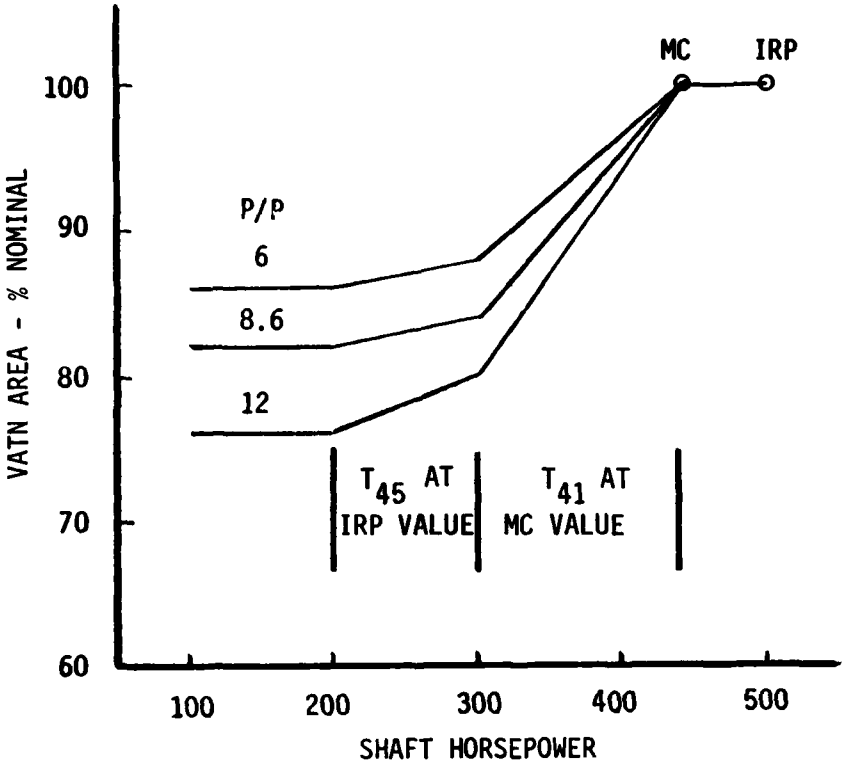

Figure 15. Typical Variable Area Turbine Nozzle Schedules.

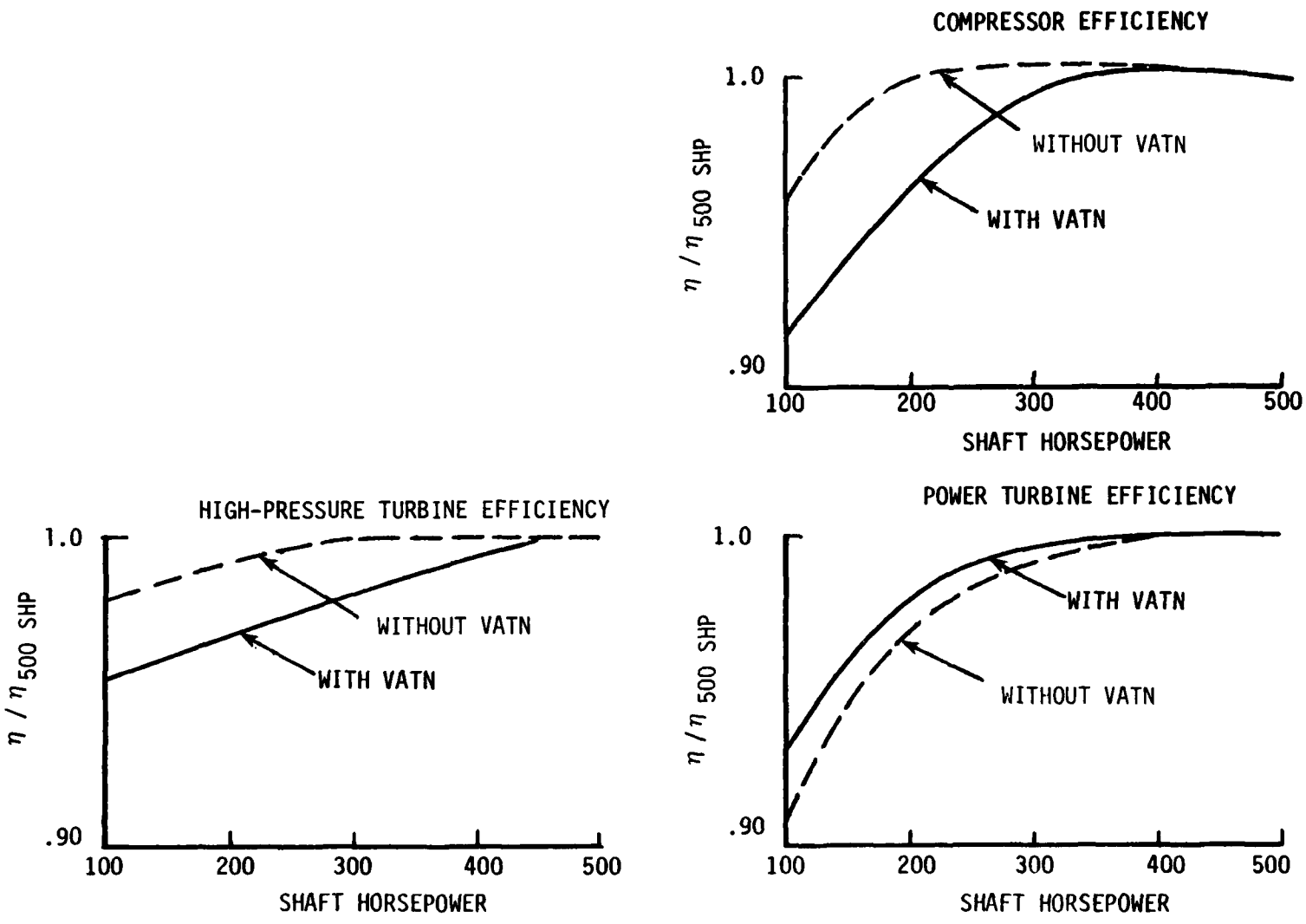

Figure 16. Typical Component Efficiency Trends With Power Level.

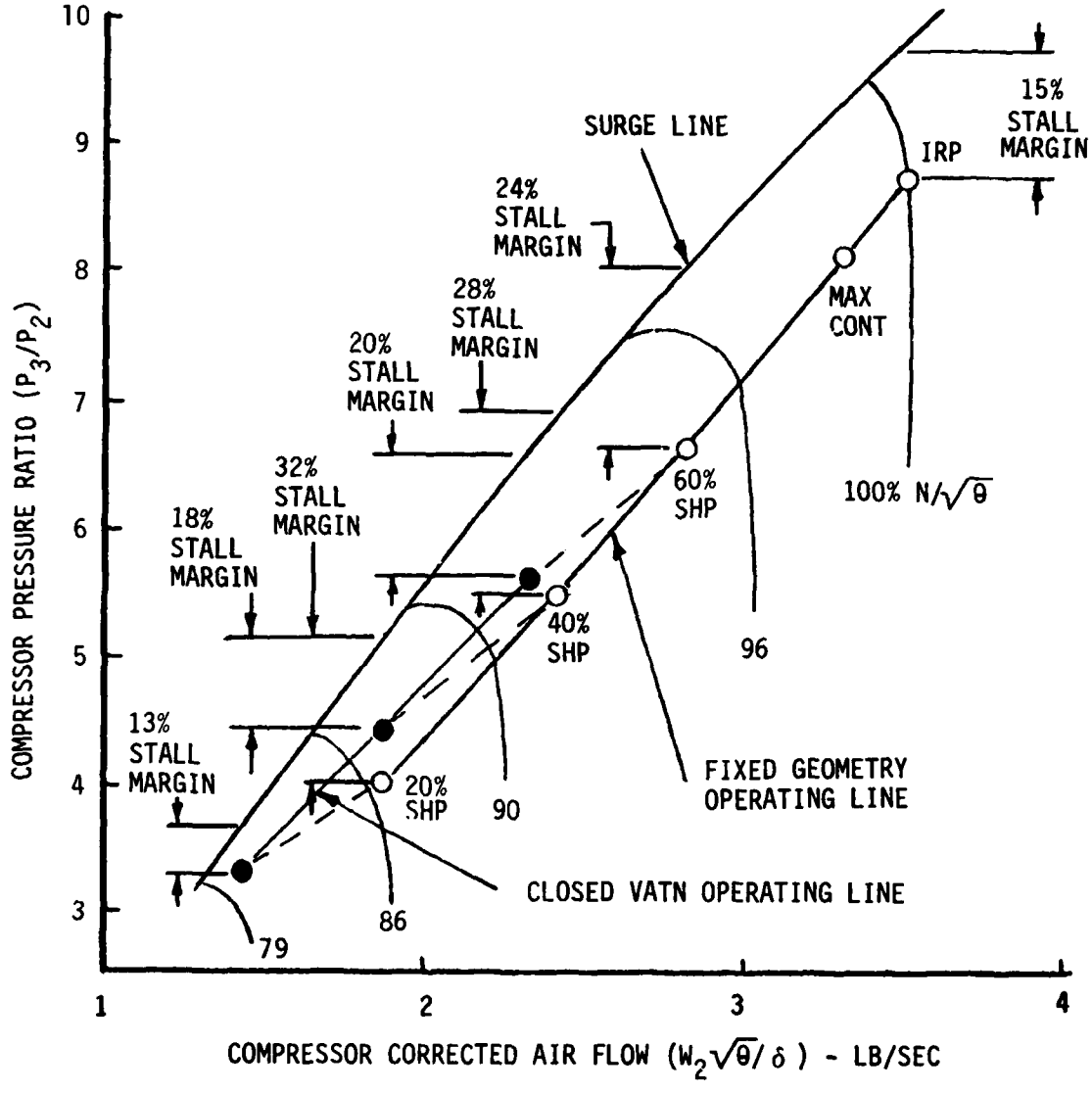

Figure 17. Variable Area Turbine Nozzle Effects on Compressor Operating Line.

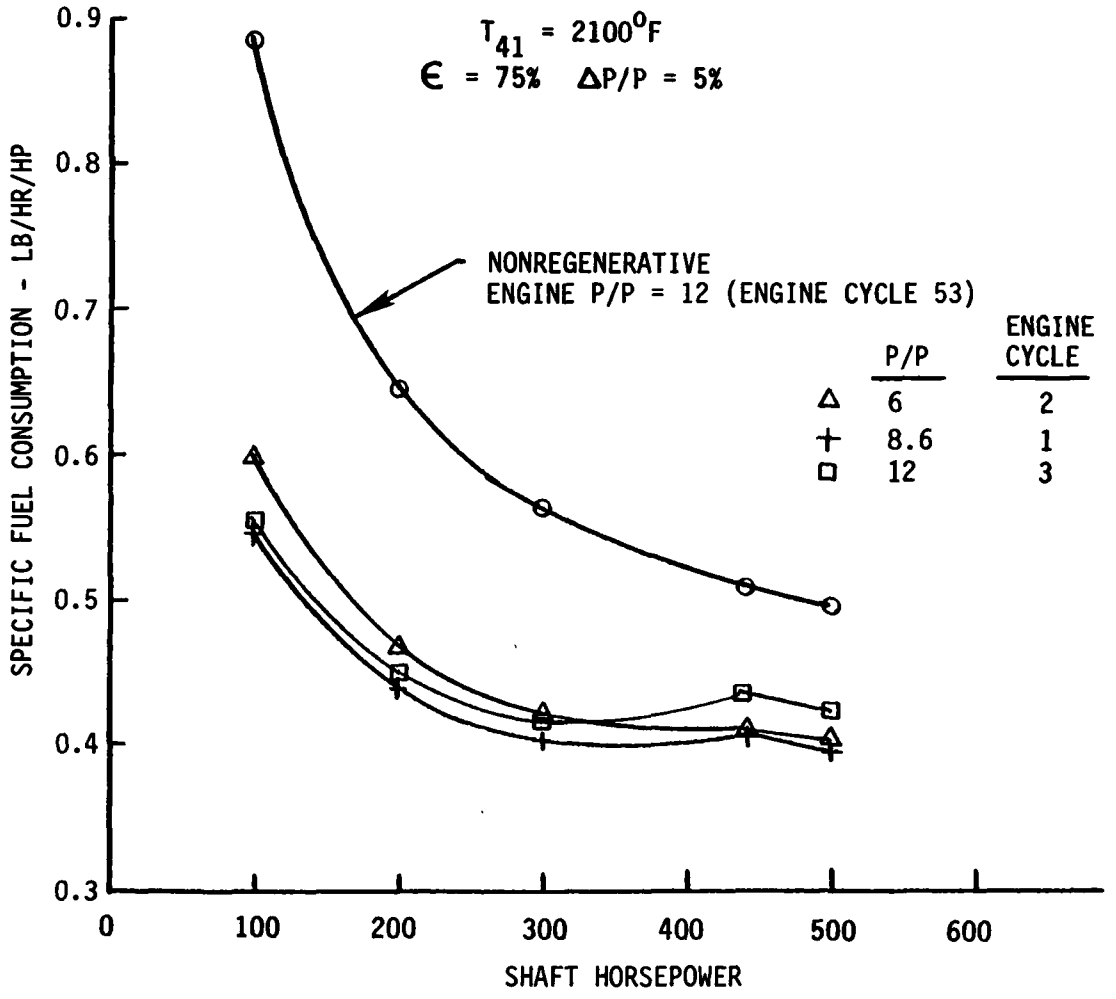

Figure 18. Sea Level Static Operating Line Performance Characteristics - Engine Cycles, 2, 3, and 53.

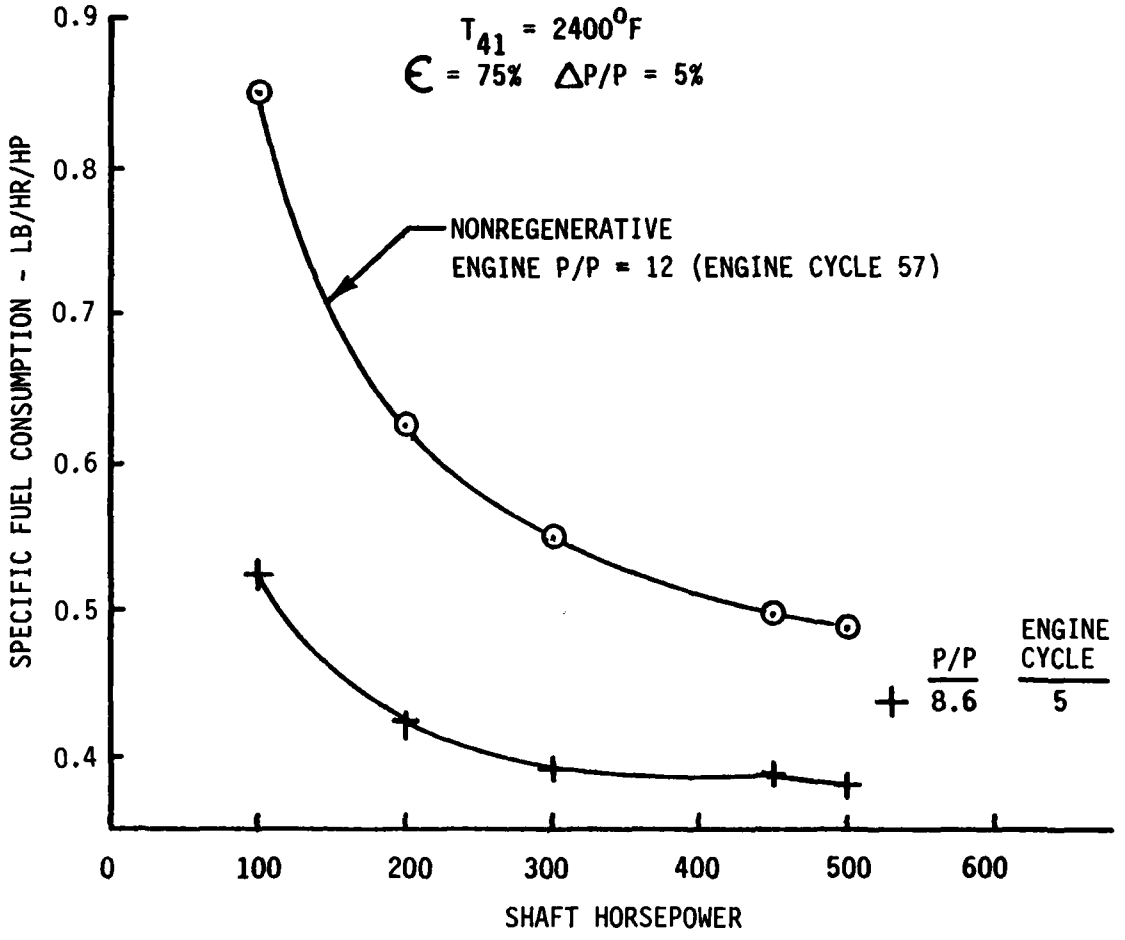

Figure 19. Sea Level Static Operating Line Performance Characteristic - Engine Cycles 5 and 57.

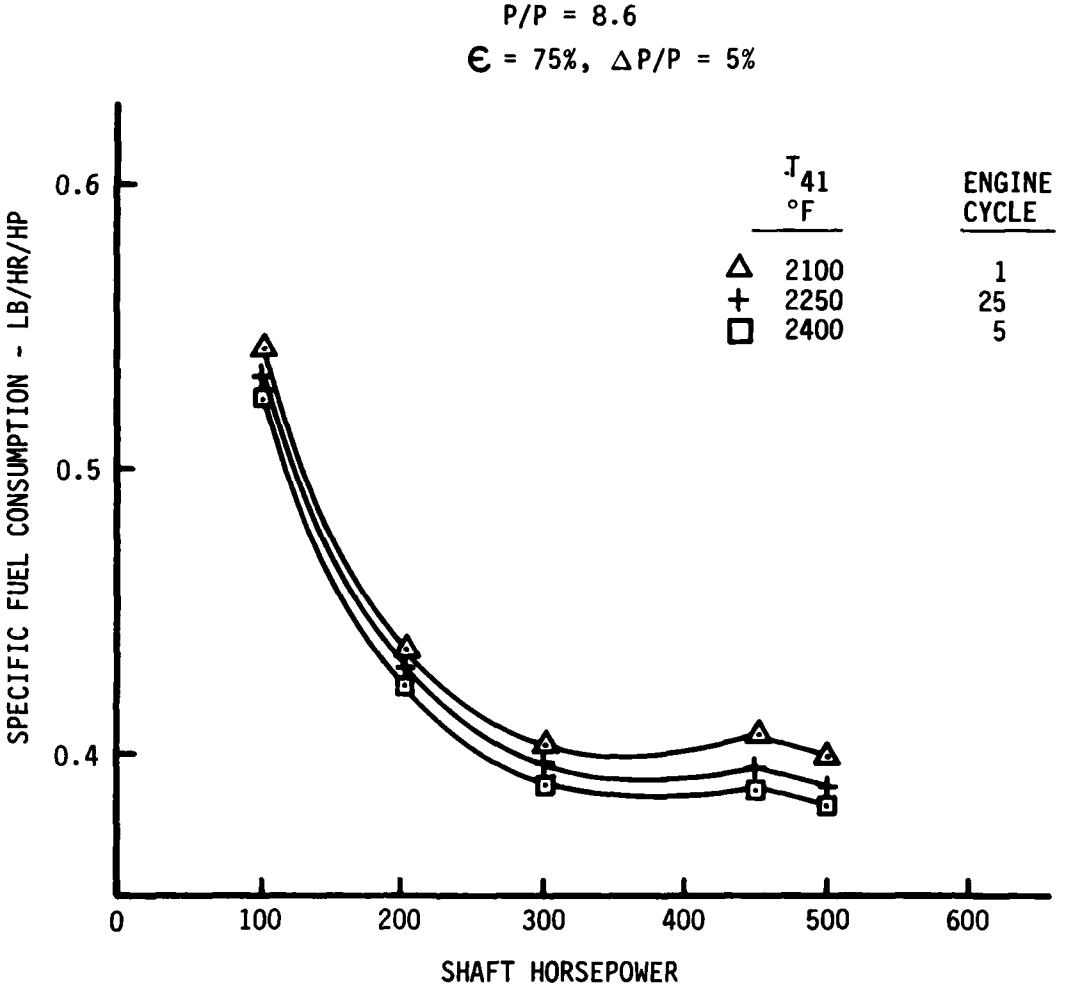

Figure 20. Sea Level Static Operating Line Performance Characteristics - Engine Cycles 1, 5, and 25.

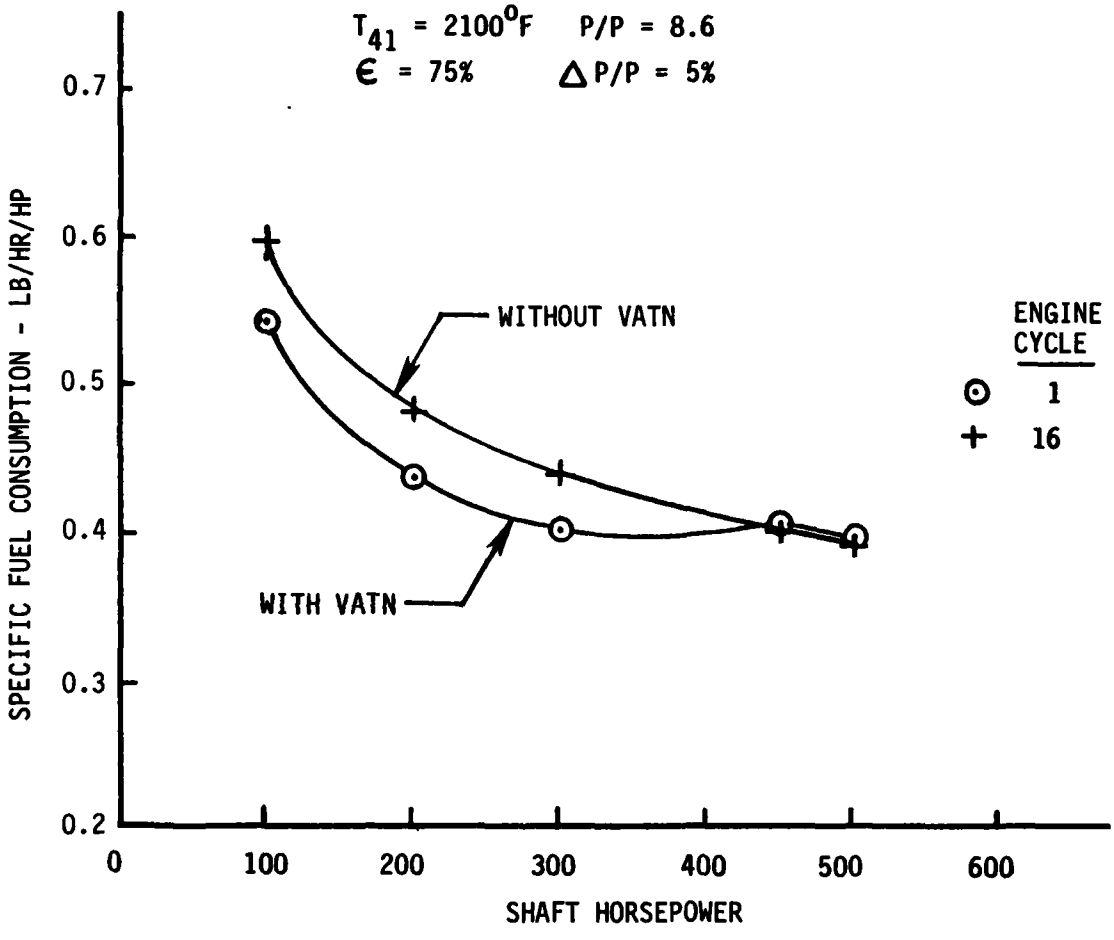

Figure 21. Sea Level Static Operating Line Performance Characteristics - Engine Cycles 1 and 16.

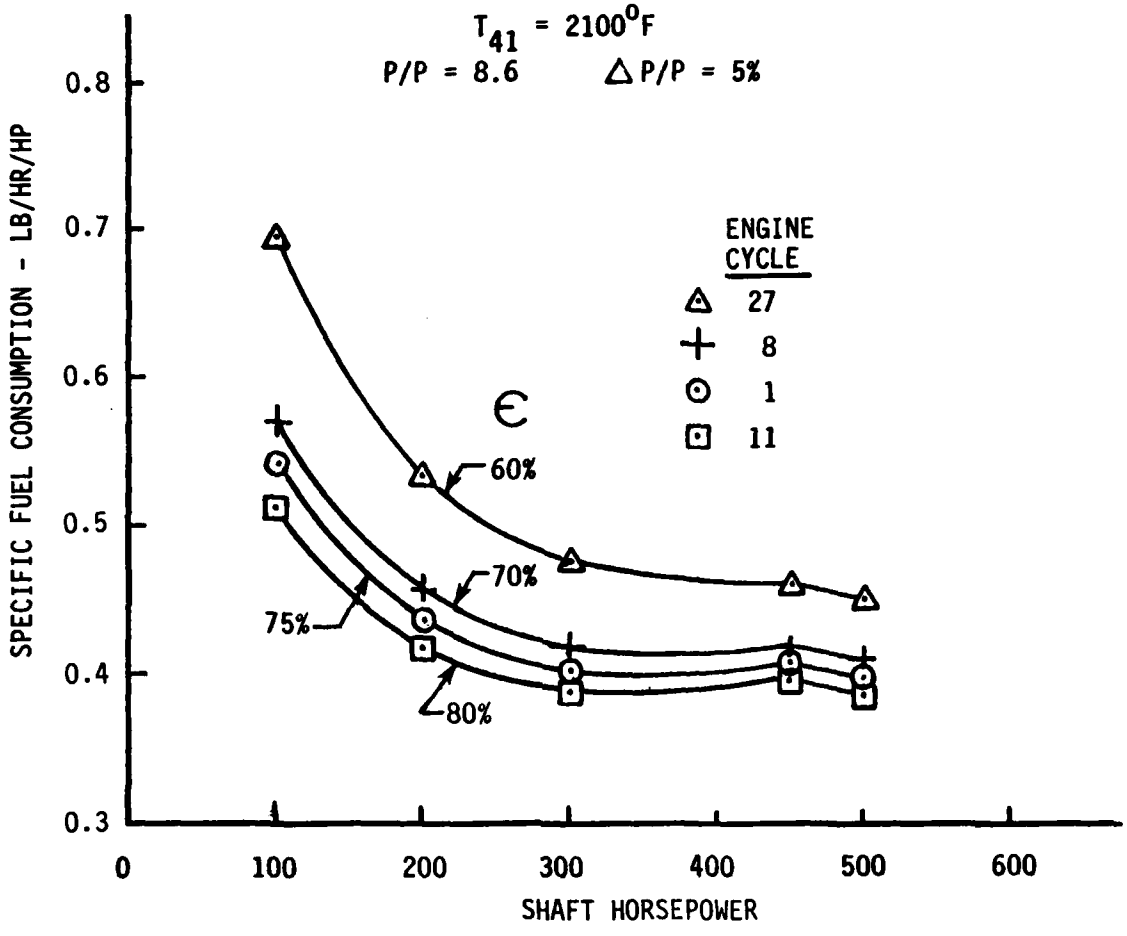

Figure 22. Sea Level Static Operating Line Performance Characteristics - Engine Cycles 1, 8, 11, and 27.

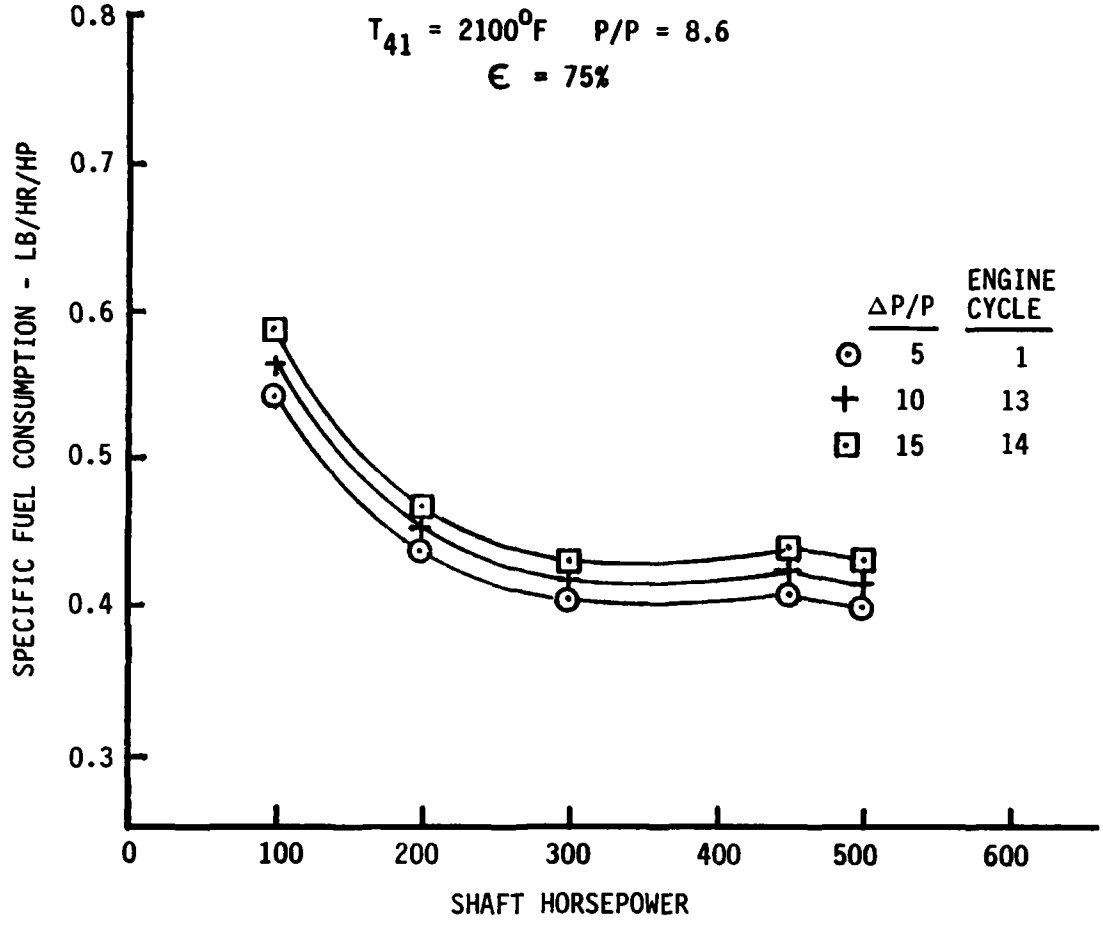

Figure 23. Sea Level Static Operating Line Performance Characteristics - Engine Cycles 1, 13, and 14.

a VATN) has slightly better high power performance due to the higher power turbine efficiency, Engine 1 with a VATN has significantly better low power performance due to the overriding cycle effects noted above.

The effects of regenerator effectiveness and pressure loss are shown in Figures 22 and 23 respectively. As might be expected, SFC continuously improves with the higher effectiveness levels and reduced recuperator pressure loss.

Figure 24 compares a plate-fin recuperator with a tubular recuperator with both configurations sized for 75% effectiveness and 5% pressure loss. The improved performance of the plate and fin configuration at part power is due to the steeper off-design effectiveness characteristic as shown previously (Figure 12).

Performance characteristics of the recuperator bypass system (engine Cycle 19) are compared to the full-time regenerative engine in Figure 25. The loss in SFC at high power is due to the loss in recuperator effectiveness with the bypass valves open while part power performance is comparable to the full time recuperator case since both engines use recuperators sized for the same effectiveness and pressure loss levels.

System payoff for the bypass system will thus depend upon recuperator weight and price reductions that may result from the smaller engine and heat exchanger size.

RECUPERATOR PARAMETRIC STUDY

The two design concepts considered most likely to be successful for aircraft recuperator applications are those involving plate-fin and tubular construction. Figure 26 shows the heat transfer surfaces typically used for each type of construction. Figures 27 and 28 are examples of tubular and plate-fin recuperator cores. The tubular unit shown in Figure 27 uses ring-dimpled tubes to increase the heat transfer coefficient on the inside of the tubes. The plate-fin unit shown in Figure 28 uses very compact offset fins (37 fins per inch) on the air side for the same purpose. The units are typical of the types of design studied for helicopter recuperator application.

For a fixed set of gas and air inlet conditions and allowable pressure drops, recuperator effectiveness is the major performance parameter influencing recuperator size and weight. For the helicopter application, the optimum overall engine cycle can be expected to be in the effectiveness range of 0.7 and 0.8. In this range, tubular recuperators tend to be lighter than corresponding plate-fin units. Their lower weight is caused partly by the simplicity of construction and partly by the excellent inherent pressure containment characteristics associated with tubes. To accomodate the high pressure differentials present between hot and cold fluids in a recuperator, the high-pressure fluid is

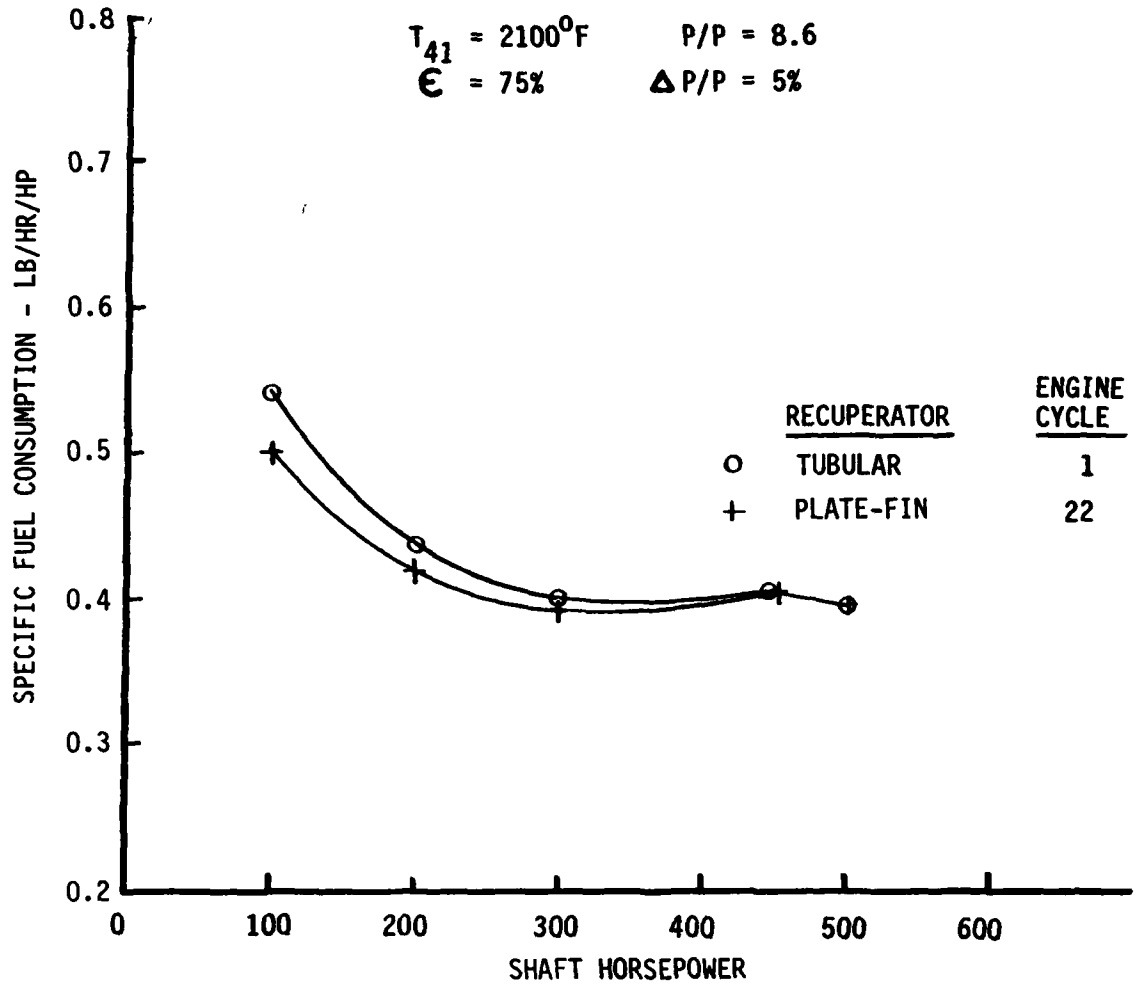

Figure 24. Sea Level Static Operating Line Performance Characteristics - Engine Cycles 1 and 22.

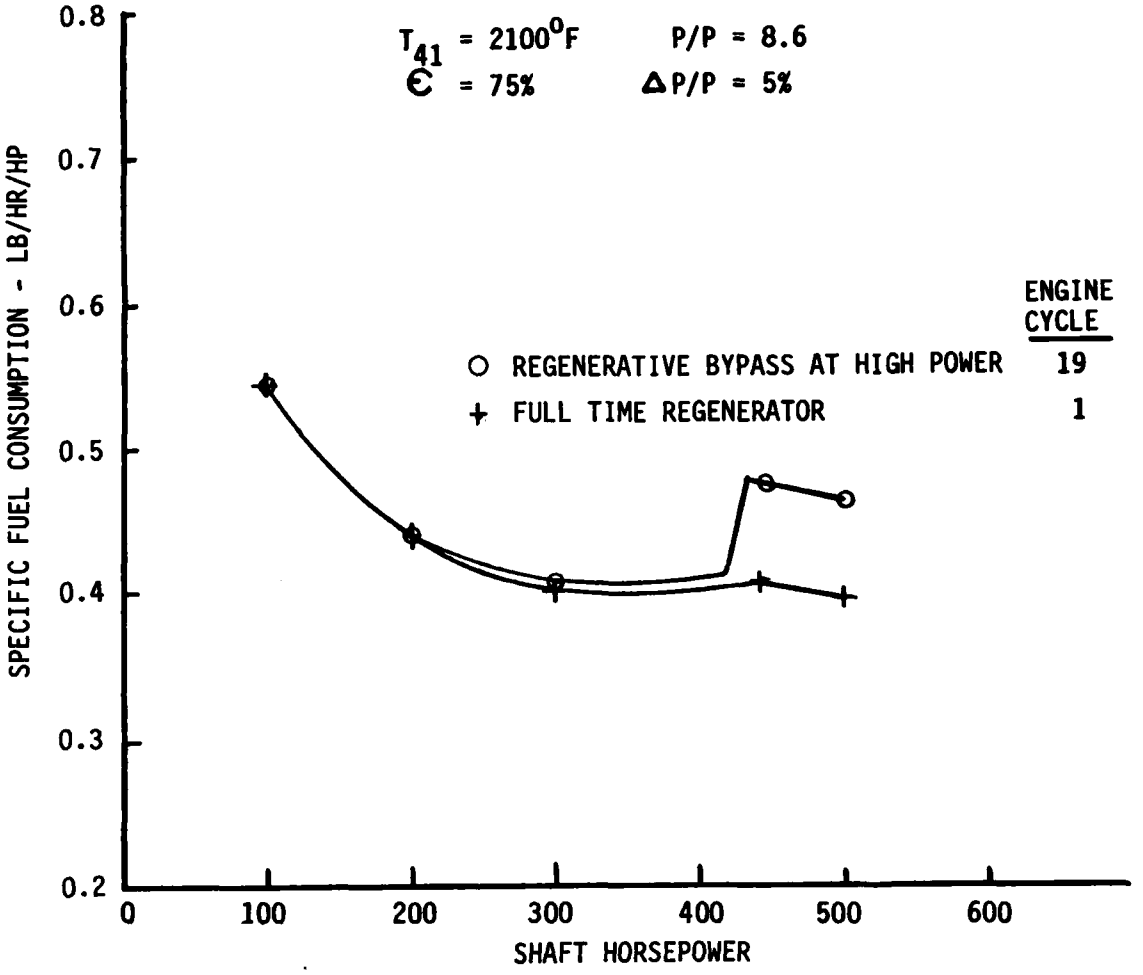

Figure 25. Sea Level Static Operating Line Performance Characteristics - Engine Cycles 1 and 19.

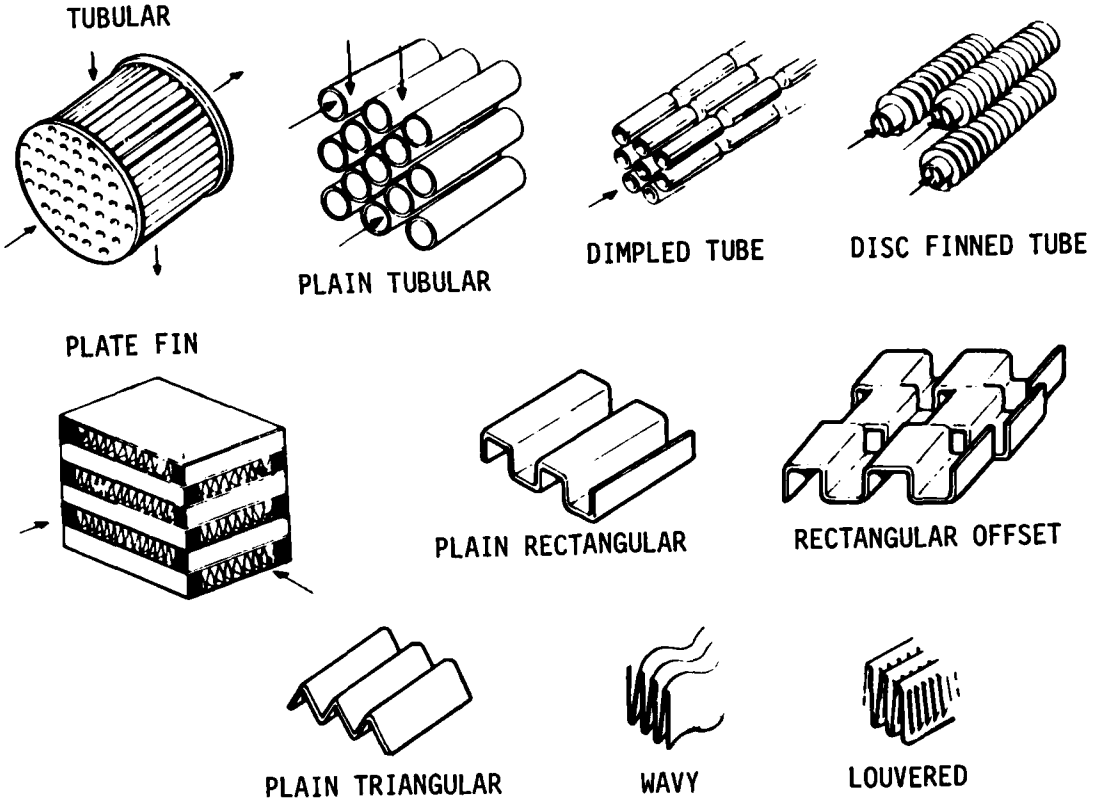

Figure 26. Typical Heat Transfer Surfaces for Tubular and Plate-Fin Construction.

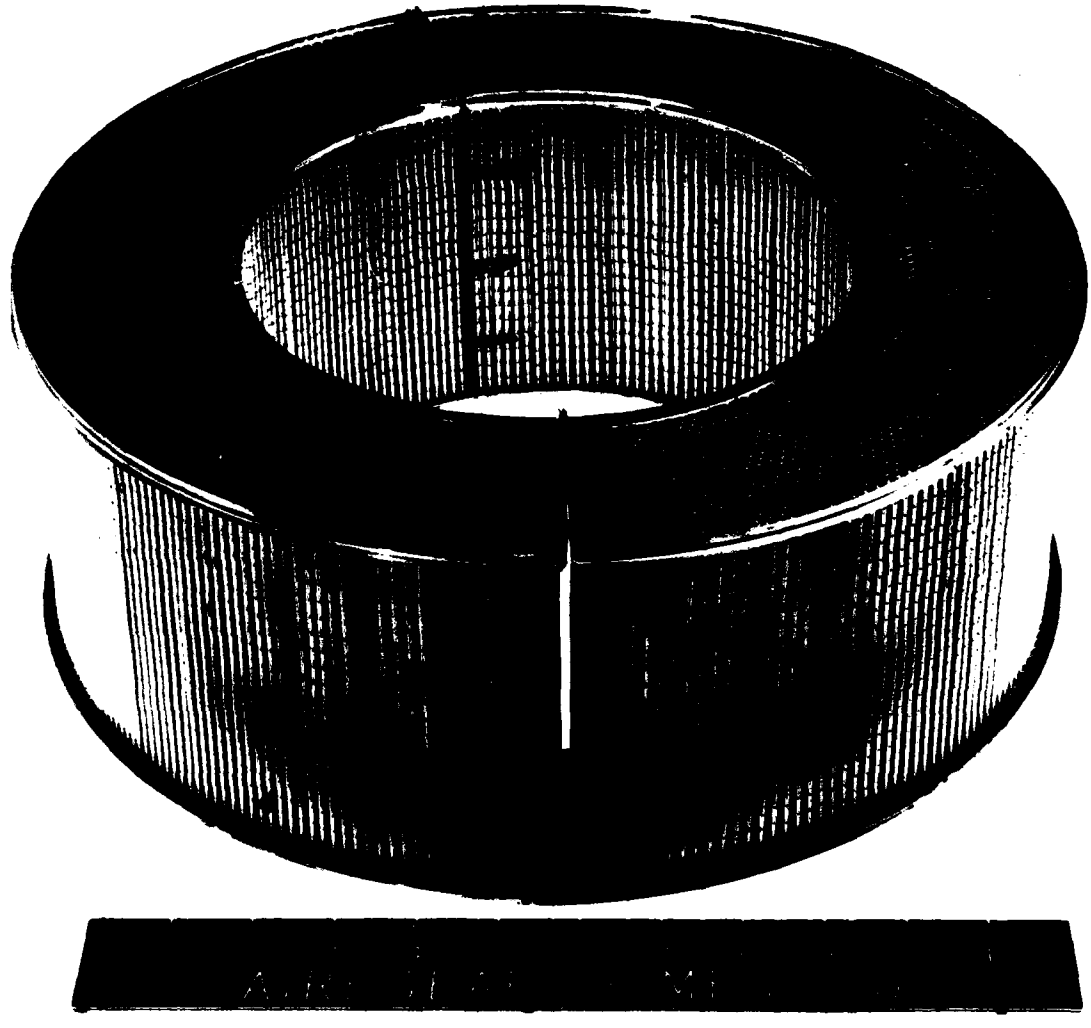

Figure 27. Tubular Regenerator Core Assembly for T63 Engine.

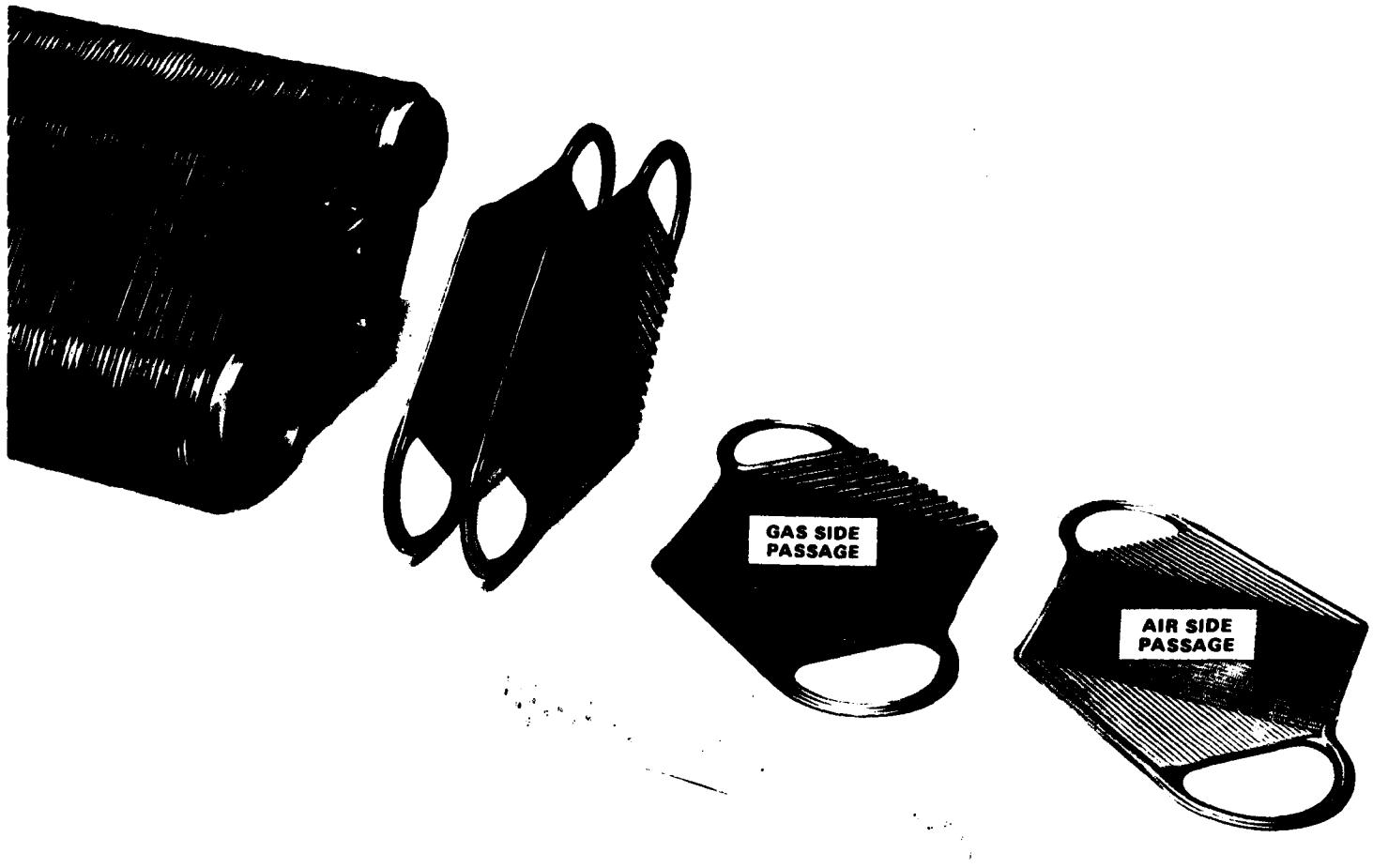

Figure 28. Subassemblies for GT-601 Plate-Fin Recuperator.

made to flow inside a bundle of small diameter tubes, while the low-pressure gas flows over the tubes. In this way, full advantage is taken of the pressure containment capability of tubes, and the weight of the external shell (which does not need to contain a high pressure) is kept low. Furthermore, because of their configuration, tubular heat exchangers can be readily packaged into an annular envelope with efficient use of space.

Although tubular heat exchanger design concepts are simpler than their plate-fin counterparts, they are less compact from a heat transfer surface viewpoint. Even though the tubes can be arranged in a staggered pattern for better heat transfer and their spacing and diameter varied to suit design requirements, tubular units do not offer the flexibility in design geometry afforded by the plate-fin units. The main disadvantage of tubular designs is the poor internal heat transfer coefficient caused by boundary layer buildup. This can be alleviated in part by using ring-dimpled tubes, which cause the boundary layer on the tube inner walls to break up, thus improving heat transfer. Ring-dimpled tubes, however, also result in a penalty in terms of pressure drop. Adding external fins to the tubes seldom results in a smaller, lighter recuperator because the heat transfer to the inside of the tubes controls the design. Thus, essentially the same surface area is available on the air and gas sides of the core.

In plate-fin recuperator construction, the hot and cold fluids are separated by parallel plates. Heat transfer in the fluid passages is enhanced by the presence of fins attached between the plates, and, because passage height and fin geometry can be varied independently for the two fluids, there is considerable flexibility in the heat exchanger design geometry. Near optimum, highly compact designs with balanced heat transfer conductances can thus be achieved.

However, because of the flow arrangement inherent in the plate-fin concept, constraints are placed on the heat exchanger minimum size. Flow distribution and pressure drop requirements dictate a minimum size for the ducting and manifolds leading the hot and cold fluids into and out of the core. In addition, structural considerations impose restrictions on minimum flow length and core aspect ratio, which also adversely affect the recuperator size from a cylindrical packaging viewpoint.

Design Parameters for Tubular Recuperator Configurations

Based on experience with other recuperators, the range of design parameters to be investigated in this study can be reduced to those given in Table 5. Then by parametric evaluation of recuperator designs over this range, the best set of design parameters can be selected. The parametric evaluation was limited to plain tubes and ring-dimpled tubes for the tube bundle arrangements shown in Figure 29. Although other tube configurations such as spiral tubes could have been included in the study, they were not expected to survive the vibration environment.

TABLE 5. TUBULAR RECUPERATOR DESIGN PARAMETER RANGES

Tube Diameter	0.1 to 0.2 inch.
Gas Stream Pressure Loss	20 to 80 percent of total $\Delta P/P$.
Air Manifold Pressure Loss Allowance	5 to 20 percent of total $\Delta P/P$.
Tube Ring-Dimple Geometry	0.03 to 0.08 and plain tube.
Tube Module Arrangement:	
Transverse spacing	1.25 to 2.0 tube diameters.
Longitudinal Spacing	Tube OD.

Figure 30 gives the influence of the ring-dimple geometry as compared with plain tubes. The evaluation was conducted using an average engine design problem statement (engine Cycle 1)--similar results can be expected for the other engines covered by this study. Several design characteristics become apparent upon review of Figure 30. The ring-dimple tubes give recuperators of lighter weight with shorter overall length; the short tube length is beneficial to overall engine CG balance. The number of tubes and core diameter both increase as the dimples get deeper. The number of tubes is an important cost consideration, since the cost increases with the number of tubes. At a ψ (see Figure 29) of 0.05, a near minimum weight is obtained with a reasonable tube count and short overall length.

Figure 31 gives the influence of tube diameter and pressure drop on core diameter, tube length, number of tubes, and tube weight. Here it is shown that smaller tube sizes result in lighter recuperators; however, as the tube size decreases, the number of tubes increases. A realistic choice of tube OD is 0.125 inch for which a lightweight design is achieved at a reasonable tube count. Figure 31 also shows that for lowest weight, the optimum pressure drop split between gas and air sides of the recuperator is around 60 percent of the total $\Delta P/P$ for the gas side (i.e., 60 percent of the total allowable of 5 percent, or 3 percent on the gas side).

- PLAIN TUBE
- RING DIMPLED TUBE ψ =.03, .05, .06, .08

$$\psi = \left(\frac{\delta}{D}\right) \Big/ \sqrt{\frac{S}{D}}$$

WHERE

D = TUBE ID
δ = DIMPLE DEPTH
S = DIMPLE SPACING

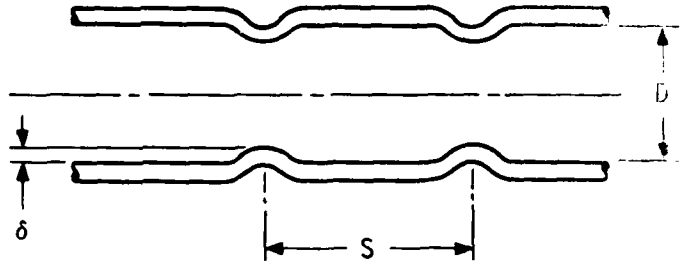

- TUBE BUNDLE ARRANGEMENT

SB 125100
SB 135100
SB 150100
SB 200100

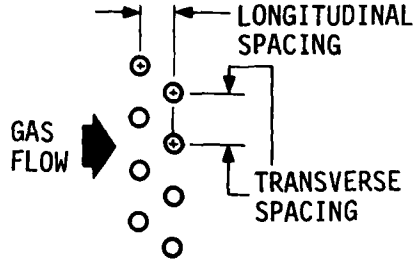

FOR EXAMPLE: SB 125100 = STAGGERED TUBE PATTERN WITH 1.25-INCH TUBE DIAMETER PITCH TRANSVERSE TO FLOW AND 1.0-INCH TUBE DIAMETER IN LONGITUDINAL FLOW DIRECTION.

Figure 29. Tubular Heat Exchanger Surface Geometries.

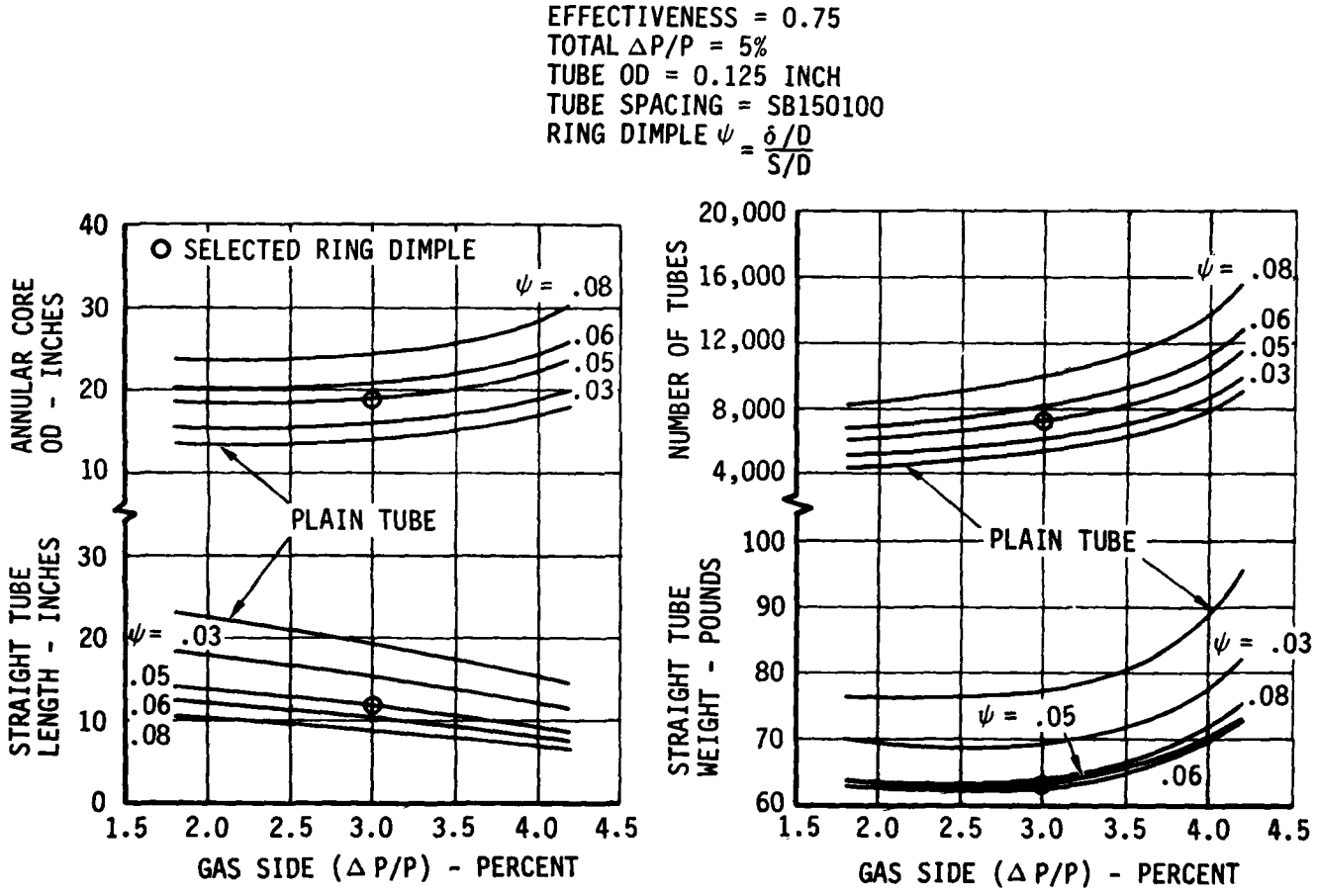

Figure 30. Effect of Tube Ring Dimple on Tubular Recuperator Characteristics.

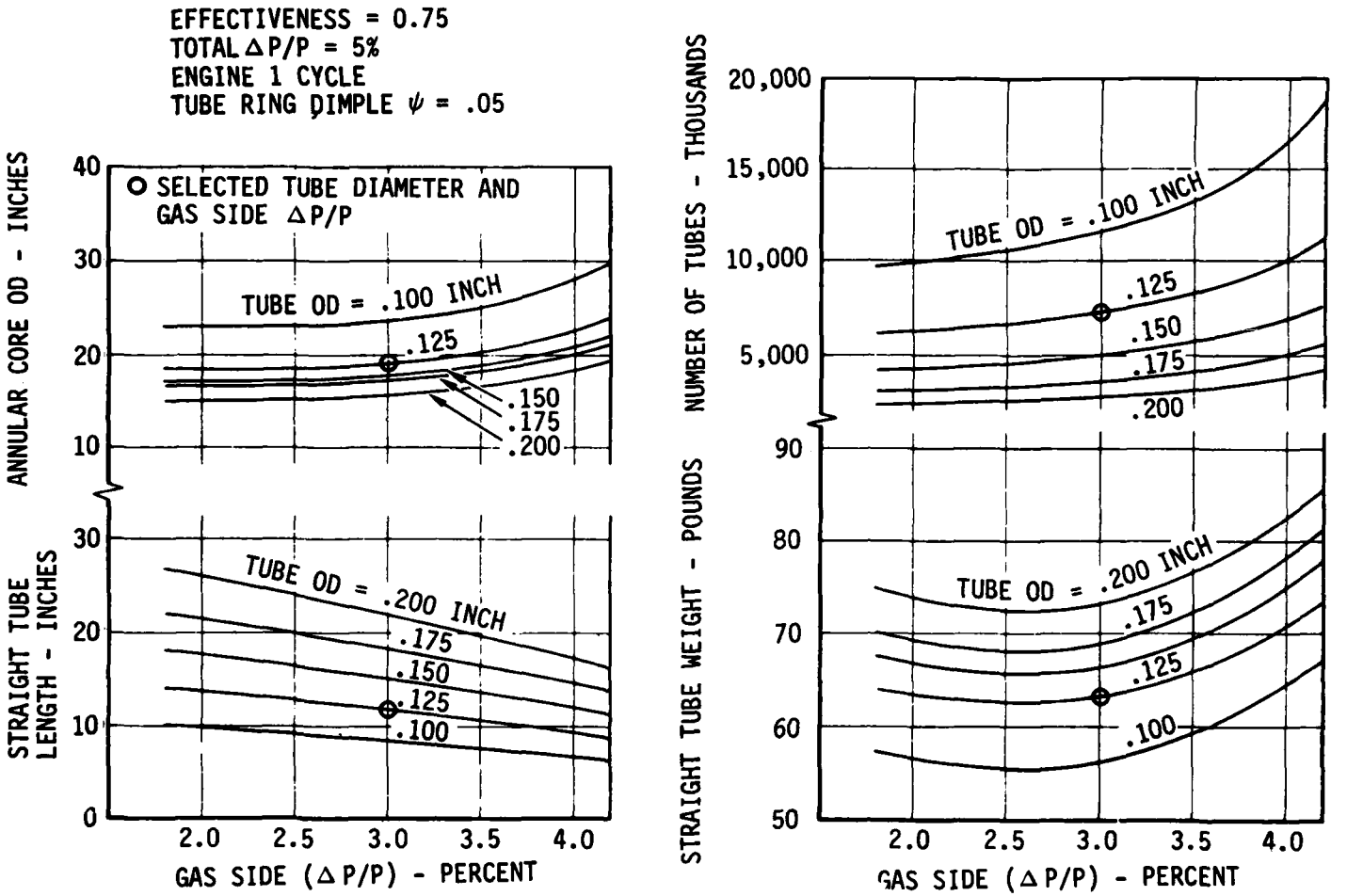

Figure 31. Effect of Pressure Drop and Tube Diameter on Tubular Recuperator Characteristics.

Figure 32 gives the influence of the ratio of transverse tube spacing to tube OD on the major design characteristics of the recuperator. For ratios below 1.5, there is a drastic change in the core diameters caused by the restricted gas flow area over the tubes. At ratios over 1.5, there is a great deal of latitude in selecting the tube spacing.

Based on the results of the parametric study represented in Figures 29 through 32, the parameters given in Table 6 were selected for use in developing recuperator designs for the engines evaluated in this study. The choice of each parameter is based on obtaining a low-weight design that allows cost-effective fabrication.

TABLE 6. SELECTED RECUPERATOR PARAMETER VALUES

Tube Diameter	0.125 inch.
Pressure Drop Used on Gas Stream	60 percent of total $\Delta P/P$.
Air Manifold Pressure Loss Allowance	5 percent of total $\Delta P/P$.
Tube Ring-Dimple Geometry, ψ	0.05
Tube Bundle Arrangement	Varied for each recuperator design.

Plate-Fin Recuperator Characteristics

To provide comparative data for plate-fin and tubular units, the detail characteristics of plate-fin units designed for the engine Cycles 8, 1, and 11 are presented. Each plate-fin unit consists of six modules; the individual module configuration is shown in Figure 33. The detail characteristics are given in Table 7 for each of the three designs. The modules are counterflow with triangular end sections as shown. Six modules are required per engine; these are arranged around the diffuser in an annular package. The air side employs very compact offset fins (37 fins per inch); the gas side also makes use of offset fins with a fin count of 22 fins per inch. Table 8 gives a weight comparison for the plate-fin units and their tubular counterparts. At the lower effectiveness of engine Cycle 8, the weight advantage of the tubular unit is significant. For the 0.8 effectiveness of engine Cycle 11, the weight advantage of the tubular unit is greatly decreased.

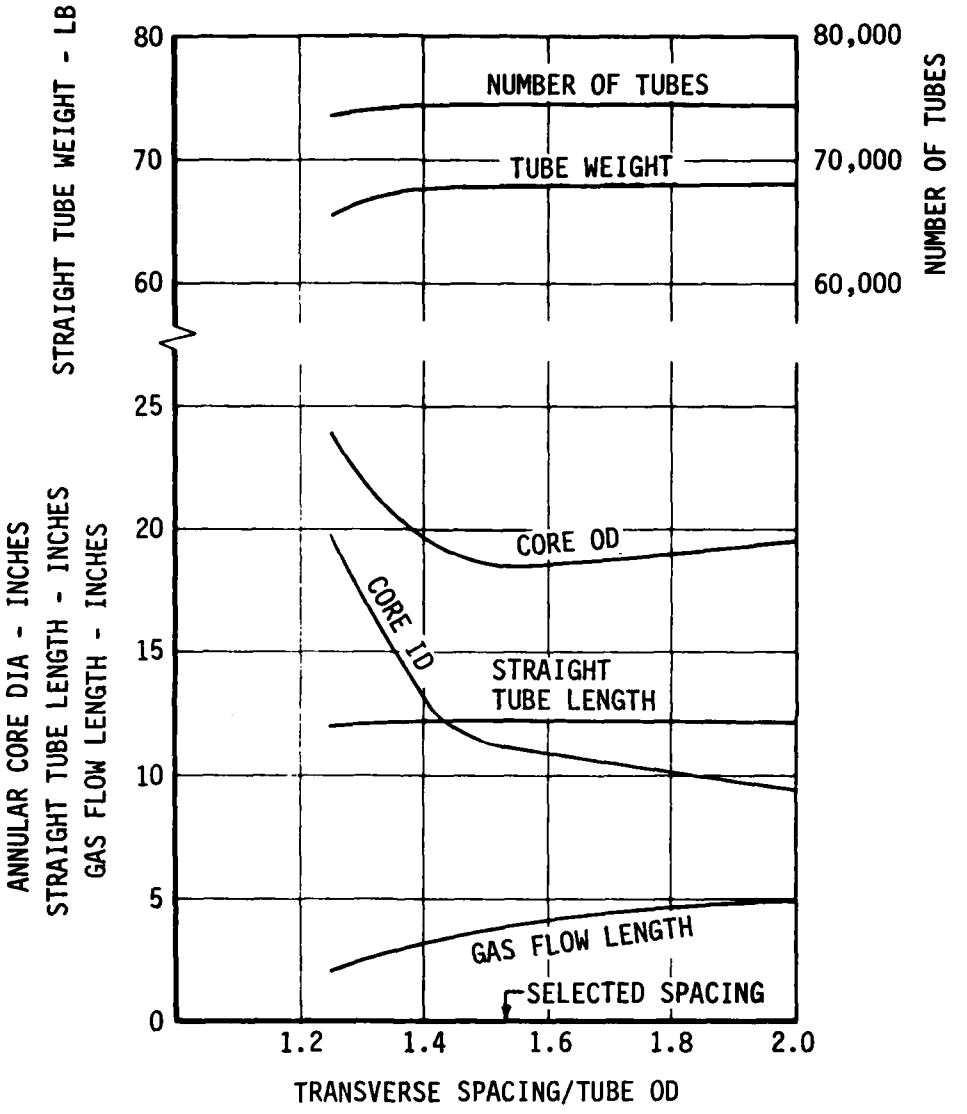

Figure 32. Effect of Tube Bundle Spacing on Tubular Recuperator Characteristics.

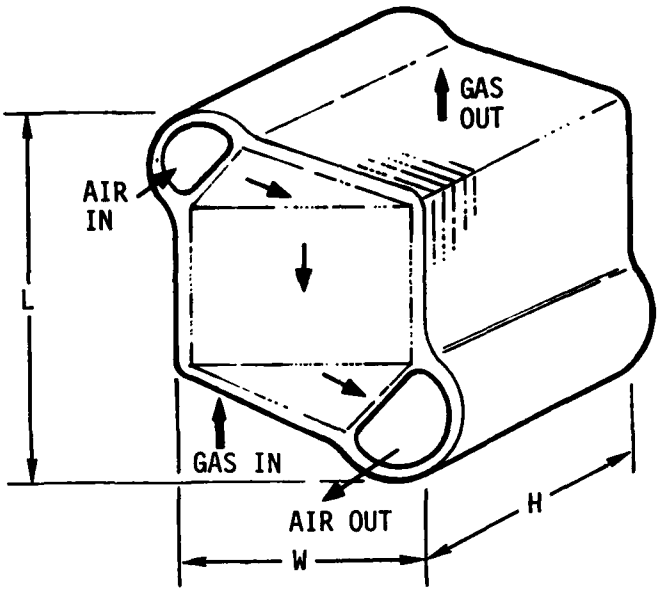

Figure 33. Plate-Fin Module Configuration.

TABLE 7. PLATE-FIN CHARACTERISTICS FOR ENGINE CYCLES 1, 8, AND 11

	Effectiveness		
	0.7	0.75	0.8
Total ΔP/P-percent	5	5	5
Engine Cycle No.	8	1	11
Module			
Width (W) - inches	5.3	5.3	5.3
Length (L) - inches	9.5	10.0	10.5
Stack Height (H) - inches	11.9	12.9	14.5
Weight - lb	22	26	32
Total (6 modules) Weight - Lb*	132	156	192

* Weight is based on stainless steel

TABLE 8. WEIGHT COMPARISON BETWEEN PLATE-FIN AND TUBULAR RECUPERATOR DESIGNS

	Engine Cycle		
	8	1	11
Recuperator Effectiveness	0.70	0.75	0.80
Plate-Fin Design Weight - lb.	132.0	156.0	192.0
Tubular Design Weight - lb.	86.0	125.0	187.0

WEIGHT AND PRICE TRENDS

Component sizing for each of the parametric engines was performed to establish weight and price trends. Recuperator trends based on AiResearch sizing data are shown in Figures 34 through 39.

Recuperator weight and cost for the baseline engine Cycle 1 were estimated at 125 pounds and $46,000 (1979 dollars) based on a total production run of 2500 units.

As shown in Figures 34 and 35, recuperator weight and price decrease with increasing cycle pressure ratio and with increasing cycle temperature. It should be noted that a change in recuperator material was made as a function of the cycle temperature and pressure ratio. While stainless steel can accommodate the hot gas side temperature imposed on the recuperator at 2100°F T_{41} and lower cycle pressure ratios of 8 to 12, the higher T_{41} and the lower cycle pressure ratios imposed a hot gas side temperature in excess of 1300°F, requiring a shift to Inconel for the heat exchanger material. This resulted in a discontinuity in the weight and price trends due to the increased weight and price of Inconel. An upper limit on hot gas side temperature of 1550°F for IN625 was used and found to be adequate for the remainder of the parametric cycles.

Figures 36 and 37 illustrate the relationships between recuperator weight and price and recuperator design requirements. As found in previous studies[1], weight and price are strong functions of both effectiveness and pressure loss.

1. McDonald, Colin F., STUDY OF LIGHT-WEIGHT INTEGERAL REGENERATIVE GAS TURBINES FOR HIGH PERFORMANCE. The Garrett Corp, AiResearch Manufacturing Co., USAAVLABS Technical Report 70-39, U.S. Army Aviation Material Laboratories, Fort Eustis, Virginia, August 1970, AD877464.

TUBULAR RECUPERATORS

$\Delta P/P = 5\%$

$\epsilon = 75\%$

HEAT EXCHANGER MATERIAL	347SS	IN625
ENGINE CYCLE	1,3	2, 4, 5, 6

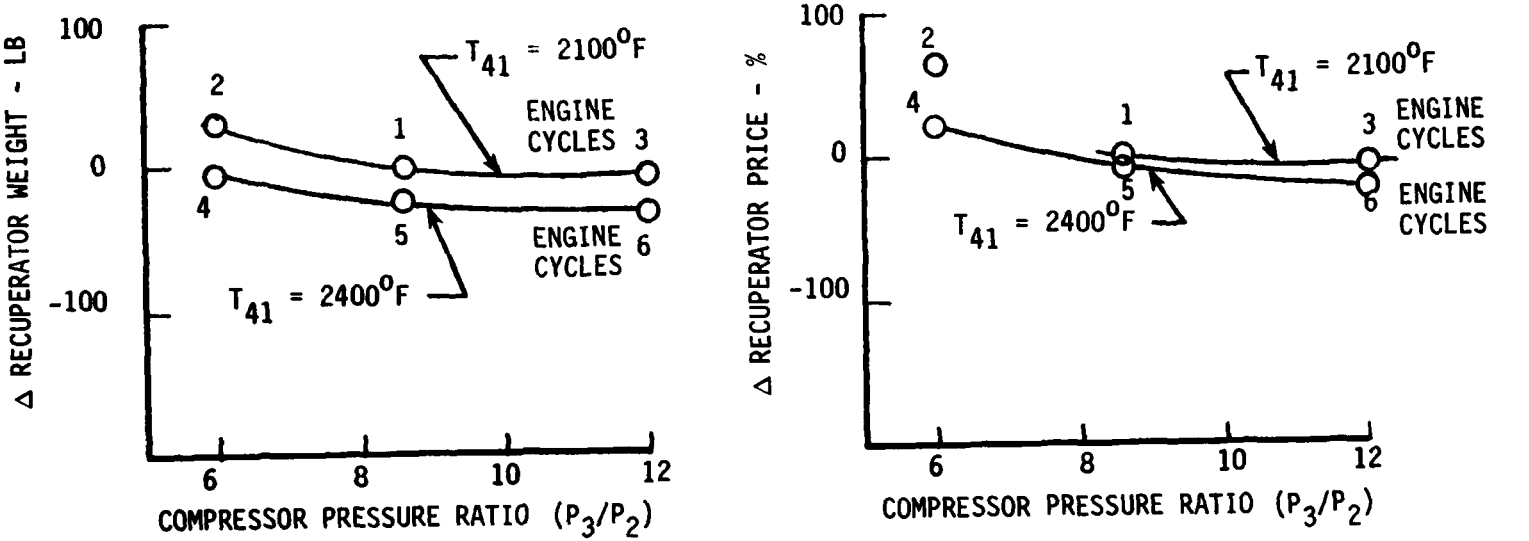

Figure 34. Cycle Pressure Ratio Effects on Recuperator Weight and Price - Cycles 1 through 6.

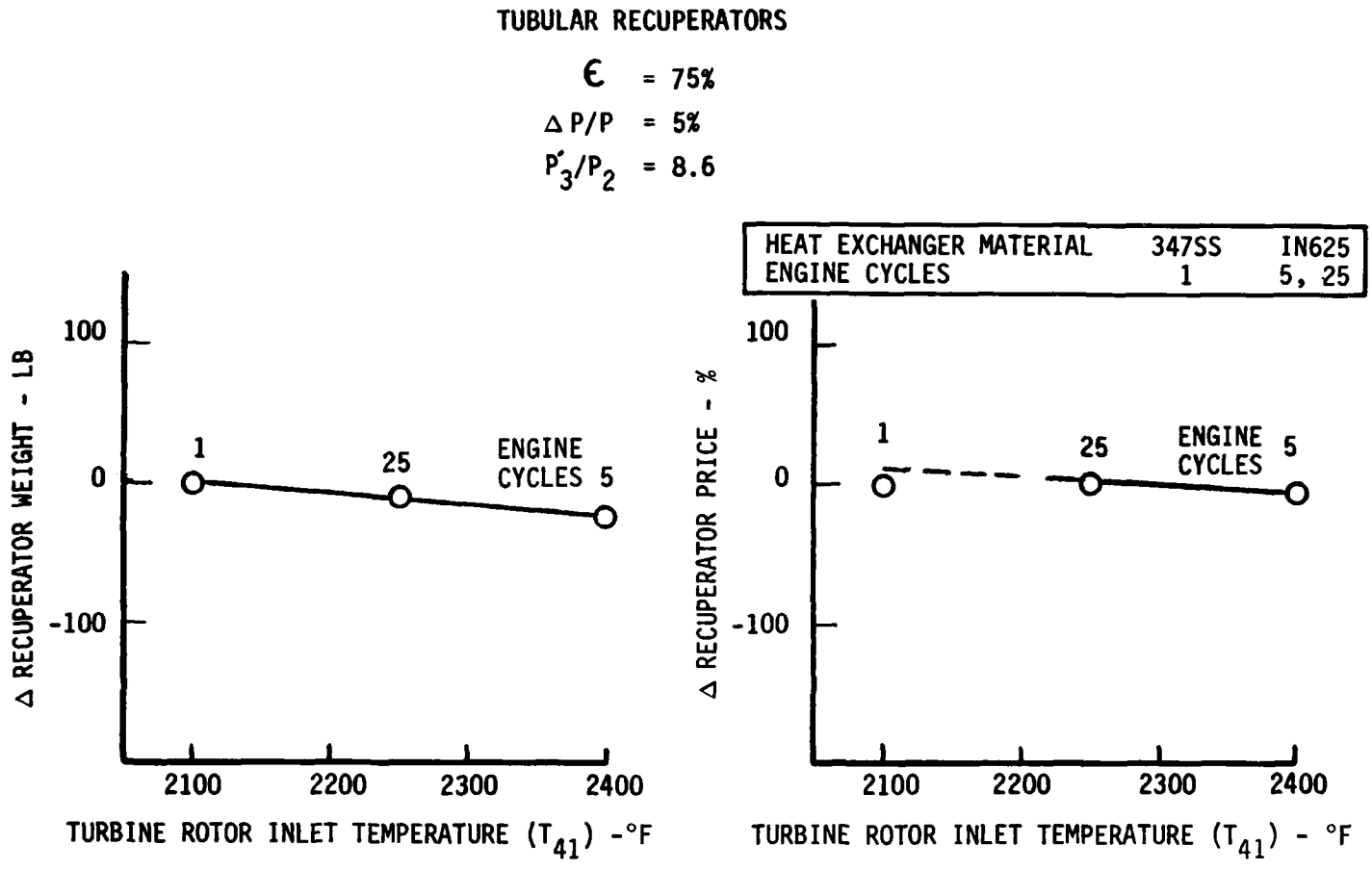

Figure 35. **Cycle Temperature Effects on Recuperator Weight and Price - Cycles 1, 5, and 25.**

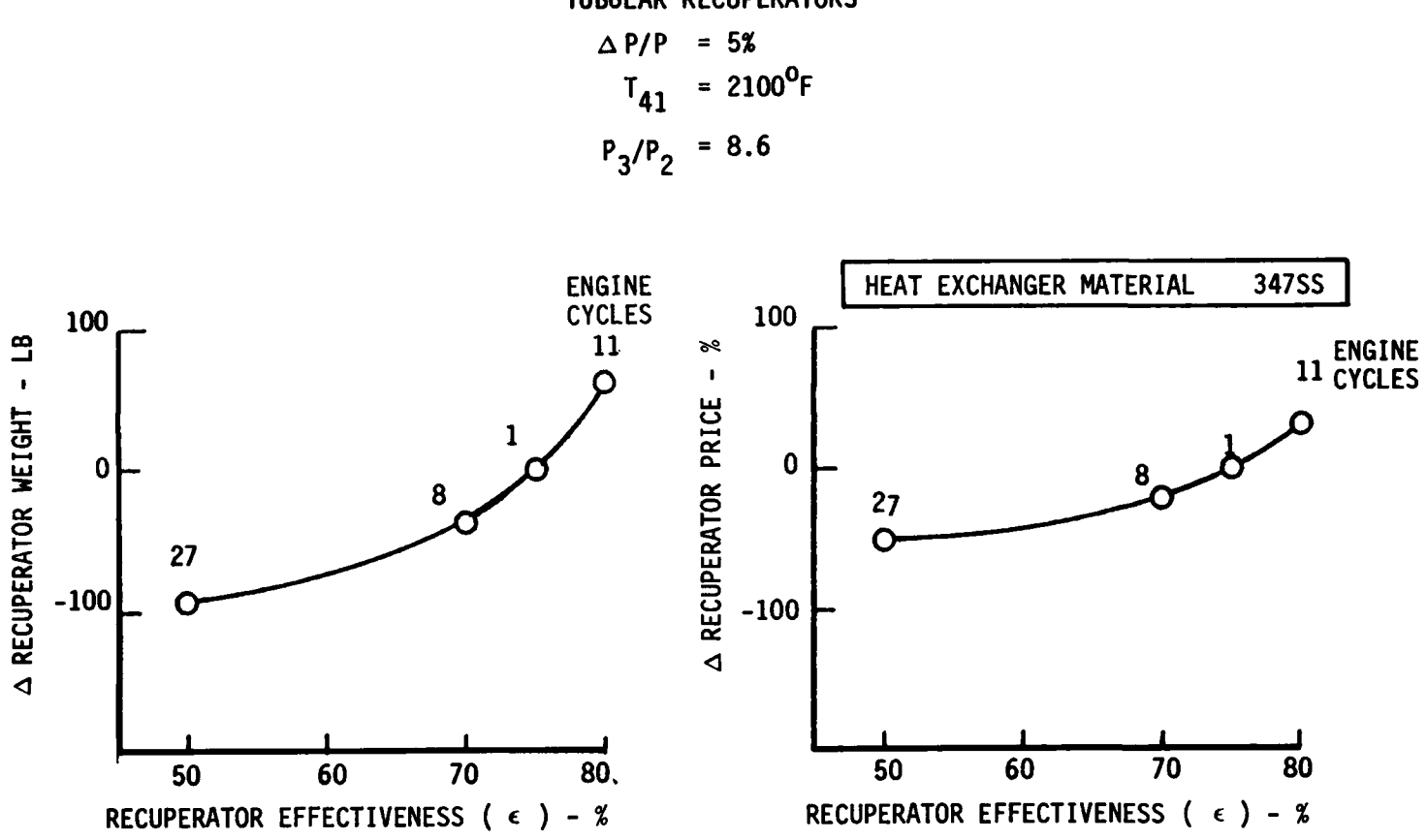

Figure 36. Recuperator Weight and Price Variation With Effectiveness - Engine Cycles 1, 8, 11, and 27.

TUBULAR RECUPERATORS

ϵ = 75%

T_{41} = 2100°F

P_3/P_2 = 8.6

HEAT EXCHANGER MATERIAL 347SS

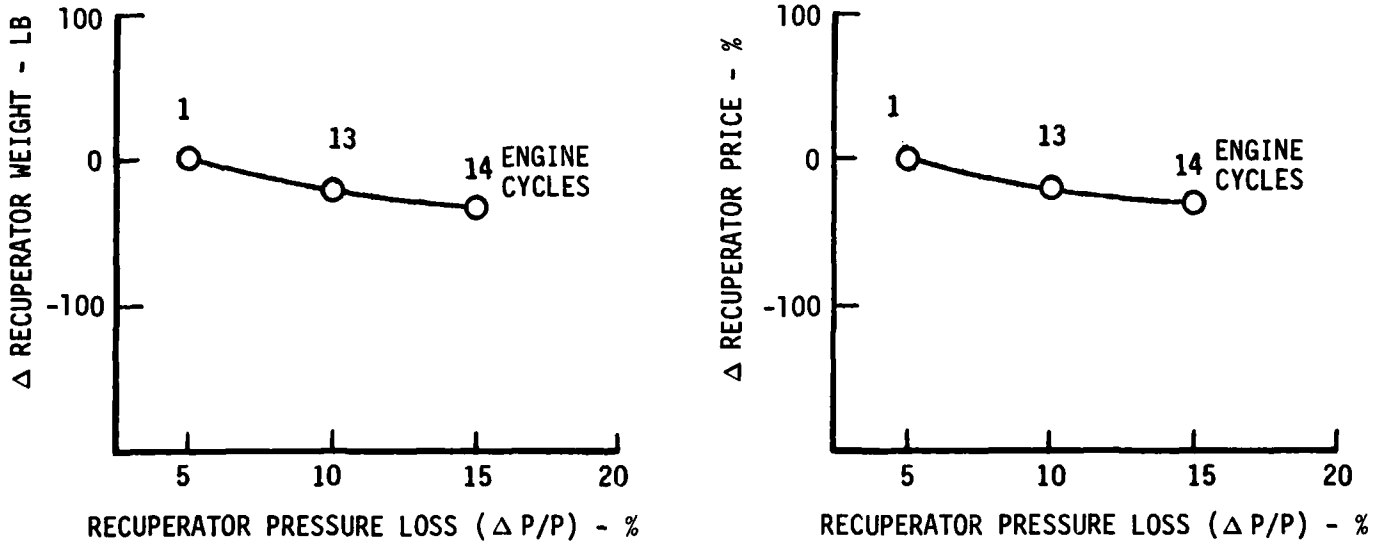

Figure 37. Recuperator Pressure Loss Effects on Recuperator Weight and Price - Cycles 1, 13, and 14.

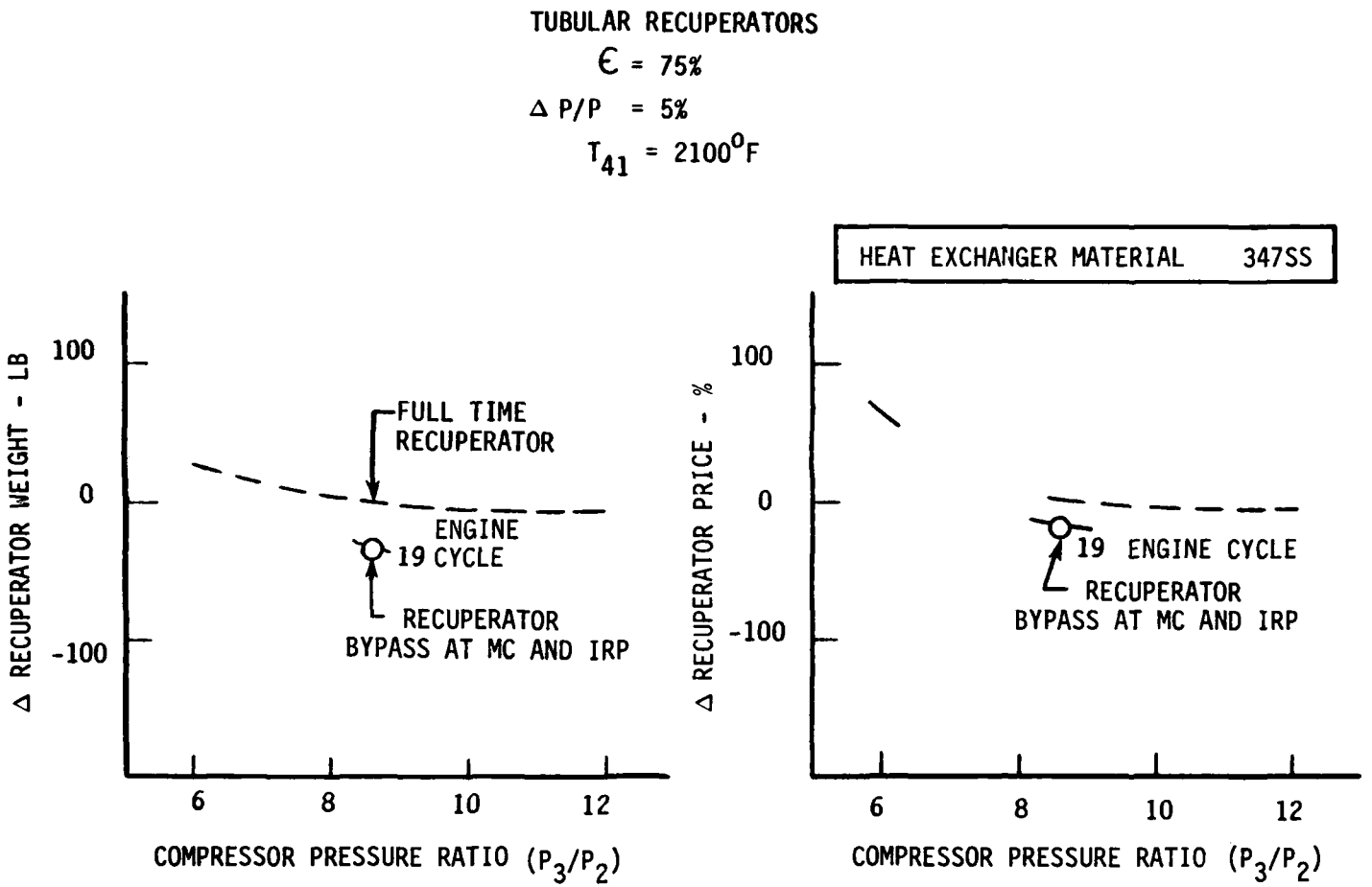

Figure 38. Recuperator Bypass Effects on Recuperator Weight and Price - Cycle 19.

$P_3/P_2 = 8.6$
$T_{41} = 2100^{o}F$
$\Delta P/P = 5\%$

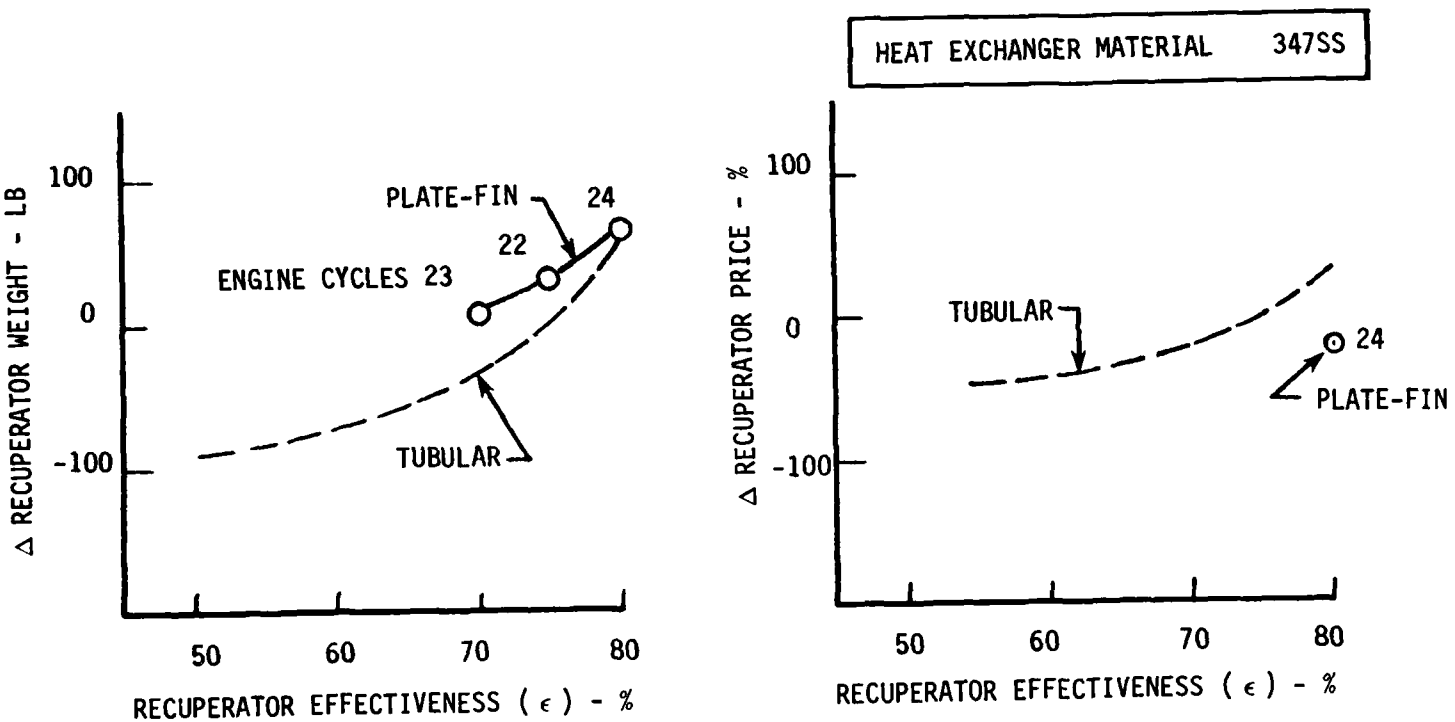

Figure 39. Effect of Recuperator Type on Recuperator Weight and Price - Cycles 22, 23, and 24.

Figure 38 shows the weight and price reduction achieved by sizing the recuperator at part power and bypassing it at high power.

Figure 39 compares weight and price trends of plate-fin recuperators with tubular configurations. As shown, the plate-fin units are heavier than comparable tubular configurations at effectiveness levels below 80% but have a price advantage

Overall engine performance, weight, and price trends are summarized in Figures 40 through 47.

Cycle pressure ratio and cycle temperature trends are shown in Figure 40 and 41. Study results show that high cycle temperature provides the best performance and lowest weight and cost while there is an optimum cycle pressure ratio which varies with T_{41}.

Recuperator design parameter trends are shown in Figures 42 and 43. With the opposing trends of performance and weight-price, it is clear that the proper choice of recuperator design parameters will be mission dependent.

Similar comments apply to VATN payoff as shown in Figures 44 and 45 to the benefit of a recuperator bypass system (Figure 46) and to the comparison of plate-fin versus tubular recuperator configurations (Figure 47).

Maintenance cost estimates were also made for each of the parametric engines using a maintenance cost model summarized in Table 9. This model relates maintenance cost to component price and a parts index defined as the cost equivalent of the number of times a component is repaired or replaced. Labor costs as well as parts costs are included and cycle parameters of pressure ratio and temperature are considered since component price and parts index are both a function of these variables. Since there is no directly applicable data to establish recuperator maintenance costs, the heat exchanger was treated as a hot frame.

TABLE 9. MAINTENANCE COST MODEL

Maintenance Cost = Material + Labor

Material/Labor Cost Ratio = 70/30%

$$\text{Material Cost} = \sum_{i=1}^{N} PI\ (i) \times \text{Price}\ (i)$$

Where Price (i) = Price of ith Component

PI (i) = Cost equivalent of number of times component is replaced or repaired during life of engine. Based on field experience and application severity factor.

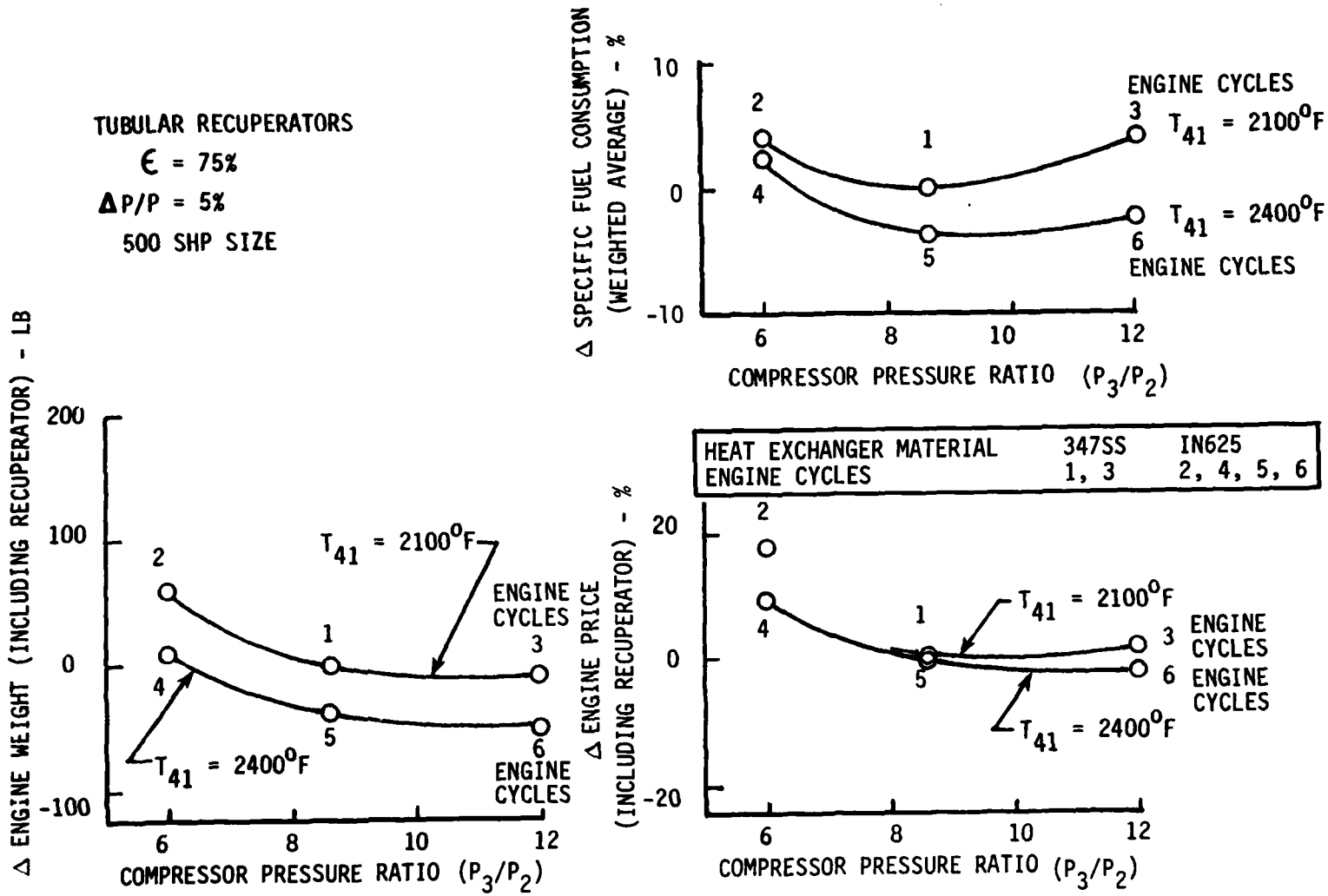

Figure 40. Specific Fuel Consumption, Weight, and Price Trends With Cycle Pressure Ratio.

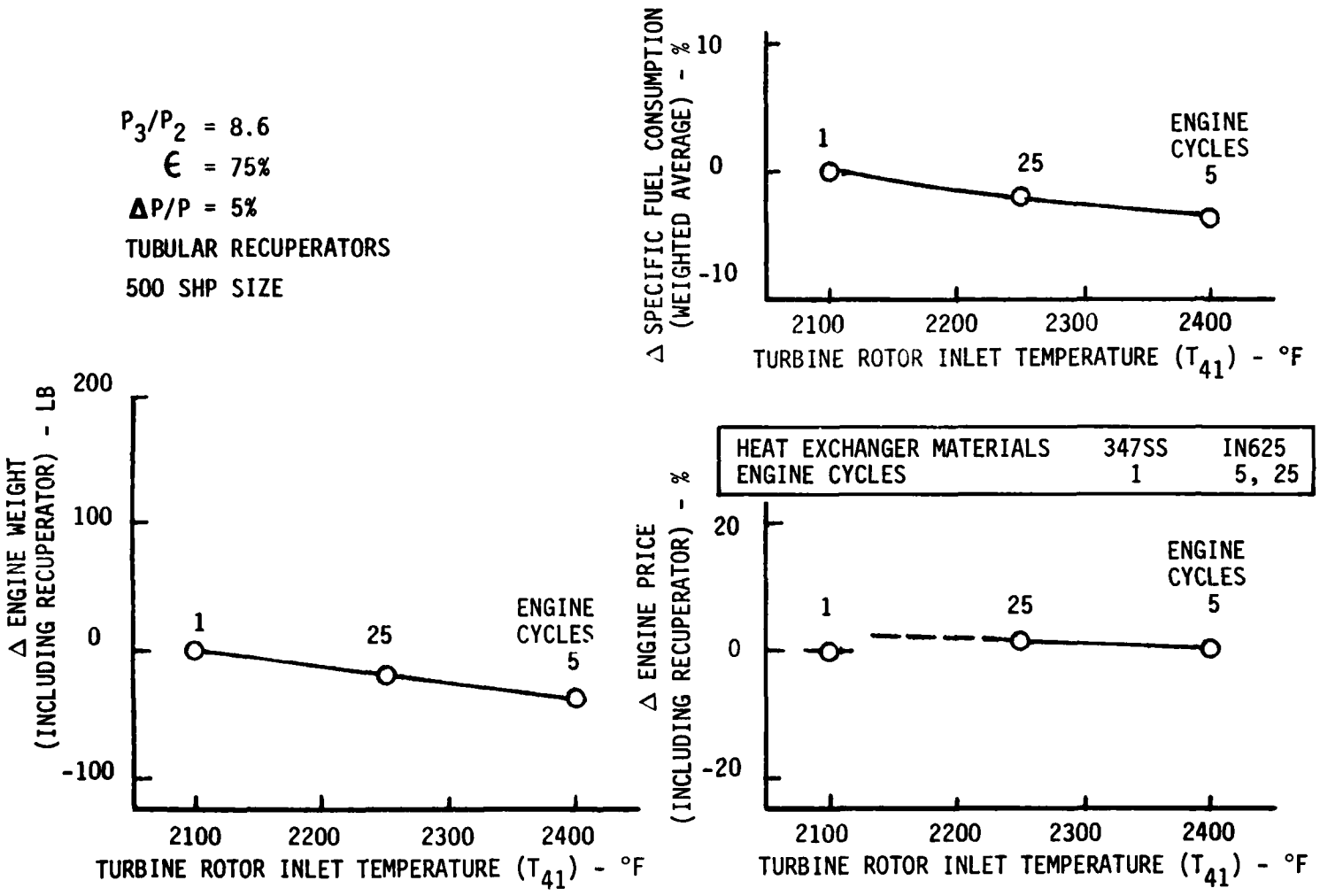

Figure 41. Specific Fuel Consumption, Weight, and Price Trends With Cycle Temperature.

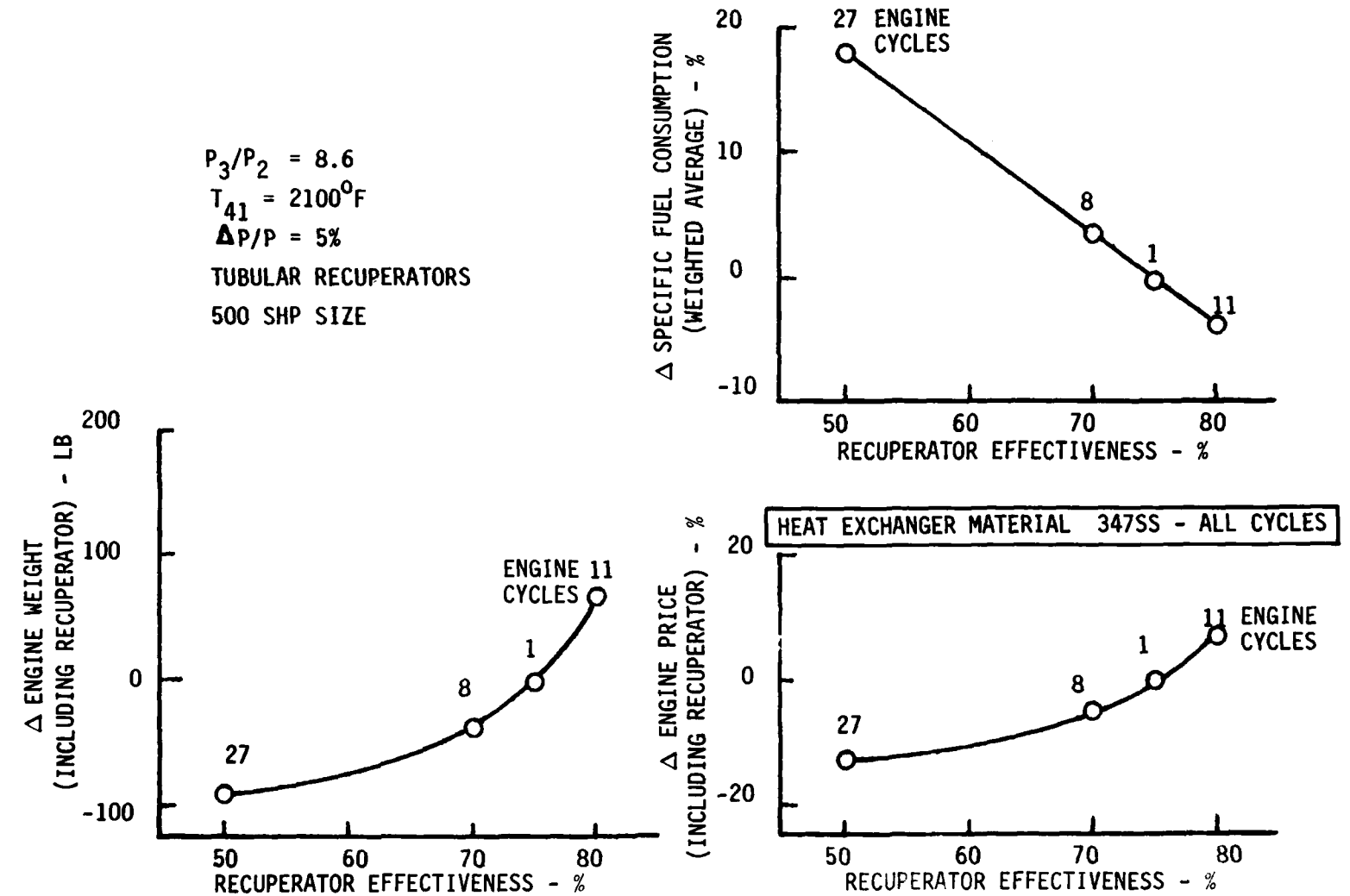

Figure 42. Specific Fuel Consumption, Weight, and Price Trends With Recuperator Effectiveness.

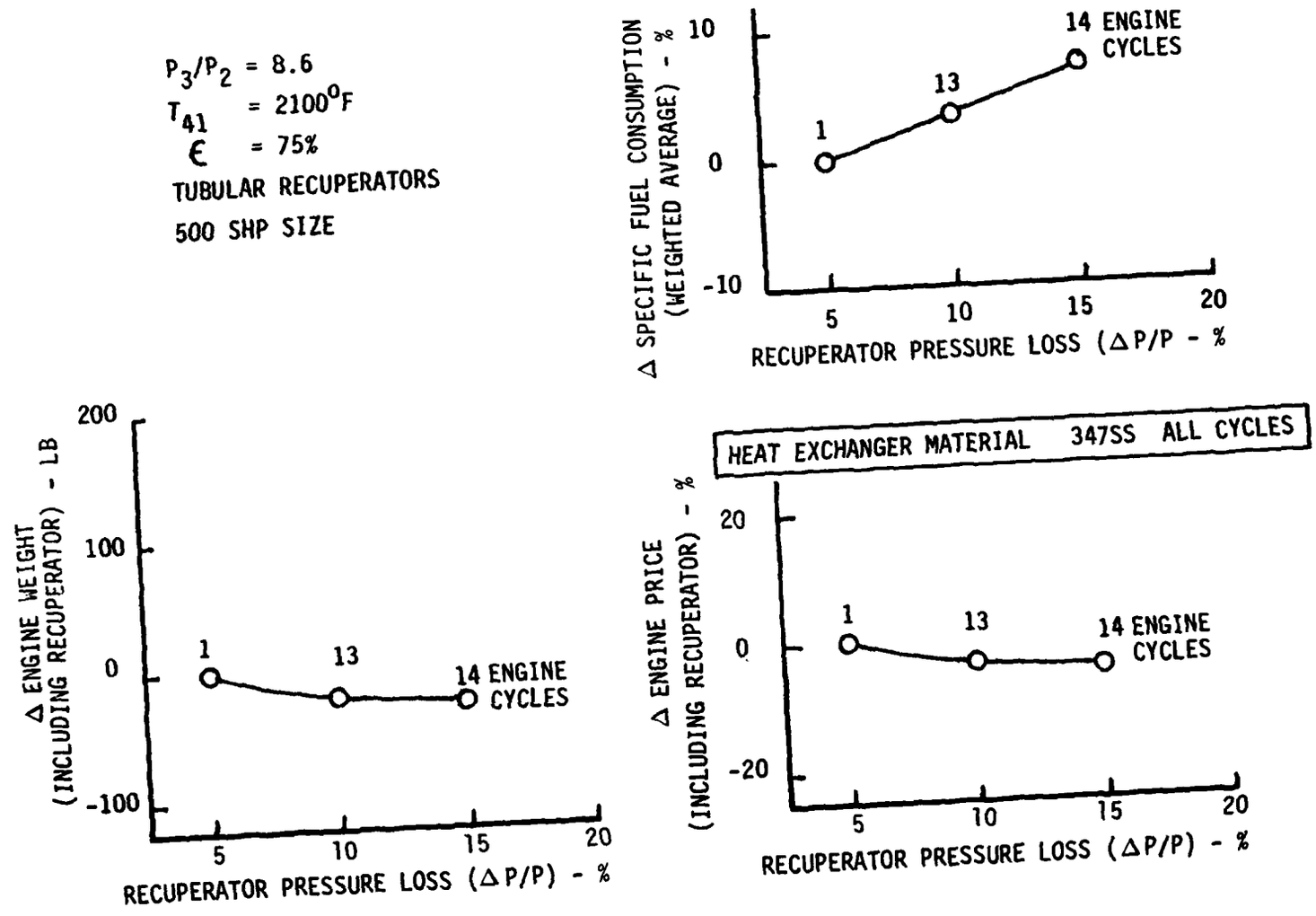

Figure 43. Specific Fuel Consumption, Weight, and Price Trends Witn Weight, and Price Trends - Cycles 15, 16, and 17.

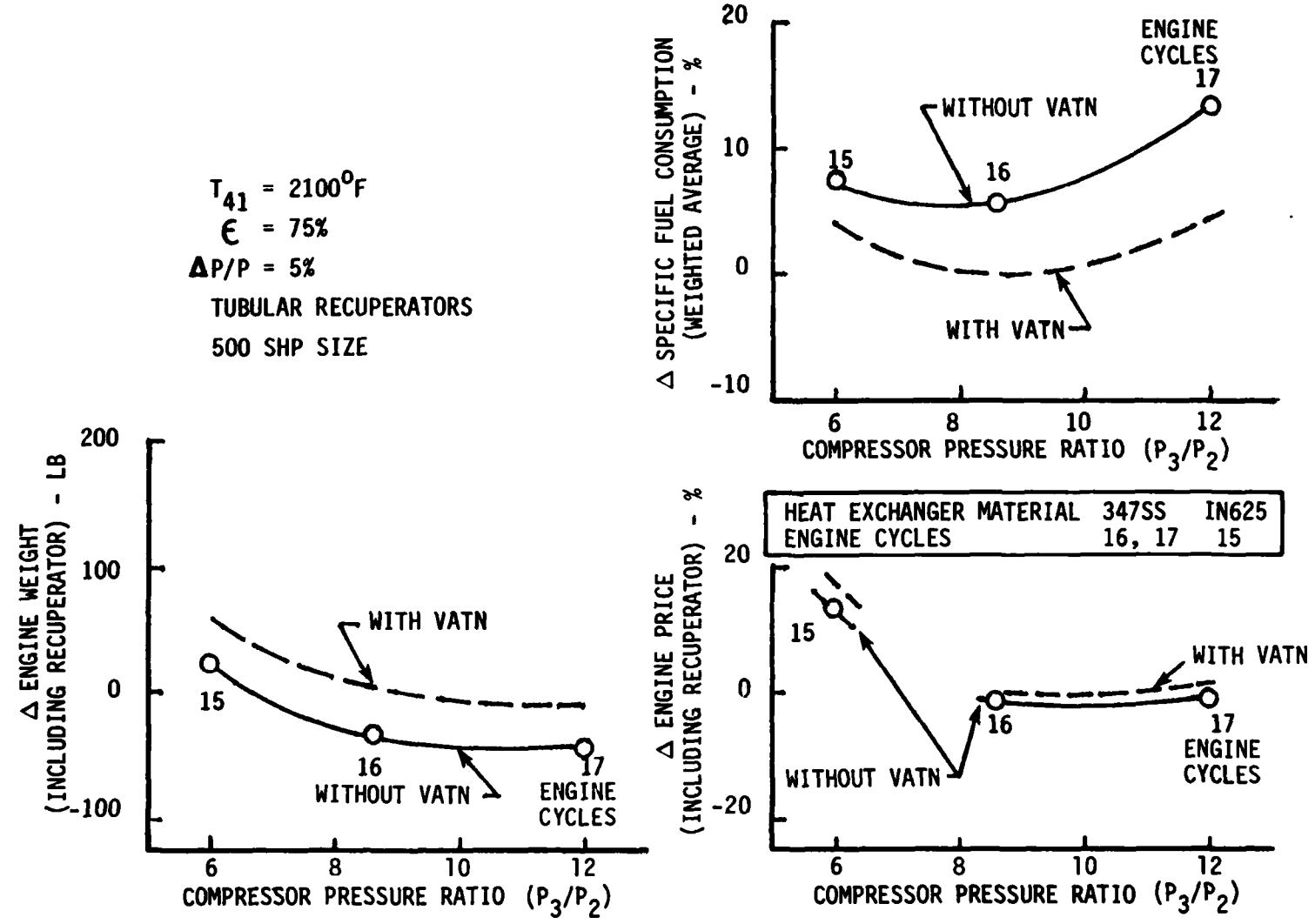

Figure 44. Variable Area Turbine Nozzle Effects On Specific Fuel Consumption, Weight, and Price Trends - Cycles 15, 16, and 17.

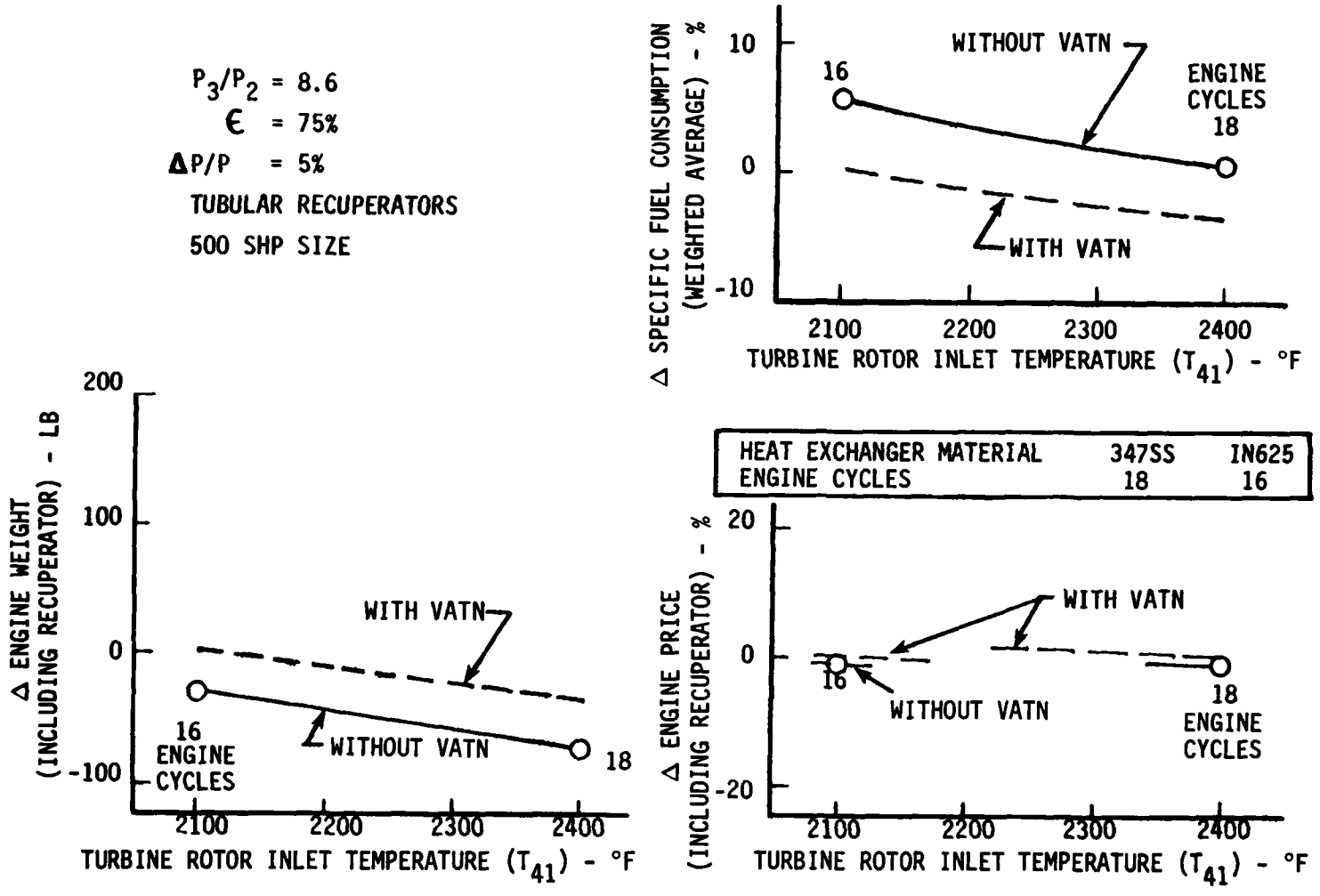

Figure 45. Variable Area Turbine Nozzle Effects on Specific Fuel Consumption, Weight and Price Trends - Cycles 16 and 18.

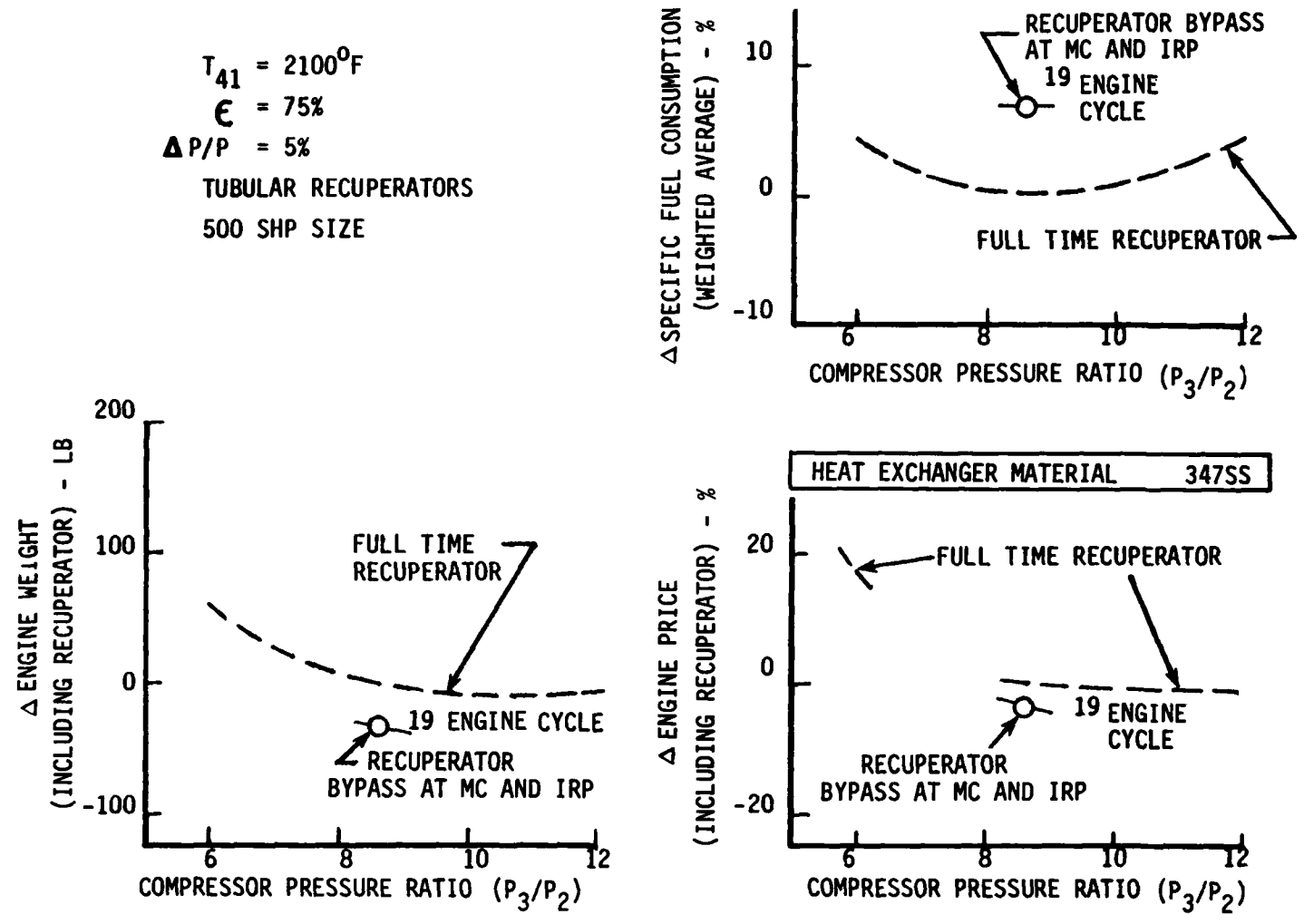

Figure 46. Recuperator Bypass Effects on Specific Fuel Consumption, Weight, and Price Trends.

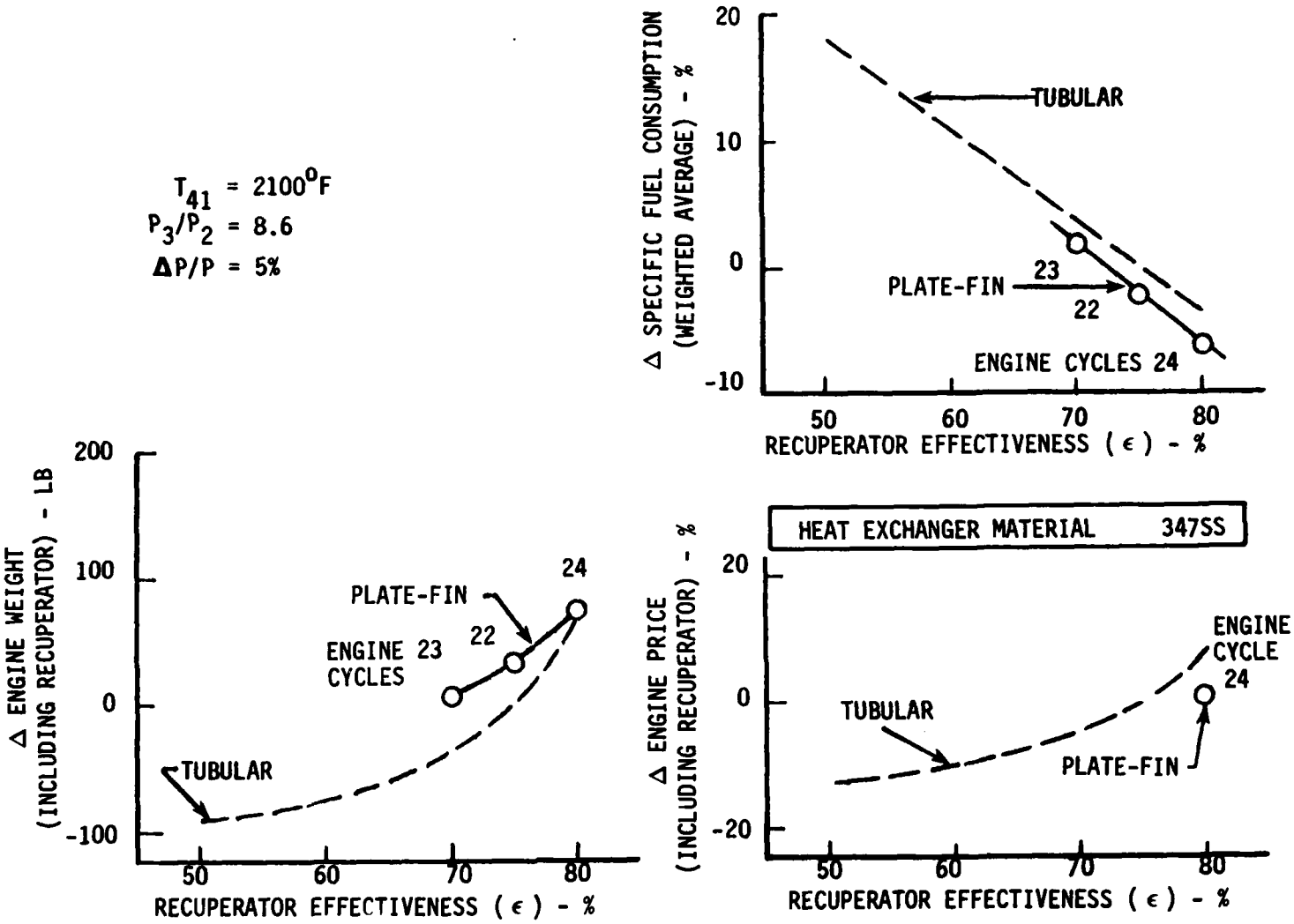

Figure 47. Recuperator Type Effect on Specific Fuel Consumption, Weight, and Price Trends.

Maintenance cost trends with principal cycle and recuperator design parameters are shown in Figures 48 through 50. As expected, the trends generally follow the engine price trends.

MISSION EVALUATION

As noted previously in the discussion of the cycle and recuperator trend curves, the proper choice of cycle and recuperator design parameters is mission dependent. That is, where performance and weight have opposite trends, trade-offs require an assessment of the relative importance of weight and performance on fuel consumption. Similarly, price effects can only be evaluated in terms of the relative impact of performance, weight, and price on life-cycle cost.

This study included a definition of light twin military helicopters and missions using engine Cycles 1 and 57 of the parametric family. The helicopters were both sized to carry a 2650-pound payload with an endurance of 2 hours plus 30 minutes of fuel reserve. Principal vehicle characteristics are summarized in Table 10. Note that the regenerative engine was scaled to 536 shp in order to meet the same mission payload and duration as the nonregenerative vehicle. The mission profile shown indicates the relative importance of SFC at the various power settings and provides a basis for combining the operating line SFC characteristics into a single average value by weighting the SFC's at various power settings in proportion to the fuel burned at the power setting.

Sensitivity of vehicle gross weight and fuel consumption to engine weight and performance was determined by assuming a rubberized vehicle and developing trade factors as indicated.

Similarly, life-cycle cost models for the two helicopters were developed by combining vehicle and engine price estimates with maintenance cost and fuel cost estimates for an assumed fuel cost of $1/gallon. Life-cycle cost trade factors were developed by perturbing each of the engine related parameters and evaluating their effect on life-cycle costs.

These trade factors then provided the basis for evaluating each of the parametric engine cycles in terms of merit factors (percent change in take off gross weight, percent change in fuel burned, and percent change in life-cycle cost) to provide a logical basis for choosing the proper combination of cycle and recuperator design parameters.

It will be noted in Table 11 that the nominal regenerative cycle (engine 1) provides a fuel saving benefit of 19.6% relative to the nonregenerative powered vehicle while incurring a penalty of 7.2% in vehicle gross weight and a life-cycle cost penalty of 14.3%.

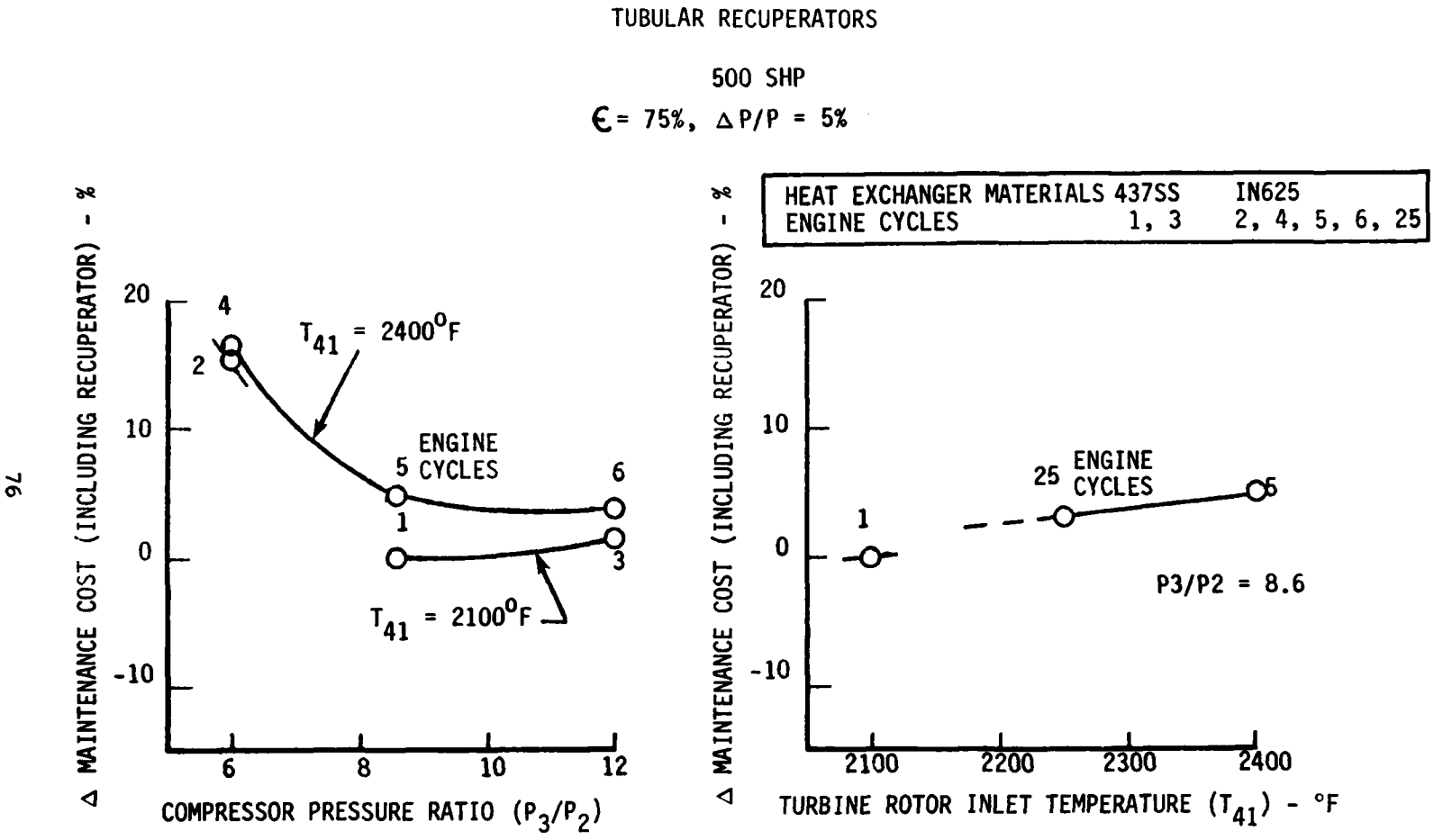

Figure 48. Maintenance Cost Trends With Cycle Pressure Ratio and Temperature.

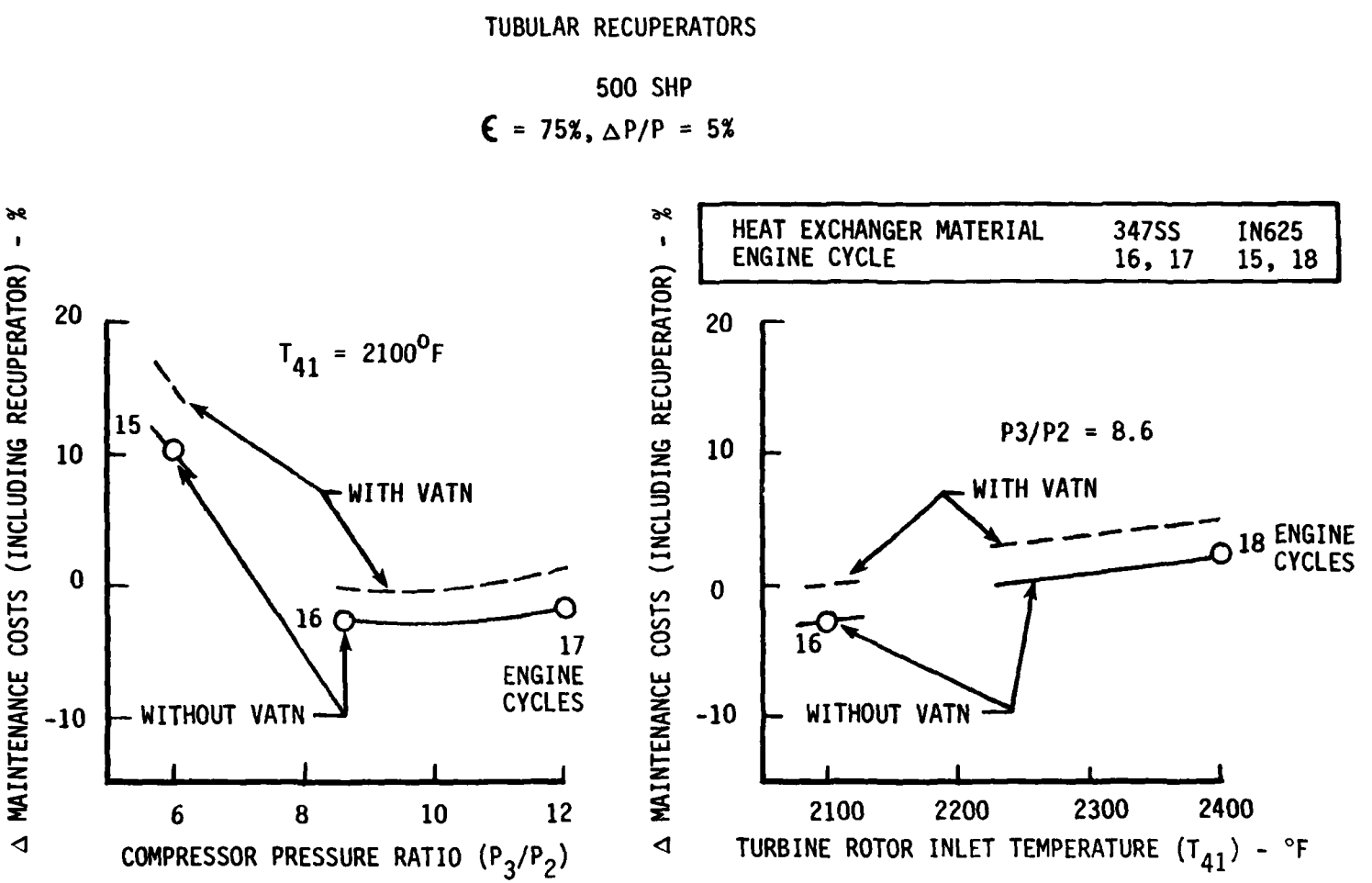

Figure 49. Variable Area Turbine Nozzle Effects on Maintenance Cost Trends.

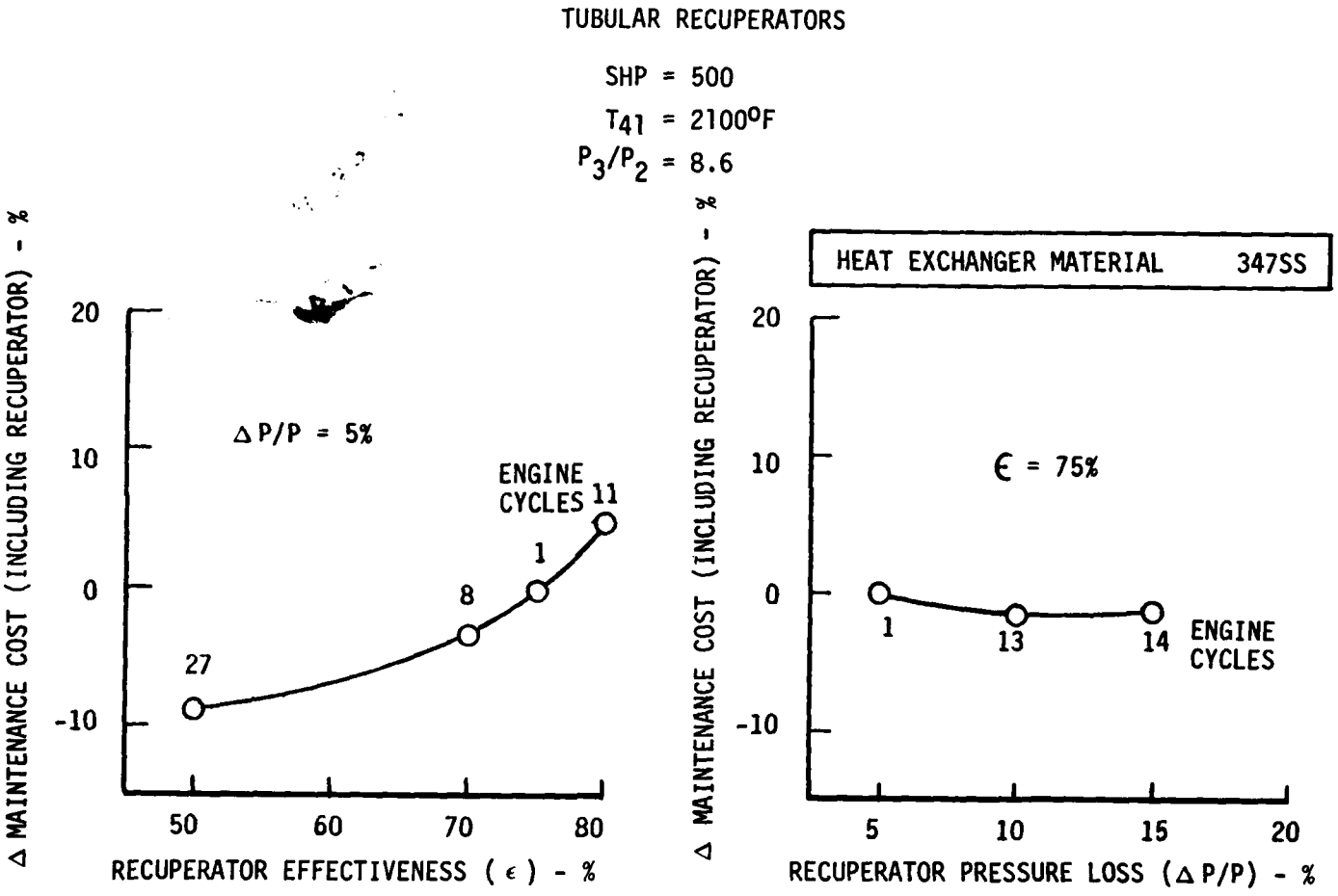

Figure 50. Maintenance Cost Trends With Recuperator Effectiveness and Pressure Loss.

TABLE 10. MISSION EVALUATION MODEL - LIGHT TWIN-ENGINE HELICOPTER

Parameter	Engine Type: Nonregenerative	Engine Type: Regenerative
Takeoff Gross Weight - lb	7250	7775
Payload - lb	2650	2650
Shaft Horsepower per Engine	500	536
Fuel Load - lb	816	650 (Including Reserves)
Mission Duration - hr	2	2 (+30-Minute Reserves)

MISSION PROFILE

% Time	Power Setting	Percent of Fuel Burned: Nonregenerative	Percent of Fuel Burned: Regenerative
5	IRP Takeoff	7.4	8.1
20	90% Hover	27.6	29.9
40	60% Cruise	40.5	39.4
25	40% Cruise	19.3	18.1
10	20% Idle	5.2	4.5

TRADE FACTORS

Change	Percent Change: Nonregenerative	Percent Change: Regenerative
10-lb Engine Weight	.70% Fuel Burned	.67% Fuel Burned
	.83% Take off Gross Weight	.71% Takeoff Gross Weight
1% SFC	1.27% Fuel Burned	1.18% Fuel Burned
	.24% Take off Gross Weight	.16% Takeoff Gross Weight

TABLE 11. LIFE-CYCLE COST MODEL

	Nonregenerative	Regenerative	
Vehicle Life - Years	10	10	
Utilization - hr/year	300	300	
Takeoff Gross Weight - Lb	7250	7775	(+7.2%)
Fuel Burned/Trip - gal.	102	82	(-19.6%)
LIFE-CYCLE COST DISTRIBUTION			
Airframe Price - %	53.9	50.6	
Airframe Maintenance - %	2.7	2.5	
Engine Price - %	25.9	32.8	
Engine Maintenance - %	3.8	4.5	
Fuel Cost at $1/gal.- %	13.7	9.6	
TOTAL	100.	100.	(+14.3%)

	Percent Change in Life-Cycle Cost	
TRADE FACTORS	Nonregenerative	Regenerative
10-lbs Engine Weight	.56%	.47%
1% Engine Price	.25%	.32%
1% Engine Maintenance Cost	.04%	.04%
1% Specific Fuel Consumption	.31%	.21%

Merit factors for each of the regenerative engine cycles (relative to the nominal engine Cycle 1) were calculated and summarized in Figures 51 through 58. Cycle pressure ratio and temperature trends are shown in Figures 51 and 52. Cycle pressure ratios of 8 to 10 and a cycle temperature of 2400°F are shown to provide minimum take off gross weight, fuel burned, and life-cycle cost for the selected helicopter mission.

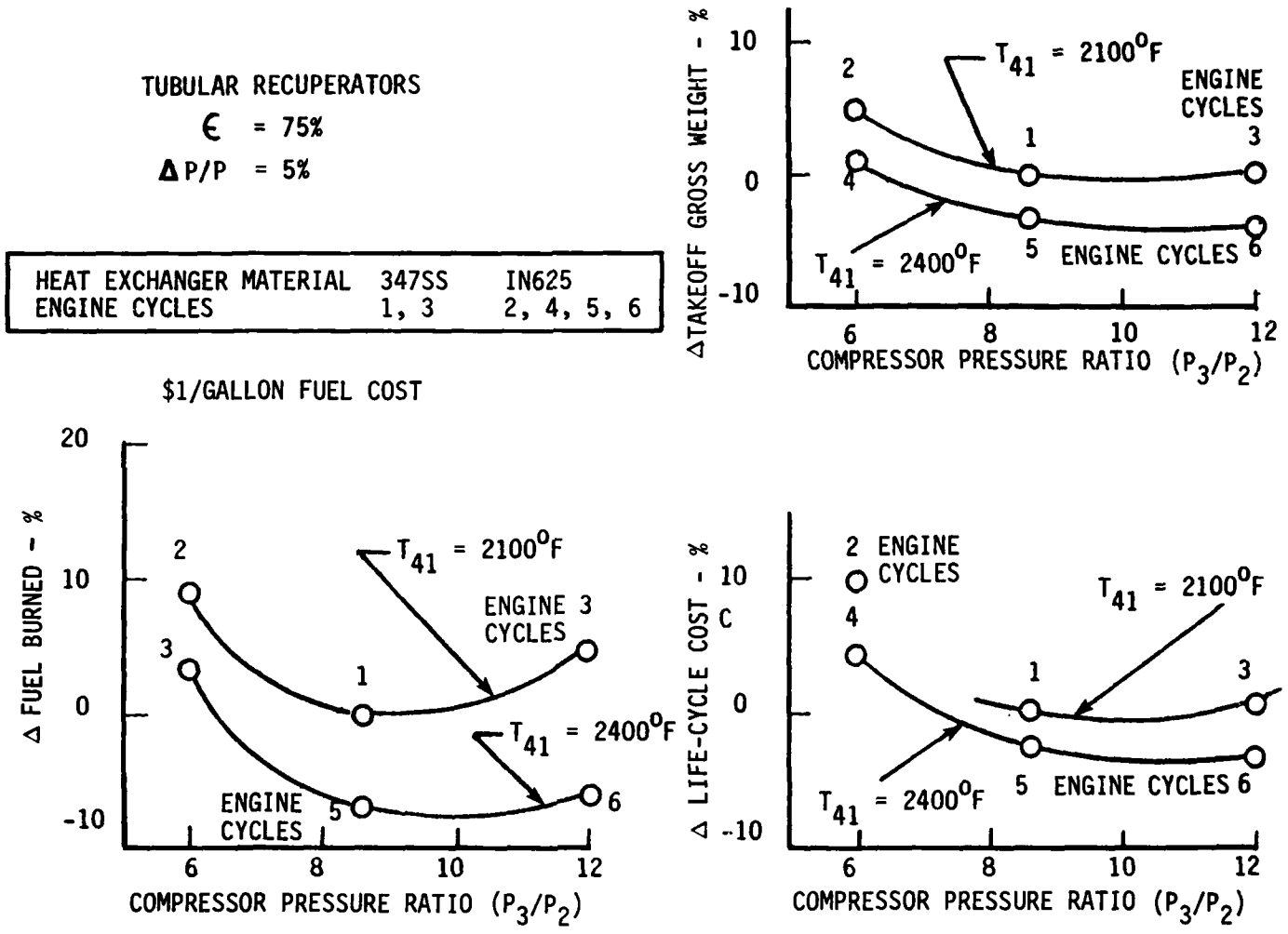

Figure 51. Merit Factor Trends With Cycle Pressure Ratio.

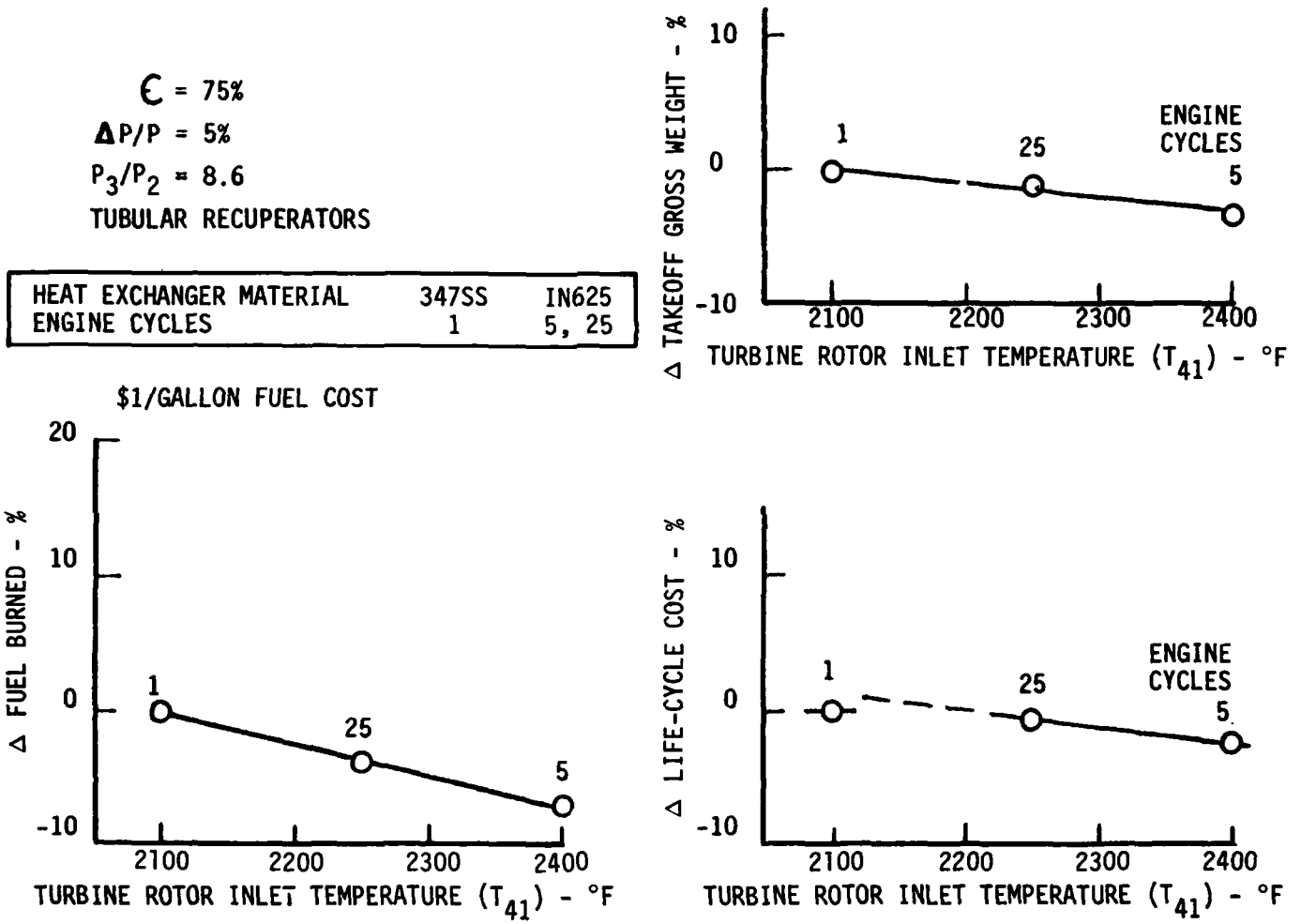

Figure 52. Merit Factor Trends With Cycle Temperature.

TUBULAR RECUPERATORS

P_3/P_2 = 8.6

Δ P/P = 5%

HEAT EXCHANGER MATERIAL	347SS	IN625
ENGINE CYCLES	1, 8, 11, 27	5, 26

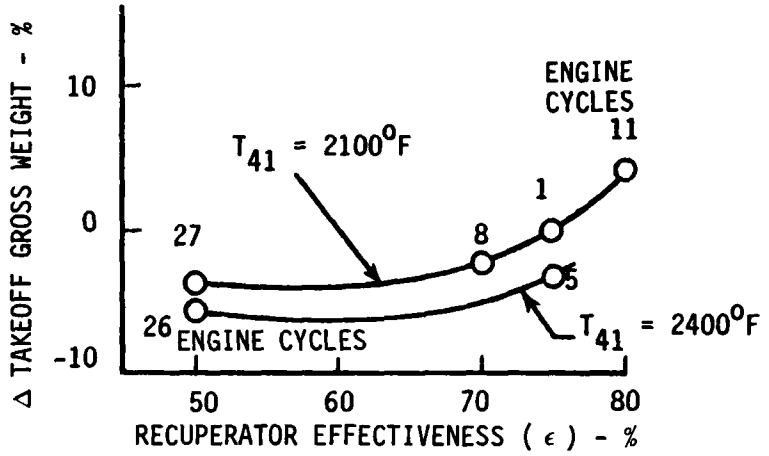

$1/GALLON FUEL COST

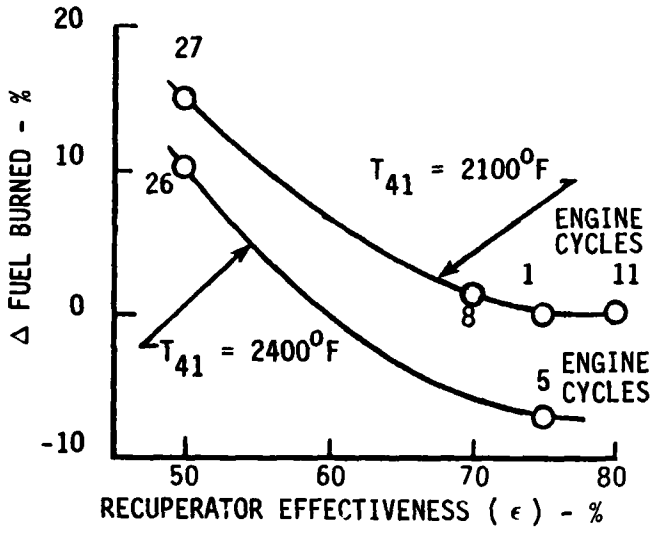

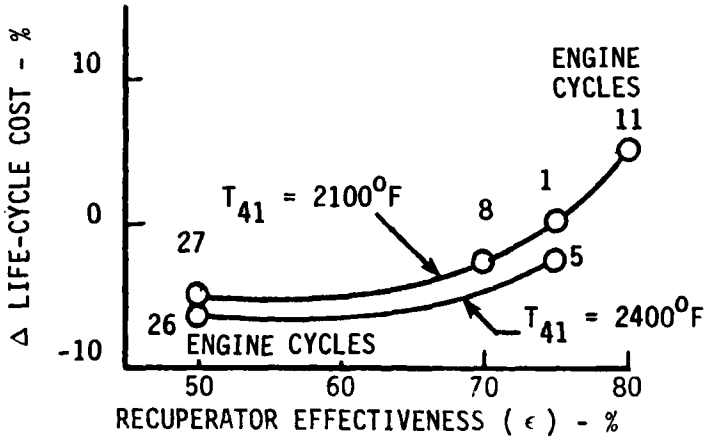

Figure 53. Merit Factor Trends With Recuperator Effectiveness.

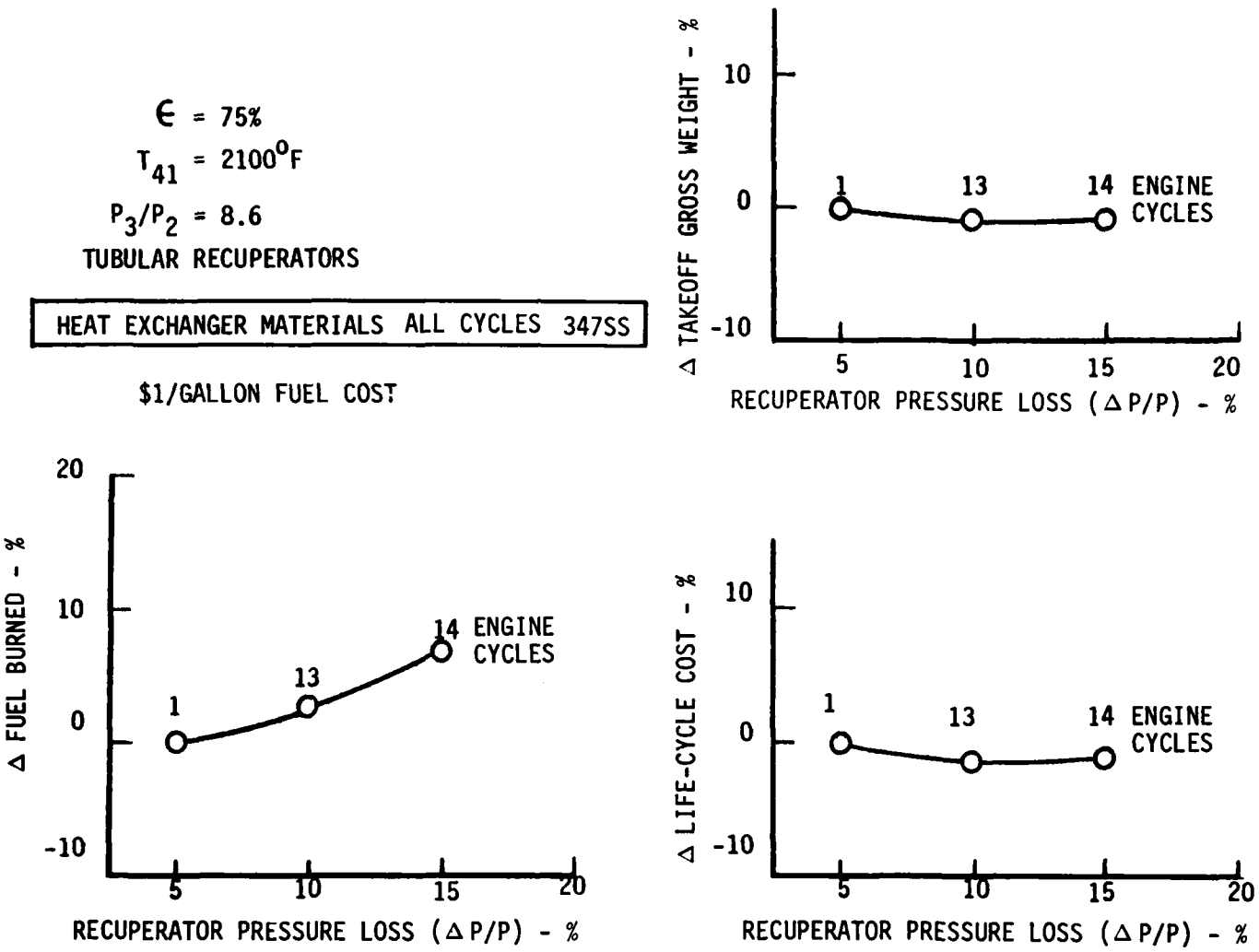

Figure 54. Merit Factor Trends With Recuperator Pressure Loss.

ϵ = 75%

$\Delta P/P$ = 5%

T_{41} = 2100°F

TUBULAR RECUPERATORS

HEAT EXCHANGER MATERIAL	347SS	IN625
ENGINE CYCLES	16, 17	15

$1/GALLON FUEL COST

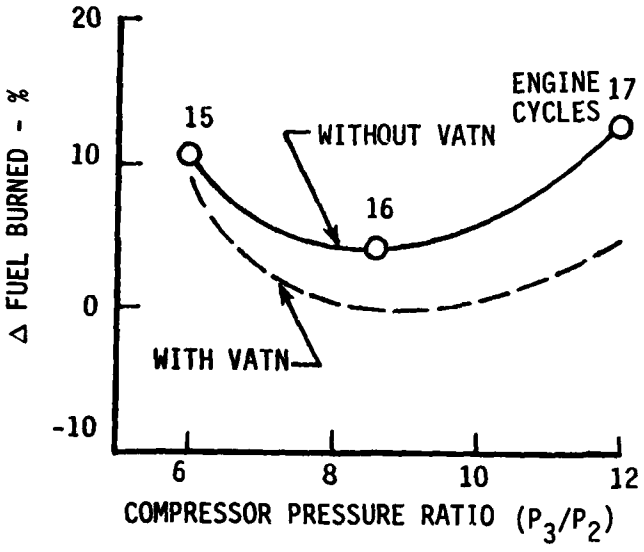

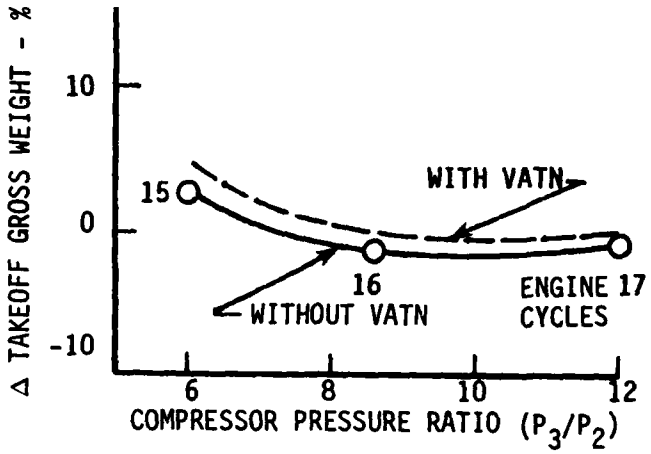

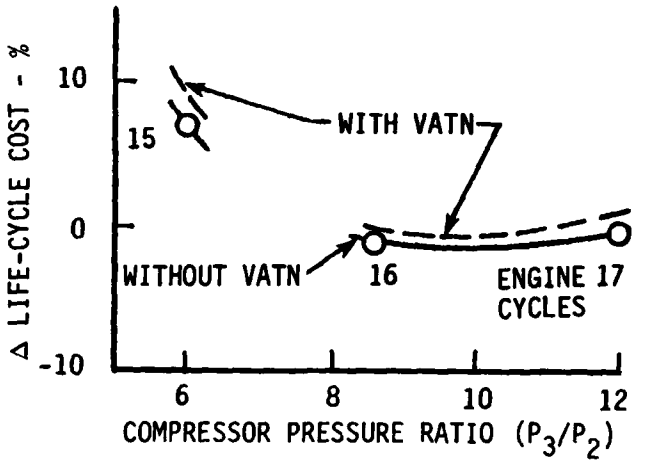

Figure 55. Merit Factor Trends With and Without Variable Area Turbine Nozzle - Engine Cycles 15, 16, and 17.

$P_3/P_2 = 8.6$

$\epsilon = 75\%$

$\Delta P/P = 5\%$

TUBULAR RECUPERATORS

HEAT EXCHANGER MATERIALS	347SS	IN625
ENGINE CYCLES	16	18

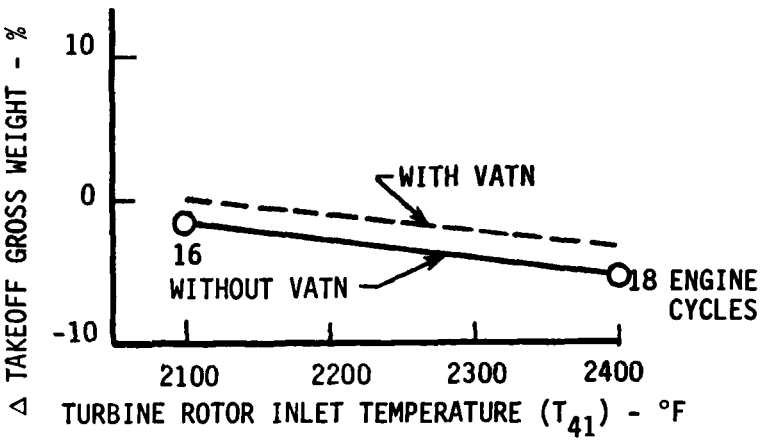

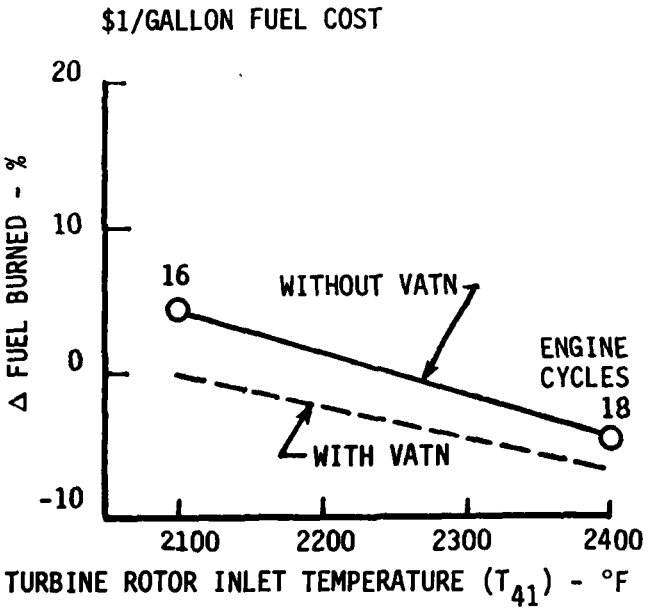

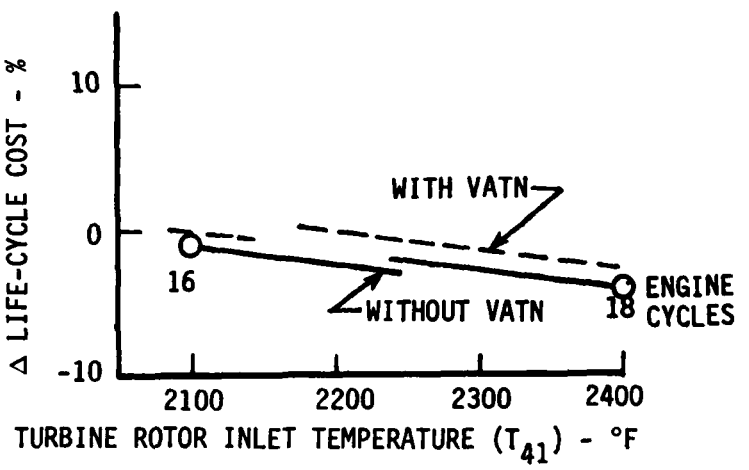

Figure 56. Merit Factor Trends With and Without Variable Area Turbine Nozzle - Engine Cycles 16 and 18.

ϵ = 75%

$\Delta P/P$ = 5%

T_{41} = 2100°F

TUBULAR RECUPERATORS

HEAT EXCHANGER MATERIALS	347SS

$1/GALLON FUEL COST

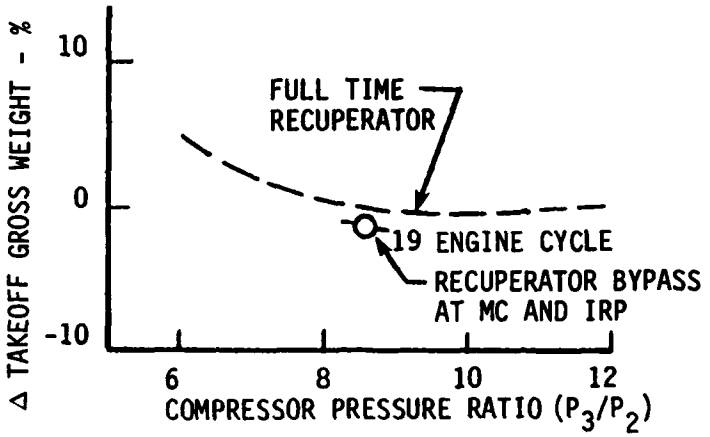

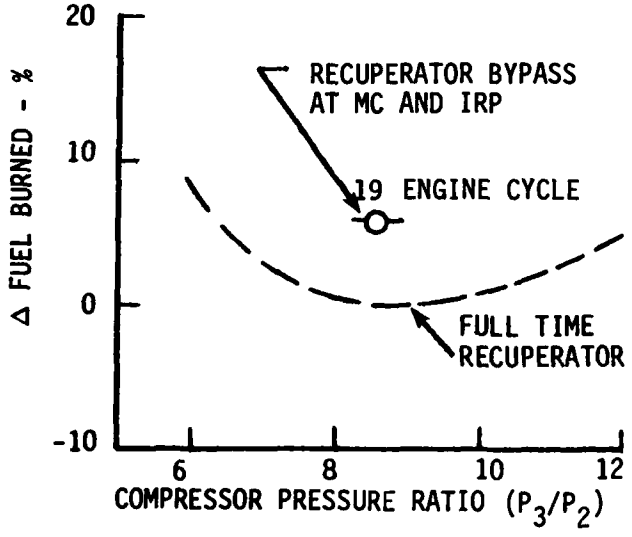

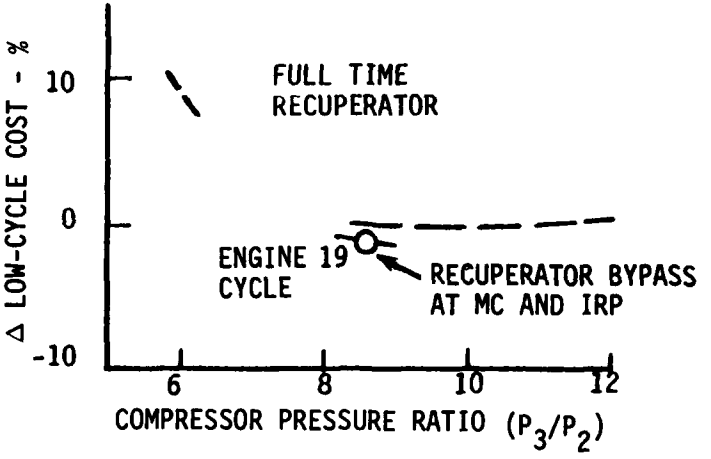

Figure 57. Recuperator Bypass Effects on Merit Factors.

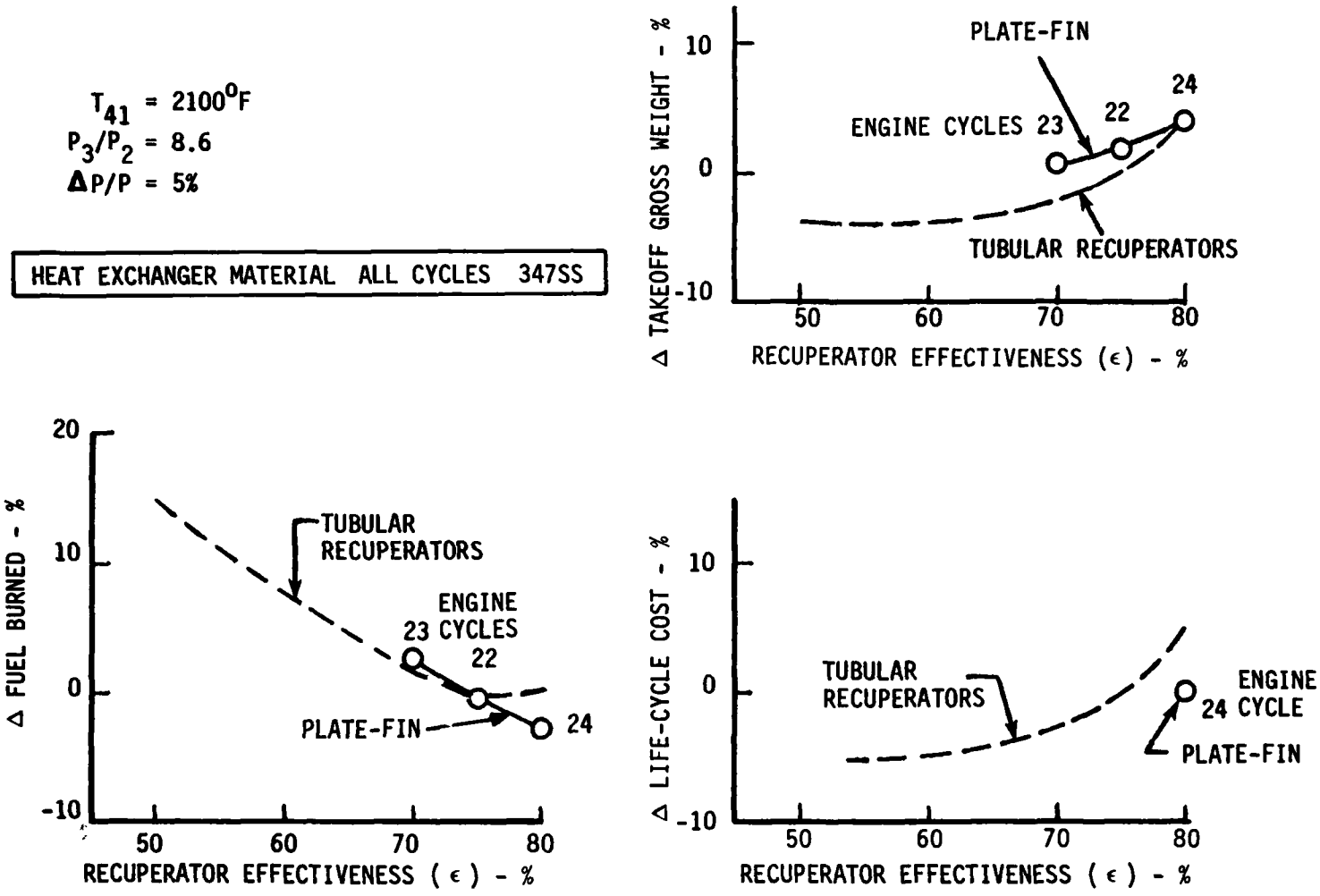

Figure 58. Recuperator Type Effect on Merit Factors.

It is of interest to note that a Navy study of regenerative turboshaft cycles[2] concluded that a cycle pressure ratio of 12:1 and a cycle temperature of 2500°F were optimum. Considering the larger flow size of interest in the Navy study (component performance levels would be relatively insensitive to size variations), those results are reasonably consistent with this study.

Figures 53 and 54 illustrate the effects of recuperator design parameters on merit factors. While recuperator effectiveness levels of 75 to 80% minimize fuel consumption, levels of 50 to 60% effectiveness provide minimum life-cycle cost. A recuperator effectiveness of 70% provides the best balance of fuel saving and life-cycle cost benefits. Similarly, the lowest value of recuperator pressure loss (5%) provides maximum fuel savings while the highest value studied (15%) provides minimum life-cycle cost. A recuperator pressure loss of 7 1/2% provides the best balance of fuel savings and life-cycle cost benefits.

VATN effects on merit factors are shown in Figures 55 and 56. The VATN fuel savings benefits are judged to more than offset the slight life-cycle cost penalty, and a regenerative engine cycle should include a VATN in the power turbine.

Figure 57 compares the merit factors of the recuperator bypass system (engine Cycle 19) with full-time recuperators. While there is a slight life-cycle cost advantage, the significant loss in fuel saving potential indicates that the bypass system does not merit further study.

Merit factors of the parametric engines using plate-fin recuperators are shown in Figure 58. While there are fuel savings and life-cycle cost benefits relative to the plate-fin recuperators at an effectiveness level of 80%, the life-cycle costs are not competitive with those of the tubular configurations at lower effectiveness. Since there is a fuel penalty associated with the plate-fin recuperators at effectiveness levels below 75%, the plate-fin recuperators were not given further consideratio in the study.

Table 12 summarized the merit factors of the two alternate flowpath configurations (engine Cycles 20 and 21). Since neither of these engine configurations provided significant fuel savings or life-cycle cost advantages, they were dropped from further consideration.

---

2. Piscopo, P.F., Lazarick, R.T., and Cyrus, J.D., FUEL CONSERVATION BENEFITS AND CRITICAL TECHNOLOGIES OF RECUPERATIVE AND ADVANCED CONVENTIONAL CYCLE TURBOSHAFT ENGINES, AIAA TECHNICAL PAPER AIAA-80-0224, January 1980.

TABLE 12. EVALUATION OF ALTERNATE FLOWPATH CONFIGURATIONS

	Engine Cycle	
	20	21
T_{41} - °F	2100	2100
P_3/P_2	8.6	8.6
ϵ - %	75	75
$\Delta P/P$ - %	5	5
Flowpath	Side-Mounted Heat Exchanger on Exhaust Pipe	Single Can Combustor in Heat Exchanger Return Pipe
MERIT FACTORS (Relative to Engine 1)		
Change In:		
SFC (Weighted Average)	0	0
Engine Weight - lbs	-4	-3
Engine Price - %	0	-1.4
Engine Maintenance Cost - %	0	-2.9
Takeoff Gross Weight - %	-.3	-.2
Fuel Burned - %	-.3	-.2
Life-Cycle Cost - %	-.2	-.6

TEN-YEAR PERFORMANCE PROJECTION

The study results presented here have been based on currently available component technology levels. Historically, turbomachinery performance levels have improved with time through a broadening of the empirical data base available to correlate the effect of various design parameters and through improvements in the analytical tools available to the designer. Improved manufacturing techniques have also contributed by providing better airfoil tolerances, reduced operating clearances and reduced surface finish roughness.

It is anticipated that these trends will continue and that approximately a 1-point gain in each of the turbomachinery components will be realized in the next 10 years.

Realization of the turbomachinery component efficiency improvements has the potential of providing an additional 3% SFC improvement relative to the current study results. As indicated in Table 13, the component improvement potential exists for the nonregenerative engines as well.

TABLE 13. 10-YEAR PERFORMANCE PROJECTION

	Regenerative Engine	Nonregenerative Engine
Component Efficiencies	-3%	-3%
Cycle Temperature and P/P	-4%	-2%
Projected SFC Improvement	-7%	-5%

Regenerative cycle study results show that the combination of higher cycle temperature and cycle pressure ratio offers potential for further SFC improvement. Continued materials and cooling technology development over the next 10 years is expected to provide an additional 100° in cycle temperature capability with no increase in cooling flow. Realization of the cycle temperature gain and a corresponding increase in cycle pressure ratio to "optimize" the regenerative engine cycle has the potential of improving the regenerative engine SFC by 4% relative to the current study results. The cycle temperature increase would also apply to a nonregenerative cycle for an estimated 2% SFC improvement.

The total projected SFC improvement over the next 10 years is 7% for a regenerative engine and 5% for a nonregenerative engine or a net improvement (regenerative versus nonregenerative) of a 2% change in SFC.

Advancements in recuperator technology are projected to result primarily from materials development. Super alloys will provide higher temperature capability with no significant weight change while nonmetallic materials offer the potential for significant weight reduction. Improved fabrication techniques are projected to provide some reduction in recuperator costs.

No significant advances in heat transfer technology are projected for the next 10 years. Reduction in the amount of heat transfer surface area required (at a given effectiveness level) would require an increase in heat transfer coefficient with no increase in pressure loss. This type of improvement is considered very unlikely.

Thus 10 years of technology advancement are projected to improve the selected regenerative cycle by 7% (2% relative to an advanced technology nonregenerative cycle) and provide some modest weight and cost reductions.

SUMMARY OF TASK I RESULTS AND SELECTION OF PARAMETERS FOR TASK II PRELIMINARY DESIGN

Table 14 summarizes candidate cycles considered prior to selection of the cycle for the Task II preliminary design. Column 1 represents regenerative engine parameters that result in maximum fuel savings, while column 2 represents engine parameters consistent with a minimum life-cycle cost penalty. Although none of the cycles represent specific engines of the parametric family, the merit factors were estimated by interpolation.

Since the cycle parameters that yield maximum fuel savings also incur a substantial life-cycle cost penalty and the combination that minimizes the life-cycle cost penalty loses much of the fuel savings potential, other combinations as noted were evaluated to guide the selection of a balanced cycle.

No combinations were found which provided significant fuel savings without incurring distinct life-cycle cost penalties. The engine cycle represented by column 4 was selected for further evaluation in the Task II preliminary design phase as representing the best balance of fuel saving potential versus life-cycle cost penalty. Study results indicate this cycle has the potential for a 26% fuel savings with an attendant 9% life-cycle cost penalty when compared to a nonregenerative engine at the same T_{41}.

TABLE 14. CANDIDATE TASK II CYCLES

	1	2	3	4	5	6
T_{41} - °F	2400	2400	2207	2250	2250	2250
P/P	10	11	8.6	8.6	8.6	8.6
ϵ - %	80	60	70	70	70	80
$\Delta P/P$ - %	5	10	7 1/2	7 1/2	7 1/2	7 1/2
Regenerative Type	Plate -Fin	Tube	Tube	Tube	Plate -Fin	Plate -Fin
Regenerative Materials	IN625	IN625	347SS	IN625	IN625	IN625
Regenerative Bypass	No	No	No	No	No	No
VATN	Yes	No	No	Yes	Yes	Yes
Flowpath	Nom	Nom	Nom	Nom	Nom	Nom
MERIT FACTORS (RELATIVE TO NONREGENERATIVE ENGINE AT SAME T_{41})						
Change in:						
SFC - %	-33	-12	-20	-24	-26	-32
Engine Price - %	+30	+16	+29	+33	N/A	+31
Engine Weight - lb	+265	+60	+137	+168	+210	+274
Takeoff Gross Weight - %	+7	-1	+2	+2	+5	+8
Fuel Burned (W_F)-%	-30	-15	-22	-26	-22	-27
Life-Cycle Cost - %	+11	+3	+7	+9	N/A	+12

TASK II - REGENERATIVE ENGINE PRELIMINARY DESIGN

With the selection of the regenerative engine design parameters, an engine preliminary design was completed. Design requirements were established, component performance levels were refined, and overall performance was estimated. Component design parameters were used to establish dimensions and relationship with other components as well as to estimate weight, price and maintenance costs. A preliminary mechanical design study was performed to guide materials selection, to establish structural integrity, and to examine rotor dynamics.

A mission evaluation relative to a nonregenerative powered helicopter was performed and an assessment of technical risk and uncertainty was made.

PRELIMINARY DESIGN OBJECTIVES AND DESIGN REQUIREMENTS

The objectives of the engine preliminary design are to:

1. Establish engine performance characteristics.
2. Establish a mechanical arrangement which integrates the regenerator heat exchanger with the engine components.
3. Provide sufficient structural and vibratory analysis to define weight and estimated price (acquisition cost).
4. Define the installation characteristics of the engine.

The design requirements for the preliminary mechanical design were based on a typical light twin engine military helicopter application. These requirements include modular construction, an integral inlet particle separator, and an integral lubrication system. Component analysis is consistent with the requirements of Military Specification MIL-E-8593A entitled Engines, Aircraft, Turboshaft and Turboprop General Specification for, 15 October 1975.

The design life for all components is 5,000 hours and 15,000 cycle low cycle fatigue life. The mission is a 2-hour mission with a time-at-power profile as shown in Table 15.

TABLE 15. TIME-AT-POWER MISSION MODEL

Power Setting	% Mission Time
IRP	5
MC	20
60% IRP	40
40% IRP	25
20% IRP	10

AD-A091 755 GENERAL ELECTRIC CO LYNN MA AIRCRAFT ENGINE GROUP F/G 21/5
REGENERATIVE ENGINE ANALYSIS.(U)
OCT 80 R P TAMEO, P W VINSON, R E NEITZEL DAAK51-79-C-0055
UNCLASSIFIED R80AEG049 USAAVRADCOM-TR-80-D-18 NL

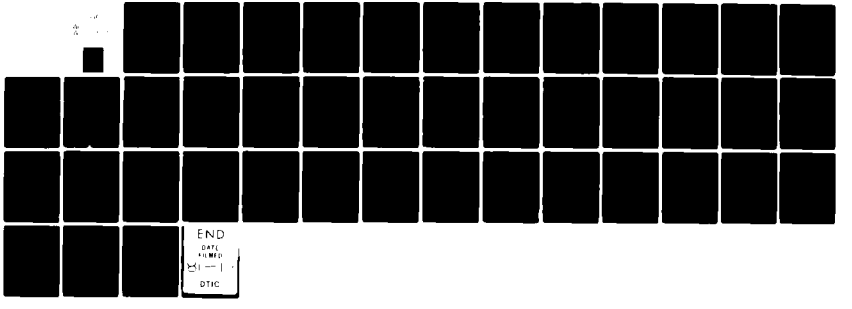

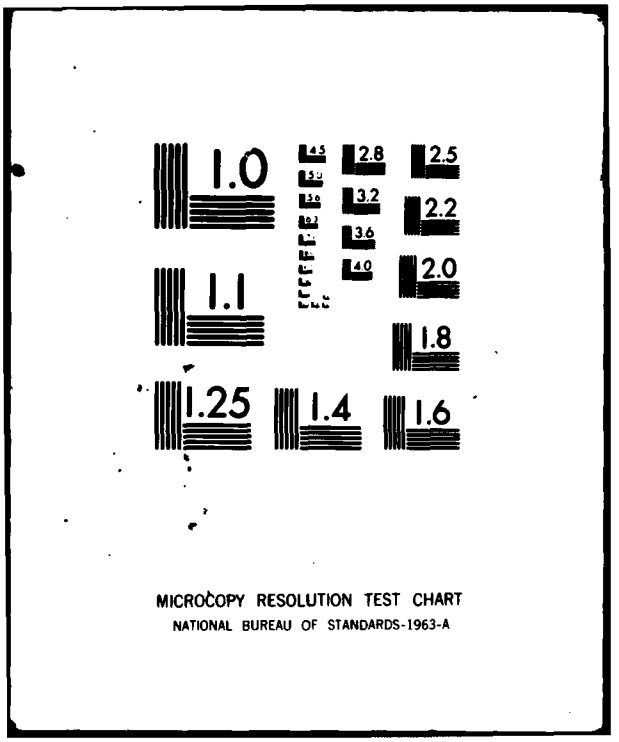
1.0
1.1
1.25
1.4
1.6
1.8
2.0
2.2
2.5
2.8
3.2
3.6
4.0
4.5
5.0
MICROCOPY RESOLUTION TEST CHART
NATIONAL BUREAU OF STANDARDS-1963-A

PERFORMANCE

Table 16 summarizes the Task II regenerative engine components at IRP and compares them to those of a nonregenerative engine. For the selected flow size of 3.5 lb/sec compressor corrected airflow, the regenerative engine delivers 539 shp at intermediate rated power while the nonregenerative engine provides that power at only 3.3 lb/sec corrected flow.

A vaneless inlet particle separator was chosen for the Task II engines for reduced pressure loss. The compressor efficiency level is consistent with the Task I parametric analyses.

The high-pressure performance level was reduced by 0.6 point relative to Task I to reflect increased cooling losses and a slight increase in stage loading.

The power turbine efficiency level is 1 point lower than Task I due primarily to a refinement of estimated aspect ratio and VATN losses.

The exhaust nozzle pressure ratio (P_8/P_0) was reduced to 1.003 to be more consistent with the very low Mach number of the exhaust gases as they exit from the heat exchanger.

The heat exchanger pressure loss objective of 7.5% was increased to 7.7% (increased cold air header loss) in order to keep feed pipe diameters small enough to line up with the recuperator headers and to clear power turbine flanges.

The power turbine discharge and exhaust scroll losses were reduced slightly as indicated and a combustor collector scroll pressure loss of 0.45% was added

Compressor discharge and mid-stage chargeable parasitic flows were increased slightly relative to the Task I values to meet hot parts life requirements and provide additional rotor purge air.

Recuperator off-design effectiveness and pressure loss characteristics are shown in Figures 59 and 60 respectively.

VATN effects on the power turbine performance were refined by estimating the efficiency-VATN interrelationships at selected off design operating conditions representative of the Task I engine operating line. As shown in Figure 61, the efficiency reduction with VATN closure was found to be more severe at part power conditions relative to the Task I assumption (Task I assumed the efficiency variation at $\Delta h/T = \Delta h/T_{IRP}$ to apply over the entire map).

TABLE 16. TASK II ENGINE CYCLES
539 SHP AT IRP

	Regenerative Vaneless	Nonregenerative Vaneless
INLET PARTICLE SEPARATOR		
$\Delta P/P$ - %	1.2	1.2
Bypass Flow - %	14	14
COMPRESSOR	2 + 1 Stages	2 + 1 Stages
$W_2\sqrt{\theta}/\delta$	3.5	3.3
$N/\sqrt{\theta}$ (100%)	58,100	62,800
P/P Total/Total	8.6	12
η Total/Total	81.5	80.0
COMBUSTOR		
T_{41} - °F	2250	2250
$\Delta P/P$ - %	4.15	4.15
$T_{39}-T_{35}$ - °F	1225	1657
η - %	99.5	99.5
HIGH PRESSURE TURBINE	1 Stage	1 Stage
ψ_P	.8	.8
$W\sqrt{T}/P_4$	1.49	.96
P/P	2.61	3.52
η - %	86.0	84.2
POWER TURBINE	3 Stages	3 Stages
RPM	20,000	20,000
$W\sqrt{T}/P_{45}$	3.71	3.14
P/P	2.70	3.04
ψ_P	.92	.92
Swirl	25°	25°
M_F	.35	.4
VATN	1ST Stator Variable	-
η - %	88	89
EXHAUST		
P_8/P_0	1.003	1.03
HEAT EXCHANGER AND DUCTS		
Change in:		
$\Delta P/P$ (HOT AND COLD) - %	7.7	-
ϵ - %	70	-
$\Delta P/P$ - Cold Side Feed Pipes - %	0.2	-
$\Delta P/P$ - Combustor Scroll - %	.45	-
$\Delta P/P$ - Power Turbine Discharge - %	3.0	2.5
$\Delta P/P$ - Exhaust Scroll - %	0.5	-

TABLE 16. TASK II ENGINE CYCLES - Continued
539 SHP AT IRP

PARASITICS	Regenerative Vaneless	Nonregenerative Vaneless
Nonchargeable - $\%W_2$	8.4	8.4
Chargeable Compressor Discharge Pressure - $\%W_2$	6.1	6.6
Chargeable Mid-Stage - $\%W_2$	.92	.92
Windage and Accessory Horsepower - %	0.9	0.9
Blower Horsepower - %	0.5	0.5

The additional part power VATN losses are associated with the power turbine work split. At part power, the rear stages tend to unload more than the front stage and VATN closure at part power tends to increase the front stage loading even further. It was therefore deemed appropriate to reexamine the Task I VATN schedules which used the more optimistic efficiency-VATN characteristic.

Figure 62 indicates that even with the more severe VATN characteristic, part power SFC continues to improve with VATN closure. Therefore, the Task I VATN scheduling logic was retained, i.e., VATN closure was allowed up to the point of reaching whichever of the following limits that was encountered first.

1. High-pressure Maximum Continuous T_{41} level.
2. Power turbine IRP T_{45} level.
3. Minimum VATN setting of 80%.

Overall performance for the Task II regenerative engine is summarized in Table 17. In addition to the sea level static operating line data used for the Task I evaluation, performance data were generated at two sea level forward flight speeds representative of the cruise portion of the selected helicopter mission. Comparable data for the nonregenerative engine are shown in Table 18. It should be noted that the regenerative engine exhaust gas temperatures (T_8) are 200° to 300°F lower than the nonregenerative engine. This would provide significantly lower infrared radiation (IR) signature for the regenerative engine cycle and reduce IR suppressor requirements.

Note that the forward flight cruise power settings were selected to provide the same net power to the rotor considering ram drag and gross thrust difference between the regenerative and nonregenerative engines.

Sea level static operating line characteristics are compared in Figure 63. Note that the regenerative engine SFC advantage of 18% at IRP increases to 34% at 20% IRP with the mission weighted SFC showing a 24.7% differential in favor of the regenerative engine.

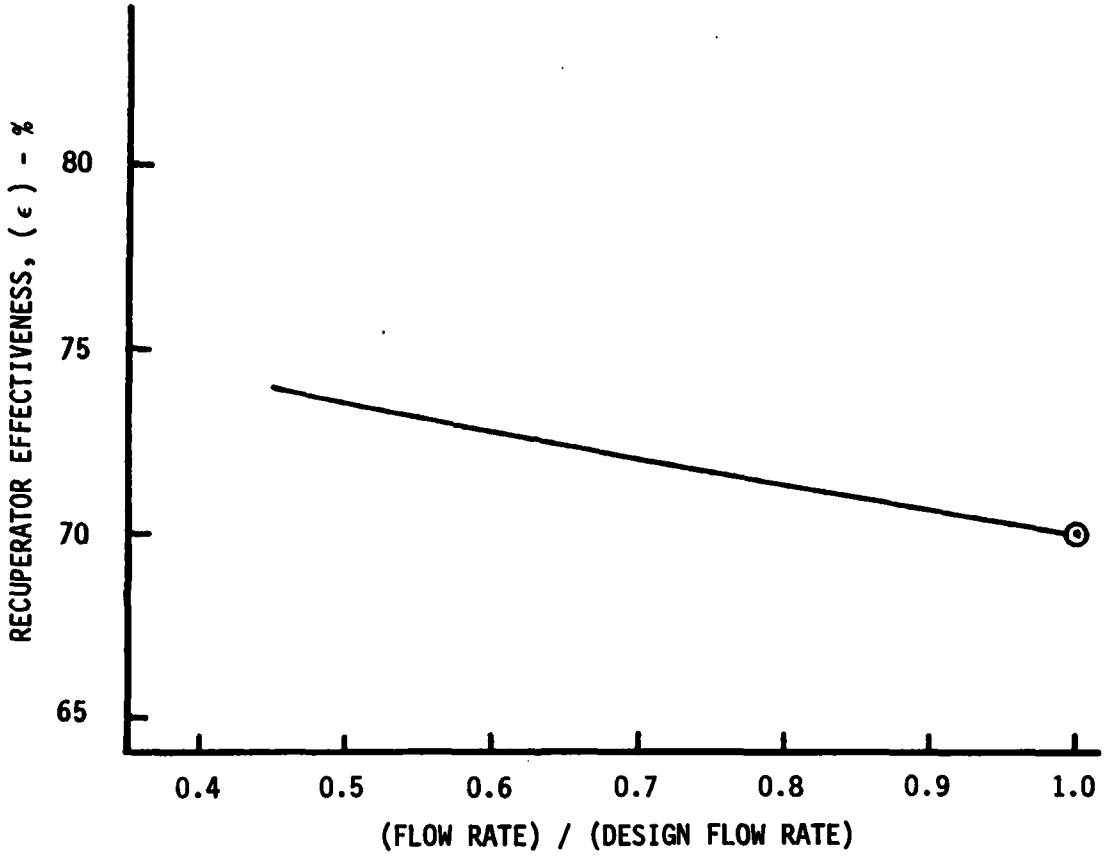

Figure 59. Task II Tubular Recuperator Off-Design Effectiveness Characteristic.

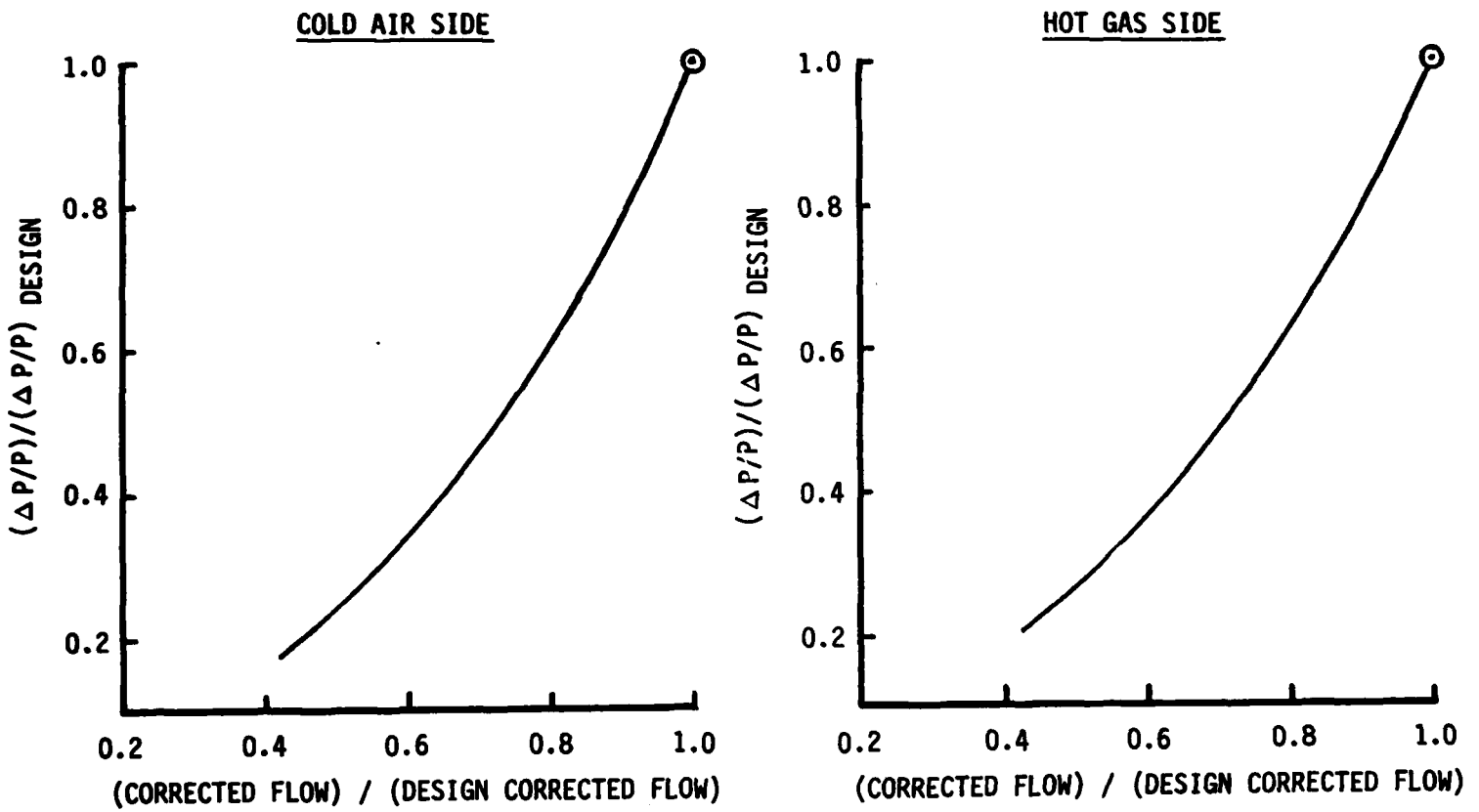

Figure 60. Task II Tubular Recuperator Off-Design Pressure Loss Characteristic.

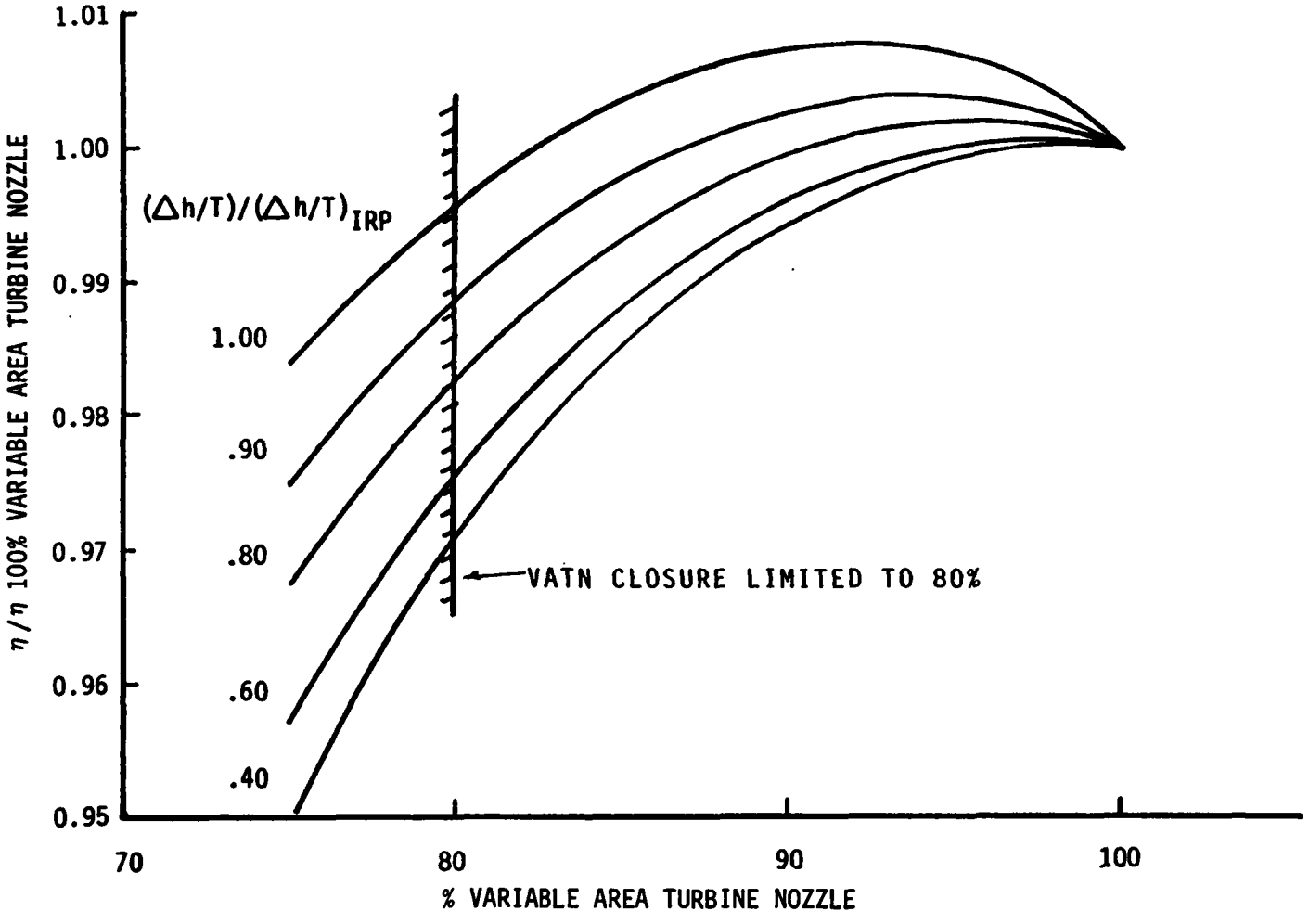

Figure 61. Variable Area Turbine Nozzle Effects on Power Turbine Efficiency Stage 1 of 3 Stages Power Turbine Variable.

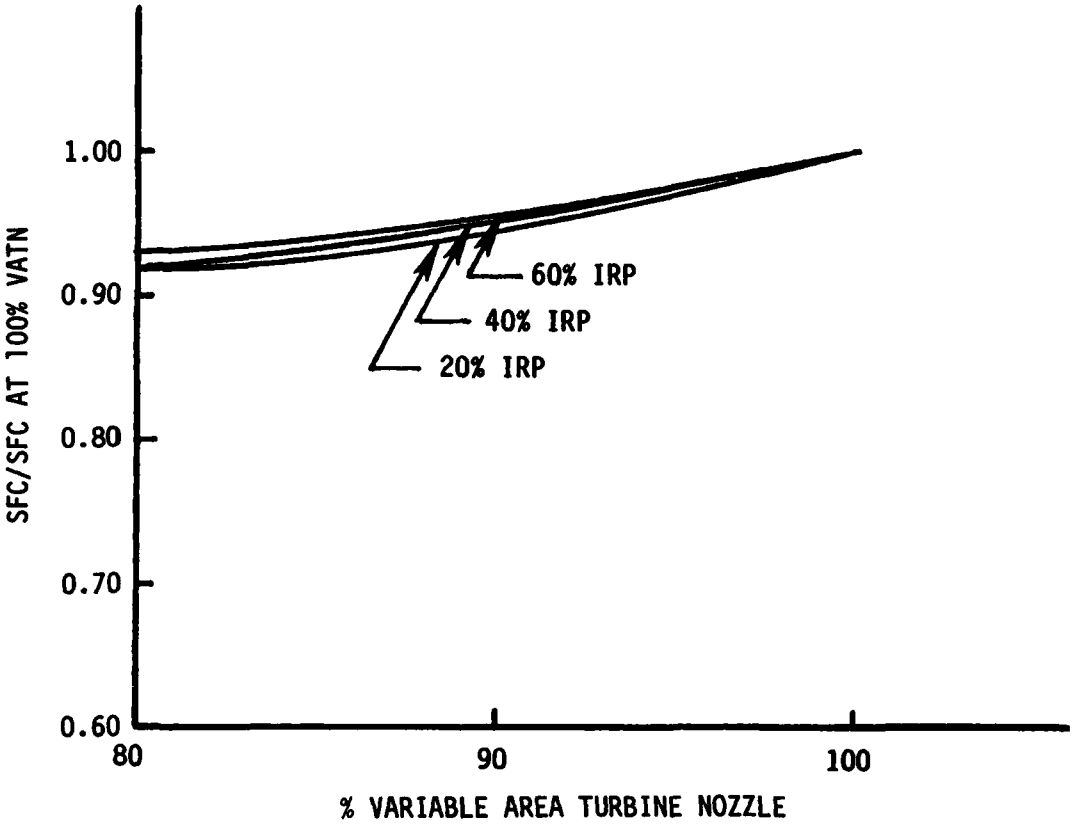

Figure 62. Effect of Variable Area Turbine Nozzle on Specific Fuel Consumption Sea Level Static.

TABLE 17. OVERALL PERFORMANCE SUMMARY - TASK II REGENERATIVE ENGINE

	Flight Condition						
	SLS	SLS	SLS	SLS	SLS	SL 150 knots	SL 80 knots
Power Setting	IRP	Max Cont	60% IRP	40% IRP	20% IRP	60% IRP	40% IRP
SHP	539	478	324	216	108	334	218
F_G - lb	15	13	6	4	2	6	4
SFC - lb/hr/hp	.405	.412	.423	.462	.578	.416	.459
$W_2 \sqrt{\theta}/\delta$ - lb/sec	3.5	3.3	2.3	1.9	1.4	2.3	1.9
P/P	8.6	7.9	5.6	4.4	3.3	5.5	4.4
T_{41} - °F	2250	2150	2145	2045	1915	2145	2040
VATN - °	100	100	84.3	80	80	83.7	80
$T_{4.5}$ - °F	1730	1650	1730	1675	1605	1730	1670
T_5 - °F	1305	1255	1360	1370	1390	1355	1360
T_8 - °F	870	835	800	760	710	800	755

TABLE 18. OVERALL PERFORMANCE SUMMARY - TASK II NONREGENERATIVE ENGINE

	Flight Condition						
Power Setting	SLS IRP	SLS Max Cont	SLS 60% IRP	SLS 40% IRP	SLS 20% IRP	SL 150 knots 60% IRP	SL 80 knots 40% IRP
SHP	539	475	324	216	108	322	214
F_G - lb	41	35	24	17	10	24	17
SFC	.492	.503	.563	.647	.873	.558	.647
$W_2\sqrt{\theta}/\delta$ - lb/sec	3.3	3.1	2.6	2.2	1.7	2.6	2.2
P/P	12.0	11.1	8.9	7.3	5.4	8.6	7.2
T_{41} - °F	2250	2150	1895	1725	1520	1860	1715
$T_{4.5}$ - °F	1625	1550	1357	1235	1100	1335	1230
T_5 - °F	1180	1135	1025	970	925	1010	965
T_8 - °F	1180	1135	1025	970	925	1010	965

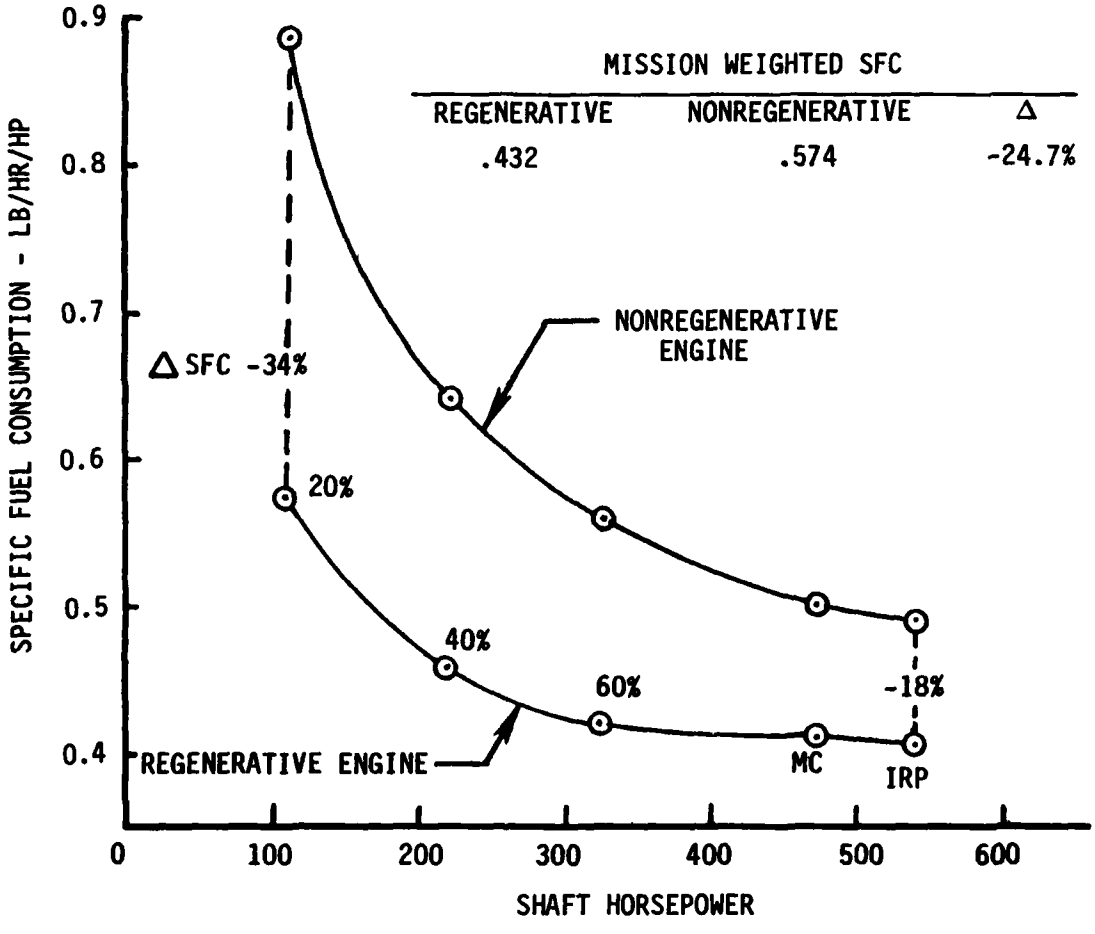

Figure 63. Task II Engine Operating Line Performance Sea Level Static, Standard Day.

ENGINE MECHANICAL DESIGN

Mechanical Arrangement

The mechanical arrangement of the selected regenerative engine, as shown in Figure 64 (Sheet 1), is a front-drive turboshaft engine featuring a single-spool gas generator section consisting of a two-stage axial, single-stage centrifugal flow compressor; a through-flow annular combustor; a single-stage axial flow gas generator turbine; an independent three-stage axial flow power turbine with a variable area turbine nozzle; and a tubular cross-counter flow regenerator. The power turbine shaft which is rated at 20,000 rpm is coaxial and extends to the front end of the engine. The engine also incorporates an integral inlet particle separator, a top mounted accessory package, a self-contained lubrication system, and a digital electronic control system.

Mechanical Description

The engine is constructed in five modules: accessories module, cold section module, hot section module, power turbine module, and regenerator module. The components of each of these modules are described below as studied for weight and cost estimates.

The accessories module includes an accessory gearbox, a fuel pump, an alternator, an electronic control, a lube and scavenge pump, an inlet particle separator (IPS) scavenge blower, a fuel filter, and a compressor variable geometry (VG) actuator. The accessory gearbox provides pads for a customer-supplied hydraulic pump and starter-generator.

The cold section module includes an inlet section, a compressor section, and the diffuser-combustor casing.

The inlet section includes the components forward of the compressor. These components include a front frame, a center body, and IPS collection scroll, an inlet guidevane assembly, and an output shaft assembly.

The front frame is a cast aluminum structure with an integral oil tank. The No. 3 bearing and the power takeoff assembly are mounted inside the front frame. The centerbody is a fabricated aluminum piece which forms the inner flowpath. It has an internal cavity for passage of hot air for anti-icing purposes. The inlet particle separator scroll is a fiberglass shell which attaches to the aft flange of the front frame. It provides a collection manifold for the air and foreign particles scavenged by the engine driven blower. An inlet guide vane assembly attaches to an aft flange of the front frame. This assembly includes the inlet guide vanes, variable vane actuation hardware, and a cast aluminum casing with integral passages for passing hot air for anti-icing purposes. The output shaft assembly is housed within the front frame and includes the No. 1 and No. 2 bearings, a carbon seal, and the output shaft. The shaft has two splines; the aft spline accepts the power turbine shaft and the forward spline is provided for customer connection.

The compressor section is comprised of a rotor section and a stator section. The rotor section is made up of a cast two-stage axial-flow blisk with an integral stub shaft and a cast centrifugal impeller. The rotor assembly is held by a tiebolt. The stator section is made up of a cast steel compressor casing with an axial flange; two stages of fabricated vane sectors; a cast impeller shroud; and a fabricated diffuser-combustor casing. The collection and distribution manifolds for the cold side air for the heat exchanger have been integrated into the fabrication of the diffuser-combustor casing. View A-A in Figure 64 (Sheet 2) shows the collection manifold at the diffuser discharge. This configuration allows the small residual swirl to be used to advantage in the manifold. View BB in Figure 64 (Sheet 2) shows the distribution manifold for the air returning from the heat exchanger. This configuration minimizes the net swirl of the air into the combustion casing. The ducts from the collection manifold to the heat exchanger pass over the distribution manifold at its smallest section to provide a compact arrangement. Eight fuel nozzles, a fuel distribution manifold and two ignitor plugs are mounted on the diffuser-combustor casing.

The power turbine module includes the turbine frame assembly, power turbine stator section, and power turbine rotor section.

The turbine frame assembly consists of the turbine frame stage 1 variable vanes, and variable vane actuation hardware. The turbine frame is a fabricated structure of cast components. The frame has three fixed-geometry struts which provide service passages to the integral sump and bearing housing. The number four and five bearings are included in the module. A carbon seal is housed in the frame sump. A support ring for the inner trunions of the variable vanes is bolted to the frame. The air-cooled variable vanes are cast Mar-M-509. The actuation hardware consists of a unison ring, lever arms, bushings, and a bellcrank. The actuator is mounted on the turbine frame.

The power turbine stator section is made up of a forged turbine casing with an axial flange, stages 2 and 3 cast vane segments with integral seals, and stages 2 and 3 shroud segments.

The power turbine rotor section is made up of uncooled cast blisks with integral seals, spacers and tip seals; a forged stub shaft; and a solid power turbine shaft.

The hot section module includes the combustor liner, high pressure turbine stator, and high pressure turbine rotor.

The combustor is an annular machined ring liner with provision for eight fuel nozzles. The high-pressure turbine stator section is made up of a 360-degree casing which supports the nozzle and the rotor shroud,

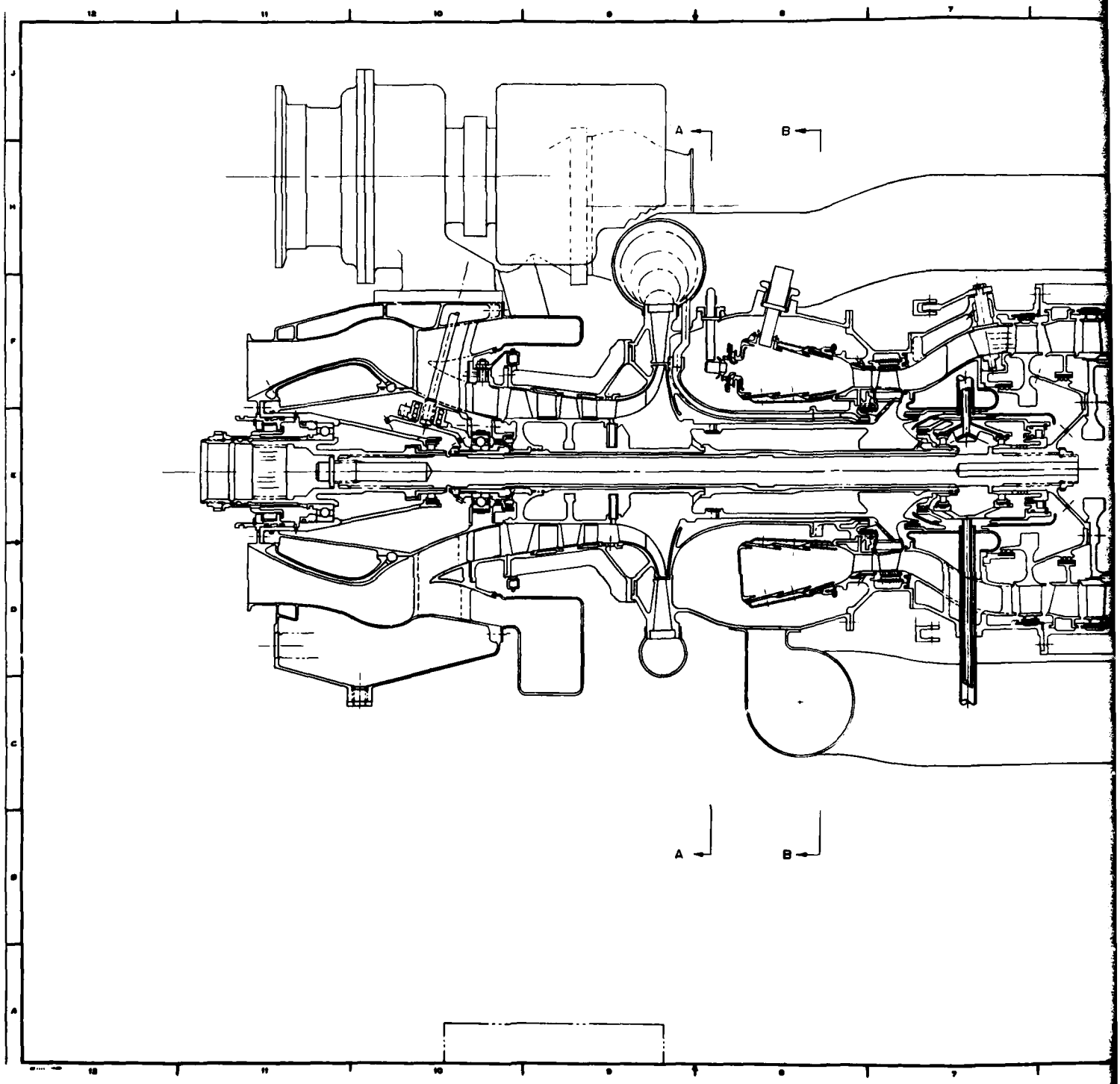

Figure 64. (Sheet 1 of 2) Regenerative Turboshaft Engine.

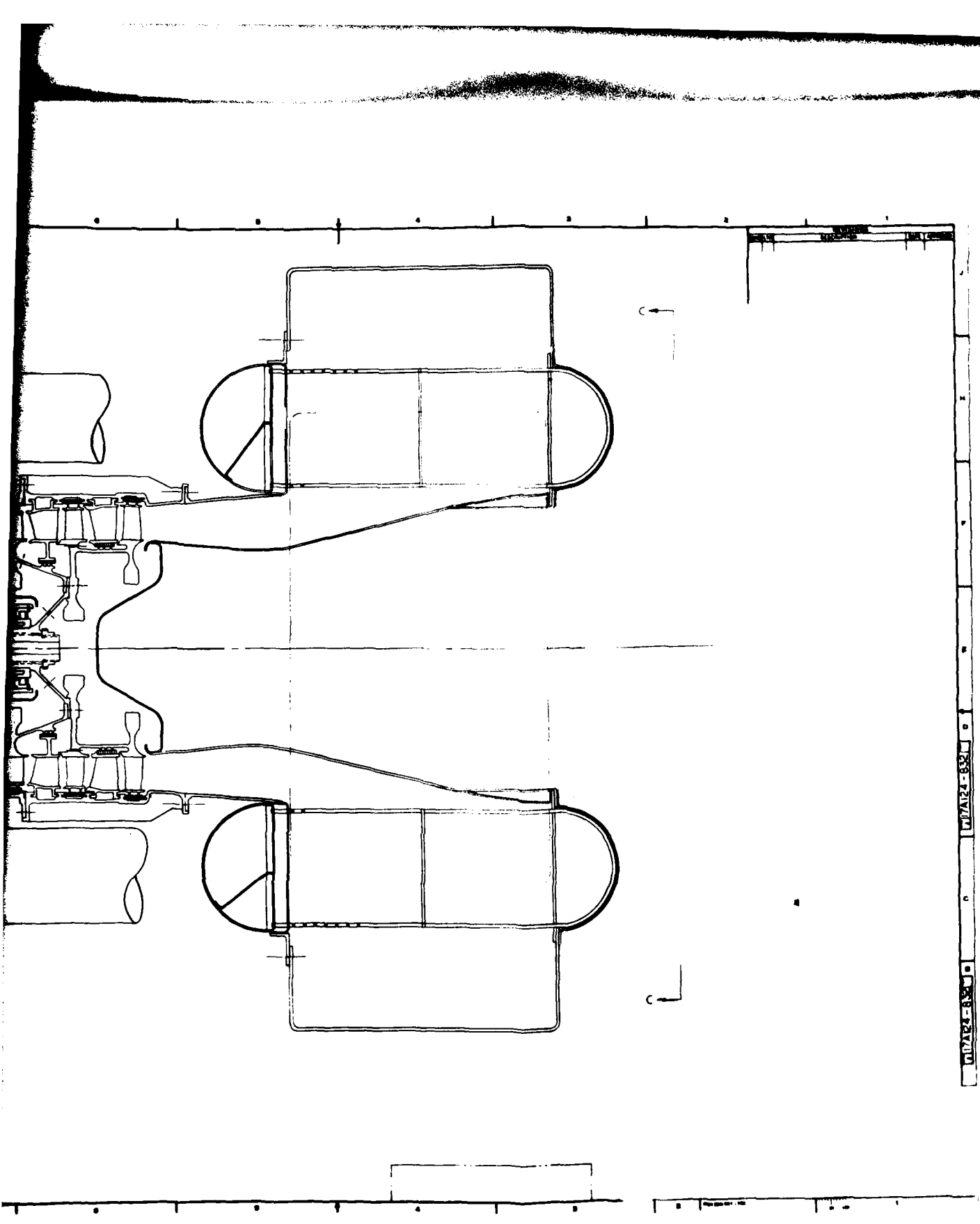

2

1

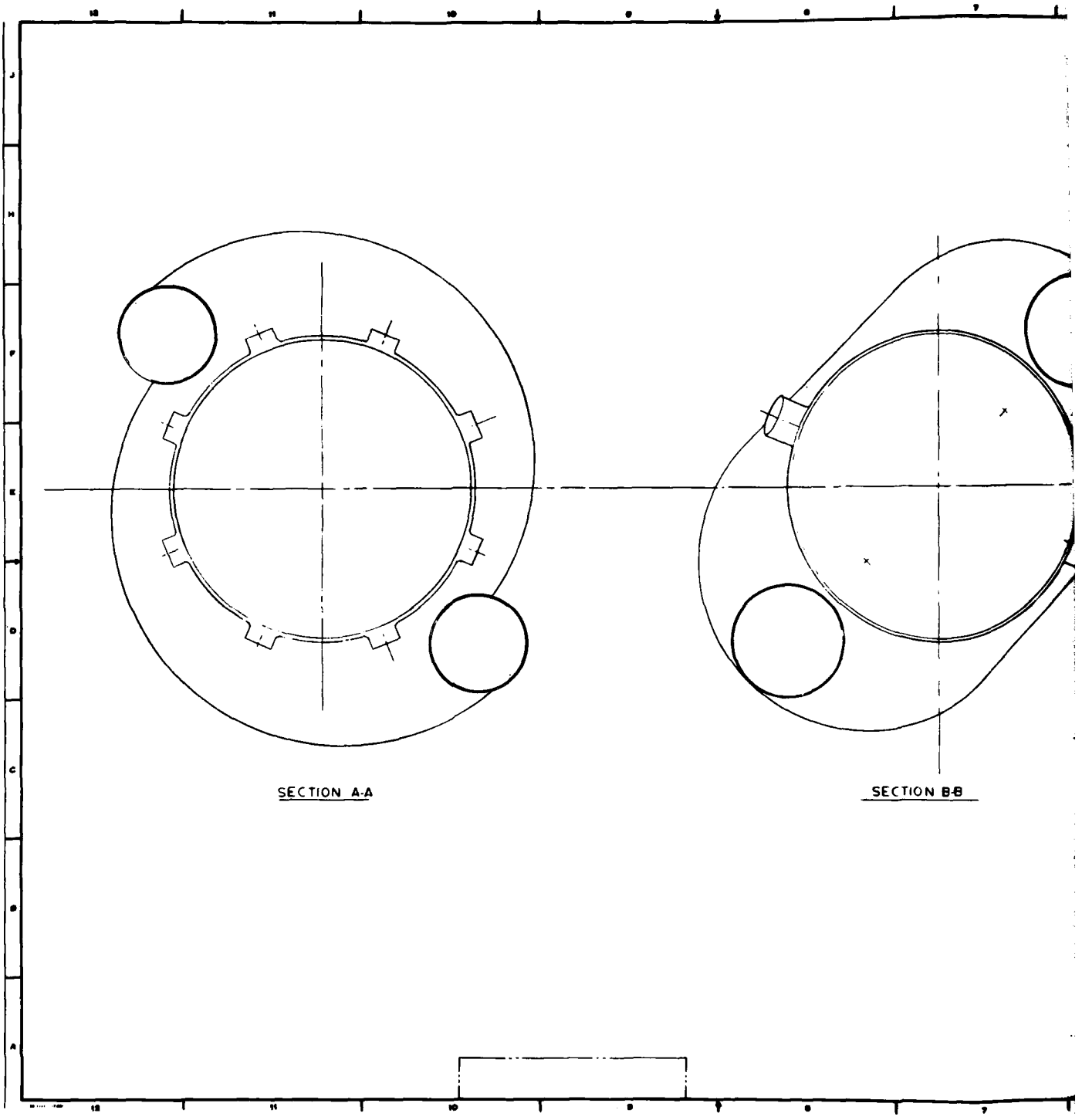

Figure 64. (Sheet 2 of 2) Regenerative Turboshaft Engine.

2

segmented shrouds, and an air cooled nozzle of an MA-754 fabricated construction. The high-pressure rotor section is made up of cast air-cooled blades supported by a machined Rene' 95 disk with integral stub shaft.

The regenerator module includes the inner power turbine discharge duct, the exhaust hood, and the recuperator. The inner power turbine discharge duct is a fabricated sheet metal structure and is attached to the recuperator and the exhaust hood at the aft flange. The recuperator is covered by a fabricated sheet metal exhaust hood which attaches to the recuperator at the forward and aft flanges.

The recuperator is the unique element of the regenerative engine. The following section provides a detail description of the design and producibility considerations.

RECUPERATOR PRELIMINARY DESIGN

The preliminary design recuperator, shown in Figure 65 (Sheets 1 and 2), is a tubular heat exchanger with tubes oriented in an axial direction and arranged in an annular bundle around the gas turbine engine diffuser outlet. The engine exhaust gas flows radially outward, making a single pass through the heat exchanger core, while the air makes two transverse passes inside the tubes in an overall counterflow direction with respect to the gas flow. Interpass turns on the air side are accomplished with U-tubes. Although a D-shaped return pan usually results in more compact packaging, the U-tube configuration provides structural advantages because the tubes are free to accommodate the large thermal expansion that will occur in this application. Because engine exhaust gas temperature will be higher than 1340°F at part-power conditions, Inconel 625 is used as the material for the preliminary design recuperator.

The physical characteristics for the recuperator are summarized in Table 19. The tubes are 0.125 inch OD with a 0.007 inch wall thickness as optimized in the parametric study. Ring-dimpled tubes are used to promote air stream turbulence and thus increase the inside heat transfer coefficient.

When tubes are arranged in an annular bundle, the U-tube configuration for interpass return normally results in a large variation in tube spacing between the first and last tube rows. However, relatively uniform tube spacing can be achieved when more tubes are used in a row as the tube bundle diameter increases. This has been accomplished by connecting two rows of inner-pass tubes to a single row of outer-pass tubes where two diameters for each pass differ greatly. For the preliminary design recuperator, the first six inner-pass rows are connected to three outer-pass rows; the first two rows to one outermost row, the next two rows to the second outermost row, and so on. Thus, 15 rows of inner-pass tubes and 12 rows of outer-pass tubes are used, which results in a total of 27 rows of tubes per bundle for a heat exchanger core. Based on this arrangement, the average center-to-center transverse pitch is 0.213 inch, and the spacing between tube rows is 0.125 inch.

TABLE 19. RECUPERATOR DESIGN SUMMARY

Tube OD - in.	0.125
Tube Wall Thickness - in.	0.007
Tube Type	Ring-dimpled
Dimple Depth - in.	0.0102
Dimple Spacing - in.	0.375
Number of Tube Rows on Outer Pass	12
Number of Tube Rows on Inner Pass	15
Number of Passes	2
Average Tube Spacing - in.	0.213
Tube Row Spacing - in.	0.125
Total Number of U-Tubes	2925
Tube Length (Core Only) - in.	9.3
Overall Gas Flow Length - in.	4.0
Core ID - in.	11.0
Core OD - in.	19.06
Air-Side Manifold Sizes	
Manifold Diameter - inch	4.3
Maximum Inlet Flow Area - sq in.	5.0
Minimum Inlet Flow Area - sq in.	0.2
Maximum outlet flow area - sq in.	6.9
Minimum outlet flow area - sq in.	2.1
Number of Inlet Ports	2
Number of Outlet Ports	2
Inlet Port OD - in.	3.0
Outlet Port OD - in.	3.25
Maximum Package Dimensions	
ID - in.	9.6
OD - in.	21.6
Axial Length - in.	16.9
Core Tube Weight - lb	42.9
Estimated Heat Exchanger Weight - lb	89.7
Material of Construction	Inconel 625

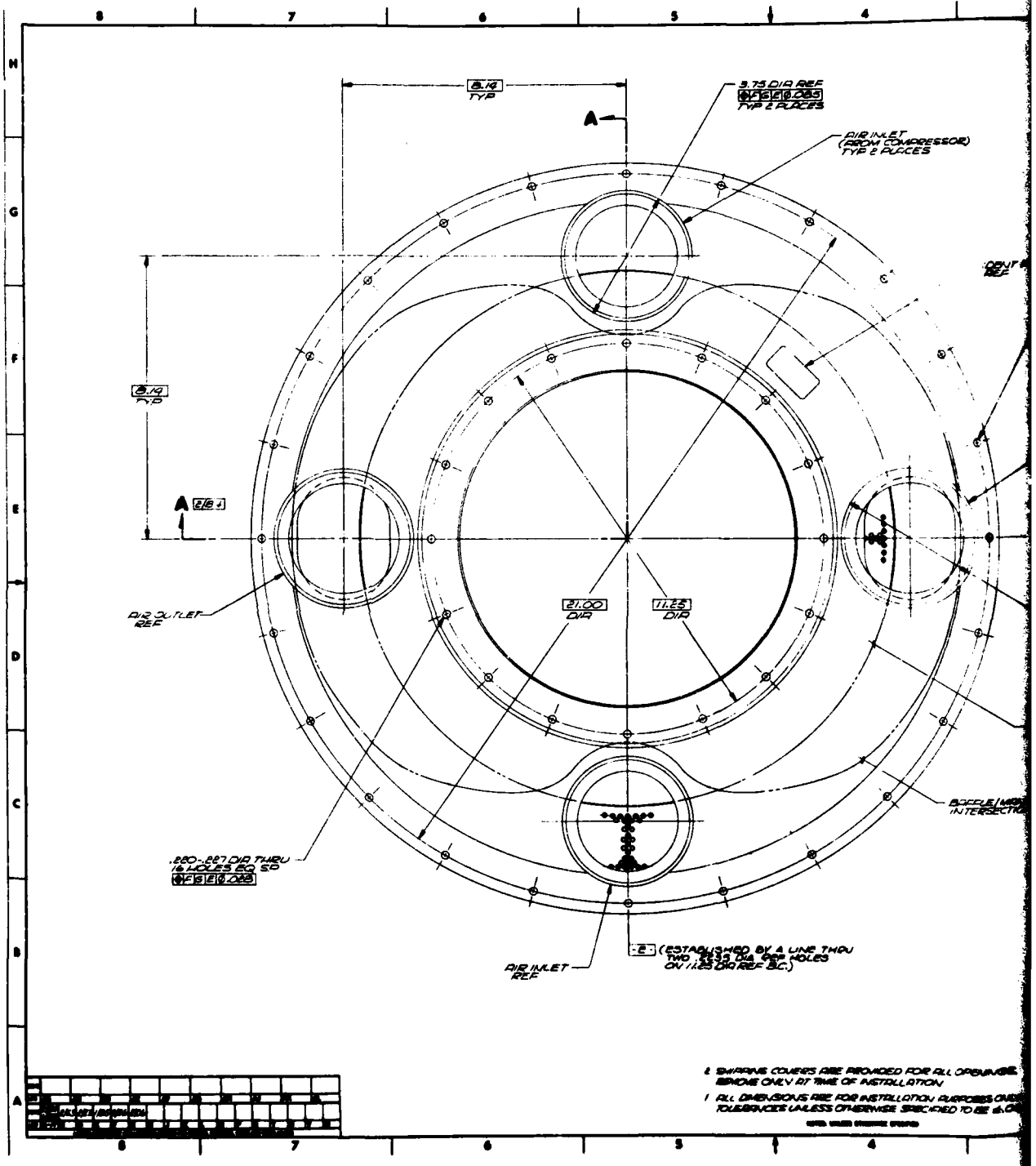

Figure 65. (Sheet 1) Recuperator Outline, Turbine Exhaust.

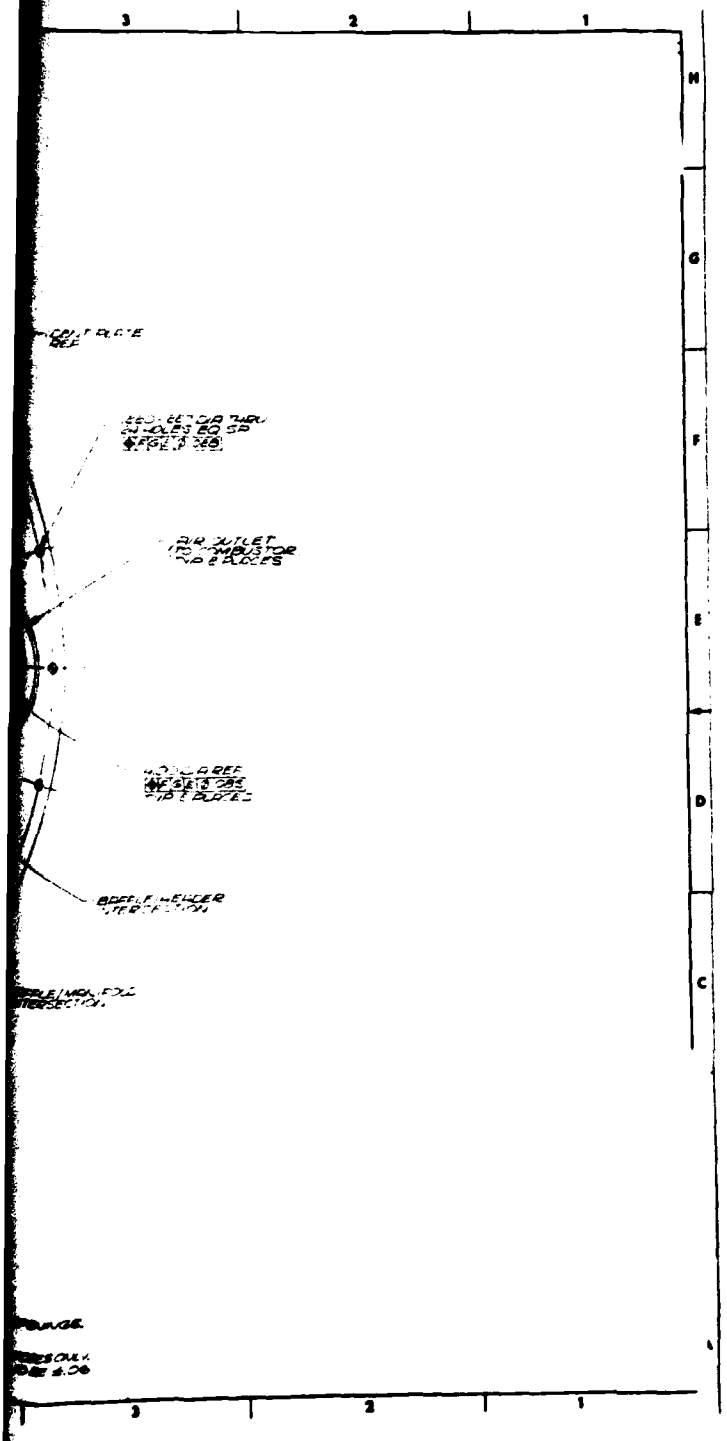
3
2
1
H
G
F
E
D
C
AIR OUTLET TO COMBUSTOR 4 PLACES
3
2
1

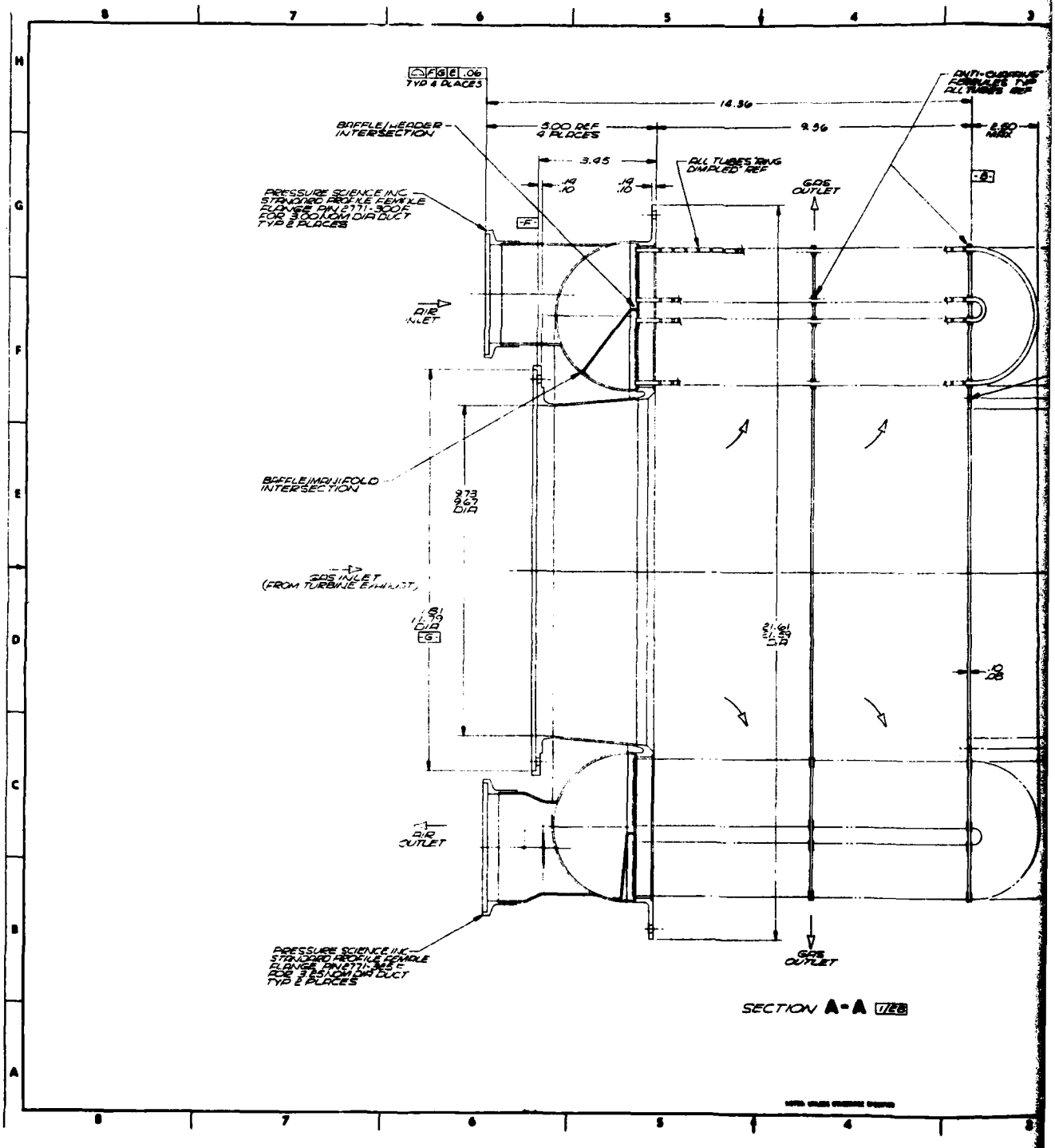

Figure 65. (Sheet 2) Recuperator Outline, Turbine Exhaust.

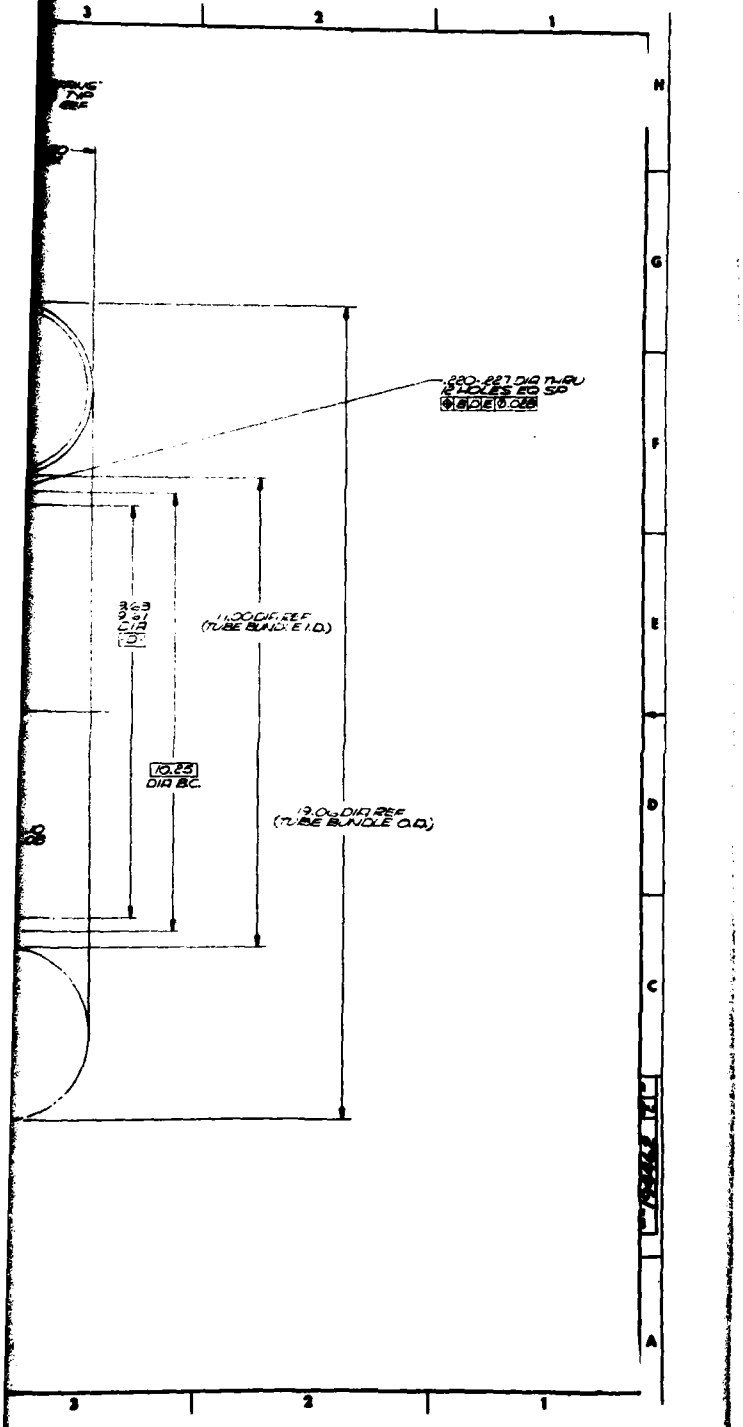
3
2
1
H
G
F
E
D
C
A
880-887 DIA THRU
12 HOLES EQ SP
⌖ B D E Ø.025
3.63
9.21
CIR
D
11.00 DIA REF
(TUBE BUNDLE I.D.)
10.23
DIA B.C.
13.0± DIA REF
(TUBE BUNDLE O.D.)

2

1

The recuperator manifolds are designed to achieve uniform airflow distribution to the tubes. This configuration using two inlet and outlet ports provides uniform flow distribution in the tubular core by employing circumferential area variation in the inlet and outlet manifold flow passages as shown in Figure 65 (Sheet 1).

Annular tube bundle core ID is 11.0 inches and the OD is 19.06 inches, and straight tube length for the core is 9.3 inches. Inlet port size is 3.0 inches OD and outlet port is 3.25 inches OD. The overall recuperator package has an ID of 9.6 inches, and an OD of 21.6 inches, and a length of 16.9 inches.

RECUPERATOR PRODUCIBILITY CONSIDERATIONS

The recuperator preliminary design configuration is expected to provide adequate structural capability to satisfy the anticipated environment of a helicopter application. The general structural design considerations for the unit are discussed below. The closely related subjects of fabrication and material selection also are briefly discussed.

Recuperator Structural Design

The structural design of the tubular core matrix must consider combined stresses due to internal pressure loadings and thermal stresses incurred by steady-state and transient metal temperature differentials among the elements in the core. To retain structural integrity during the design life of the unit, the level of steady-state, long-term operating stresses should be kept below the stress for 1 percent creep in 10,000 hours (or the specified design life), and, where possible, the peak short-term stresses should be kept below the yield strength of the material. In each case, the material strength at the appropriate metal temperature should be considered. Where local transient stresses exceed the material yield strength, a plastic analysis must be used to demonstrate that the number of cycles to failure is well above the expected number of load cycles. Also, where vibratory stresses are involved, the relevant steady and alternating stress levels must be evaluated to demonstrate fatigue resistance. The recuperator must be designed for sustained-pressure operation at maximum operating temperature throughout the entire design life. Established analytical techniques are used to ensure that acceptable pressure stress levels exist in the core, headers, and manifolds.

Thermal stresses in recuperator modules are of: (1) the steady-state, long-term type, which exist during most of the operational life; and (2) the transient type, which occur during engine startup, shutdown, and load changes. Transient metal temperature differentials are more elusive, and are the most critical in determining the gages and materials that must be used to give the required life. The U-tube configuration and anti-chaffing ferrules in the spacer plates accommodate transient and steady-state temperature differentials without developing large thermal stresses.

Recuperator Fabrication Processes

The basic processes for fabrication of the recuperator of this study have been fully developed and most are used daily in the production of aircraft heat exchangers. The required quality control procedures are also in daily use, and assure compliance with specifications. The major processes are described briefly below.

The first critical process is ring dimpling of the tubes. The inner diameter of each dimple must be controlled to close tolerances in order to assure the proper turbulence of the air and thus provide the correct heat transfer without exceeding the allowable pressure drop. AiResearch produces large quantities of ring-dimpled tubes. The dimples are roll-formed in a machine which automatically feeds the plain tubes from a hopper and deposits the completed tubes in another hopper. Thus the process operates on a nearly "hands-off" basis. Quality control is provided on a sample basis. The pressure drop of a representative number of tubes is measured upon initial setup, at selected intervals during the production run, and at the end of the run. The allowable pressure drop will vary for the different radii U-bends, but the basic procedure works well and consistently produces heat exchangers that meet requirements.

The next process is that of forming the U-bends in the tubes. The smaller radius bends must be formed by special techniques in order to avoid wrinkling and thus excessive pressure drop. Filling with oil and pressurizing during bending has proved to be superior to low melting temperature alloys from a time standpoint. This procedure is also capable of automation.

The headers and tube support plates have the holes drilled on a numerical control tape machine with multiple heads. One method of quality control that has been successfully utilized is the use of properly sized balls as go-no-go gauges. The thin gauge tube support plates may be stacked during drilling, which reduces the required machine time. The anti-chafing ferrules are presently installed by hand.

The other major detail parts of the recuperator are the manifolds, the internal flow divider, and the air ports. These are formed by standard sheet metal processes, and the degree of automation will depend on production rate.

The next step after all detail parts are on hand is stacking of the core. All parts are cleaned and maintained in an oil-free state. The headers and tube support plates are assembled in a stacking fixture and the tubes are then installed. The stack is built up from the smallest radius U-bend tubes and proceeds both radially inward and outward. Quality control during this process is primarily visual in order to assure that no header holes are left empty.

The next process is brazing the assembled core, thus forming a pressure-tight assembly. Nickel base braze alloy is employed which melts in the range of approximately 1800° - 2000°F. Depending on the alloy combination utilized, either a vacuum or a controlled atmosphere furnace may be used. The quality control procedure utilized is pressurization, usually under water, and repair procedures may include re-braze or plugging of tubes.

Once the core is leak tight, final assembly is completed by welding on all manifolds and attaching hardware. Final acceptance procedure generally consists of a proof pressure and leakage test and may include a pressure drop test on each core, or on a sampling basis.

These processes, as discussed above, are well developed and are utilized on a regular basis. They have proven to yield consistent, high quality heat exchangers. The only area where development would be required is in automation of some of the processes. This would only be required when production quantities become appreciably high.

RECUPERATOR MATERIALS CONSIDERATIONS

In selecting heat exchanger materials, a number of factors must often be evaluated beyond the normal considerations of mechanical properties, corrosion resistance, and cost. In particular, for very high temperature operation of metals, e.g., 1600° to 2000°F, oxidation and hot corrosion characteristics can be the most important issues to consider during development of a lightweight unit for airborne applications.

A second area of concern is fabricability, since many of the materials capable of providing the required strength have poor workability, resulting in limited availability of forms. Such metals inherently are difficult to form and join, particularly by welding. Furnace brazing, which is generally the preferred method for fabricating these heat exchangers, requires large joint overlaps for success. The brazing alloys are the weak links at higher temperatures, since they cannot be strengthened to the same degree as the parent metal. An alternative solution is some form of activated diffusion bonding wherein a lower melting point form of the parent metal (prepared typically by adding boron to it) is used as a filler metal and is then diffused away during a subsequent isothermal solidification operation.

For most of the Phase 1 parametric study, type 347 stainless steel was considered as the material of construction for the recuperators. Later analysis of the off-design performance conditions indicated operating temperatures in excess of 1340°F, which exceeds the capability of stainless steel. For this reason, Inconel 625 was selected as the material of construction due to its superior high-temperature properties. Inconel also has very good corrosion resistance and good fabricability.

Structural, Vibrational, and Dynamics Analyses

Structural and vibration analyses were made for certain components, which would significantly affect weight, performance, or price. These analyses were made either by direct calculation or by scaling of stress analyses made for similar parts. Examples of these analyses are: disk and blisk sizing to meet burst speed requirement, and high-pressure turbine blade stress to determine cooling flow requirements. Component prices reflect these analyses by material section and component weight.

A rotor dynamics analysis was made using a computer model. The purpose of the analysis was to assure an acceptable mechanical arrangement. The analysis provided the fundamental critical speeds for the high-pressure and power turbine rotors. The results are depicted in Figure 66. The high-pressure turbine rotor has two critical speeds well below the idle range and all bending mode critical speeds well above the operating range. The power turbine rotor has two critical speeds well above the operating range. The power turbine rotor has two critical speeds below its operating range, and all other critical speeds are well above the power turbine operating range. The second bending mode does occur in the range of possible secondary excitation by the high-pressure turbine rotor, but this is judged to be a minor risk. Since the solid shaft has substantial buckling margin, this mode could easily be "tuned" by modifying the shaft diameter in a detail design if required. In summary, no major dynamics problem is identified for the selected mechanical arrangement.

Installation Characteristics

The installation dimensions of the engine are shown in Figure 67. The engine is supported by two connections at the front frame and a single connection at the power turbine aft flange; alternate mounting schemes could be considered. The output drive is supplied with an internal spline for customer connection. Spline lubrication is supplied by the engine lubrication system. The output shaft is rated at a speed of 20,000 rpm. The separator is provided with a quick-disconnect flange. The accessory gearbox has pads for customer hydraulic pump and for a customer starter-generator. Provision is made for bleed air for customer use. The exhaust hood is supplied with a flange for exhaust duct connection. The exhaust is shown with side discharge in Figure 67. Alternate locations of the discharge can be considered.

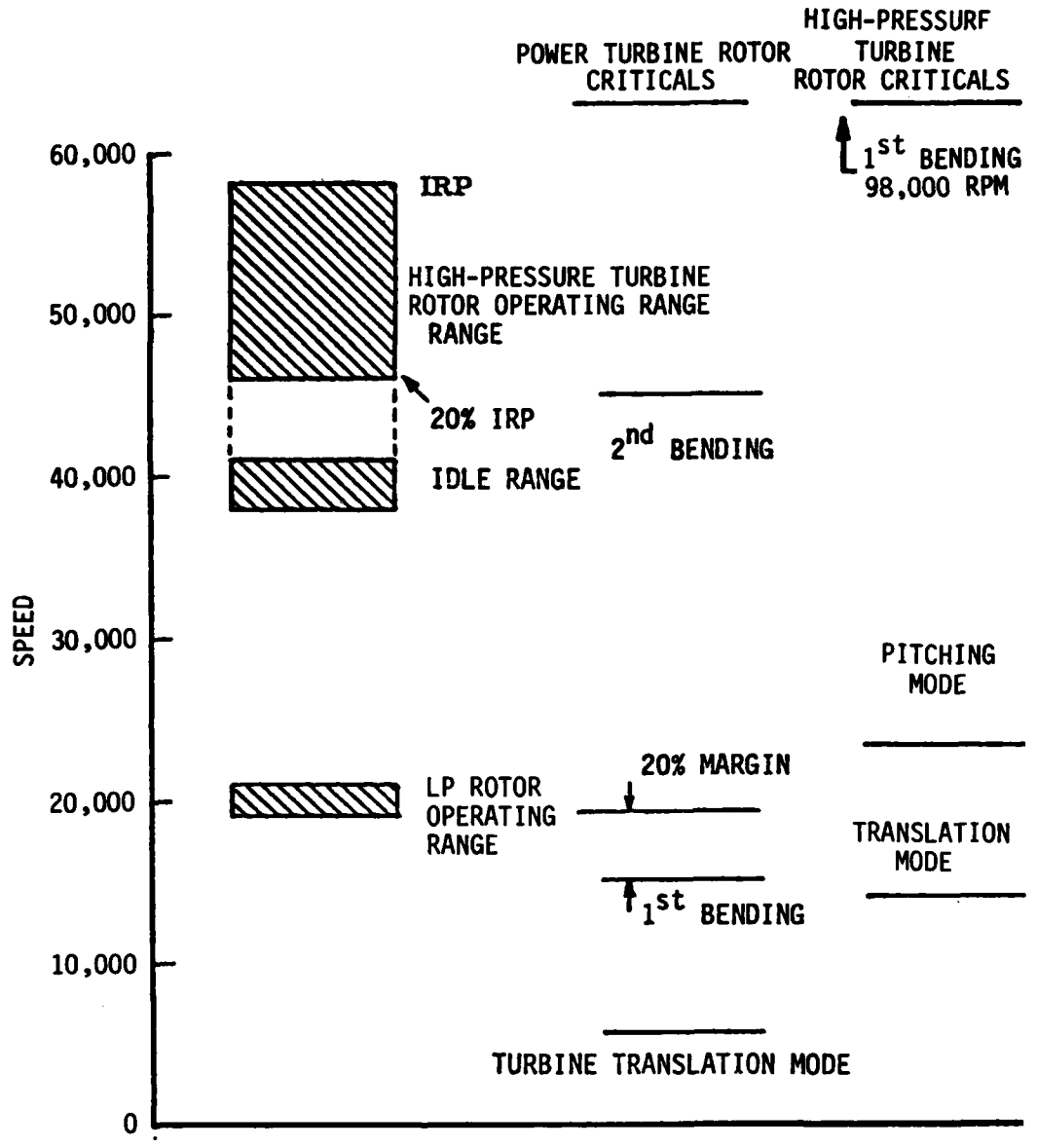

Figure 66. High-Pressure and Power Turbine Rotor Dynamics Summary.

WEIGHT AND PRICE ESTIMATES

Weight Estimate

Weight calculations were made for each of the engine components. The calculations for the power turbine, the exhaust system, and the combustor casing with scrolls were made using the component definitions and hardware arrangement for the regenerative engine shown in Figure 64. The weight for the regenerator heat exchanger including cold side manifolds and flanges was supplied by AiResearch. The weights for the other components were obtained by scaling similar components from other General Electric engines and by calculation of unique features for the regenerative engine shown in Figure 64. The results of the weight study are listed in Table 20. Also listed are the results of a weight study of a comparable conventional cycle engine. The regenerative cycle engine is 71% heavier than the conventional cycle engine.

TABLE 20. WEIGHT SUMMARY
539 SHP AT IRP

Component	Regenerative Engine (pounds)	Conventional Engine (pounds)
Inlet Particle Separator	38.6	35.6
Compressor	24.6	23.8
Combustor	35.5	17.0
High-Pressure Turbine	22.0	22.1
Power Turbine	57.3	47.3
Exhaust System	26.6	6.5
Controls and Accessories	45.7	42.8
Sumps and Drives	10.0	9.9
Regenerator	89.7	---
TOTAL	350.0	205.0

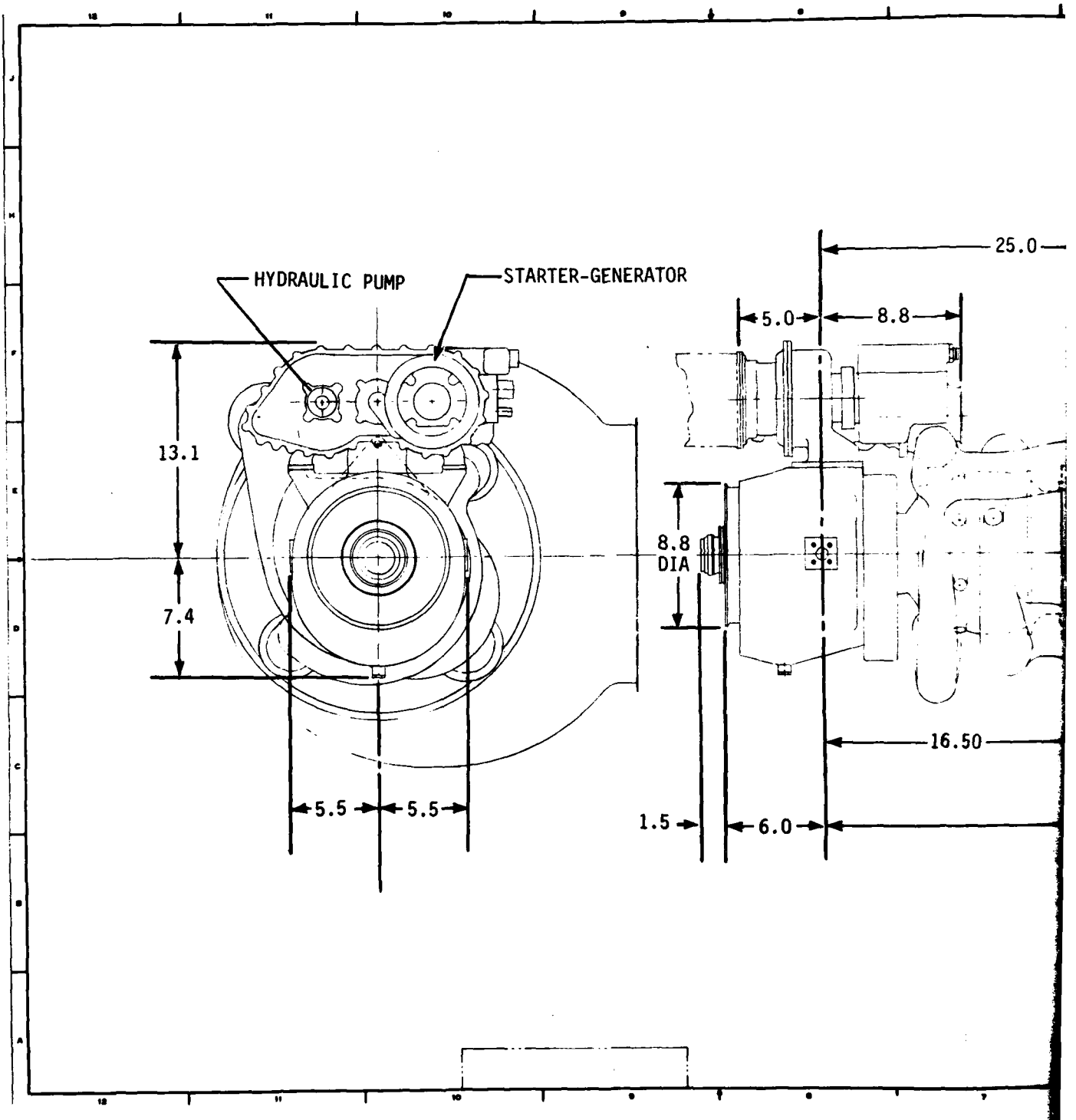

Figure 67. Installation Dimensions.

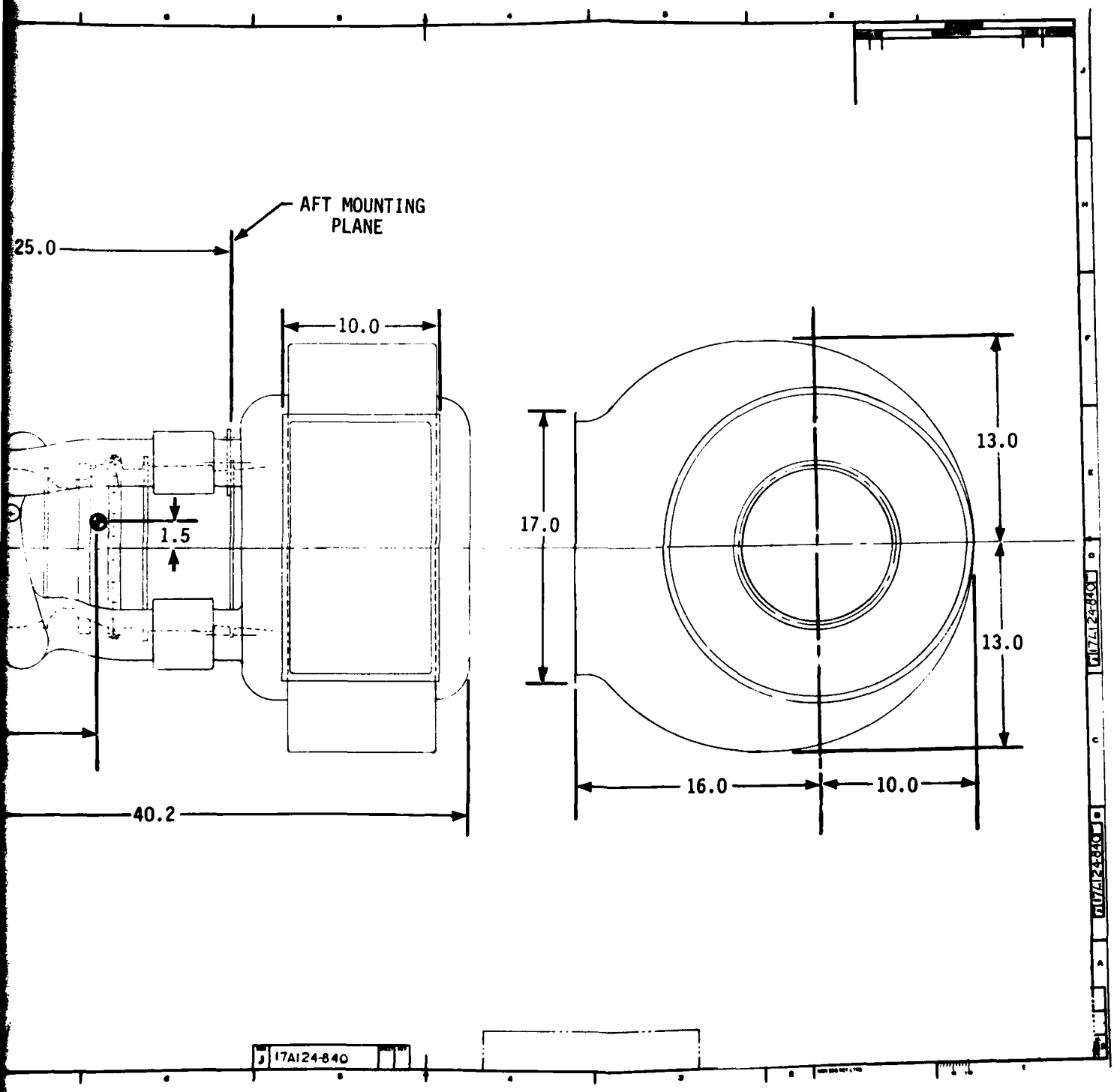
AFT MOUNTING PLANE
25.0
10.0
1.5
40.2
17.0
13.0
13.0
16.0
10.0
17A124-840
17A124-840
17A124-840

2

1

Price Estimate

Estimates of component prices were made on the basis of prices for similar components on other General Electric engines. The price of the regenerator heat exchanger including cold side manifold and flanges was supplied by AiResearch. Table 21 lists the percentage breakdown of the engine price by major component sections. Also listed is the component breakdown of a comparable conventional cycle engine. The overall price of the regenerative cycle engine is 30 to 50% greater than the overall costs of a comparable conventional engine.

TABLE 21. PRICE ESTIMATE SUMMARY
539 SHP AT IRP

Component	Regenerative Engine (% or Price)	Conventional Engine (% of Price
Inlet Particle Separator	5.3	7.1
Compressor	6.1	8.3
Combustor	10.2	11.2
High-Pressure Turbine	12.7	16.5
Power Turbine	16.0	17.4
Exhaust System	1.3	1.3
Control and Accessories	17.8	24.1
Sumps and Drives	7.0	9.7
Regenerator	20.4	0.0
Assembly Inspection and Testing	3.2	4.4
	100*	100*

* Estimated acquisition cost of the Conventional Engine is $150,000 (1979 dollars) based on a total production run of 2500 units at the rate of 300 units/year. The regenerative engine acquisition cost is estimated to be 30 to 50% higher.

SCALING EFFECTS

Since the component technology used in the study is currently available in the 500 shp size range, there are no size related effects that would require special emphasis during engine development. Performance is, however, size dependent. This is illustrated in Figure 68 where engine airflow, weight, performance and price trends for ±25% variations in IRP power rating are shown. While airflow, weight and price follow regular trends with power rating, SFC is adversely affected by size reduction and favorably affected by size increase.

Relative to the current study, a 25% size reduction (approximately 400 shp) would increase SFC by 1.2%, while a 25% size increase (approximately 675 shp) would reduce SFC by 0.9%.

MISSION EVALUATION

The Task II engine mission evaluation was performed by combining the performance, weight, and cost characteristics as shown in Table 22 and using the trade factors developed in Task I (Tables 10 and 11) to quantify the merit factors. In addition to the SLS operating line performance used in the Task I analysis, the 60% IRP and 40% IRP forward flight conditions were utilized in Task II in order to assess installation differences between the regenerative and nonregenerative engines.

TABLE 22. TASK II ENGINE CHARACTERISTICS

	Regenerative	Nonregenerative	
SHP	539	539	
$W_2\sqrt{\theta}/\delta$	3.5	3.3	
P/P	8.6	12.0	
T_{41} - °F	2250	2250	
Power Turbine VATN	Yes	No	
Recuperator Effectiveness - %	70	-	
Recuperator Total ($\Delta P/P$) - %	7.7	-	Change:
Weighted Average SFC - lb/hr/hp	.432	.574	-24.7%
Engine Weight - lb	350	205	+145 lb
Relative Engine Price - %	1.39	1.0	+39%
Relative Engine Maintenance Cost - %	1.30	1.0	+30%

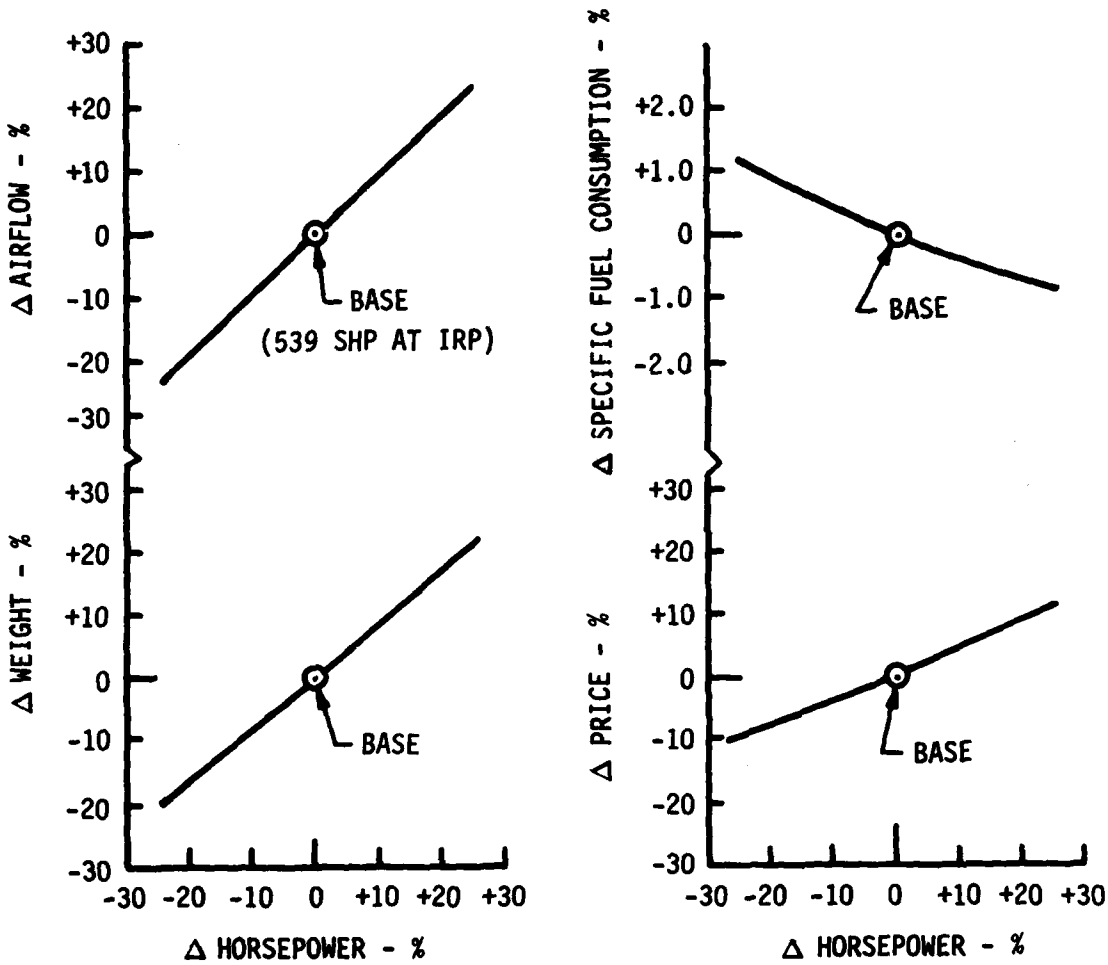

Figure 68. Engine Size Trends.

Three specific installation effects judged to be of significance were:

1. Nacelle enclosure weight.

2. Nacelle scrubbing drag.

3. Ram drag and gross thrust effects.

Since the regenerative engine is longer and of larger diameter for a given power size, a larger nacelle enclosure is required. The nacelle weight differential between the regenerative and nonregenerative engines was estimated at 25 pounds of airframe weight per engine. The approximately 8 ft^2/engine of additional exposed surface area will result in increased vehicle drag and thus require additional power to obtain a given flight velocity. The equivalent SFC differential due to the scrubbing drag difference was estimated at 1.5% at 150 knots and 0.4% at 80 knots for an overall mission weighted average SFC penalty of 0.5% for the regenerative engine.

Tables 16 and 17 indicate that the regenerative engine obtains cruise power at lower air flows than the nonregenerative engine and has less gross thrust (lower airflow and lower P_8/P_0). Moreover, since the regenerative engine exhaust is side mounted, no propulsive thrust is available from the engine. The combined ram drag and gross thrust differential was thus estimated as a 1.6% penalty in equivalent mission weighted SFC for the regenerative engine.

Table 23 summarizes the installation effects and the impact on merit factors. Table 24 shows the regenerative engine merit factors on both an uninstalled (Task I) basis and on an installed basis considering the installation factors noted above.

Figure 69 illustrates the sensitivity of the life-cycle cost differential to two factors with large degrees of uncertainty; fuel cost and recuperator maintenance cost. As indicated, fuel costs of $4.00/gallon are required to break even on life-cycle cost at the current utilization rate of 300 hours/year. Doubling the utilization (smaller fleet size) would reduce the break-even fuel cost to approximately $2.60/gallon.

Since there is little relevant flight experience, recuperator maintenance costs carry a high degree of uncertainty. As noted previously, the recuperator was treated as a hot frame for maintenance cost purposes in this study. As shown in Figure 69, this assumption would have to be in error by an order of magnitude to have significant impact on regenerative engine life-cycle costs.

TABLE 23. INSTALLATION EFFECTS - NONREGENERATIVE TO REGENERATIVE

	Change
Nacelle Weight (+25 lb/engine)	1.0% in Takeoff Gross Weight
	1% in Fuel Flow
	.7% in Life-Cycle Cost
Nacelle Scrubbing Drag (+0.5% ΔSFC)	.1% in Takeoff Gross Weight
	.6% in Fuel Flow
	.1% in Life-Cycle Cost
Ram Drag and Net Thrust Effect (+1.6% ΔSFC)	.3% in Takeoff Gross Weight
	1.9% in Fuel Flow
	.3% in Life-Cycle Cost
Total Installation Effects	+1.4% in Takeoff Gross Weight
	+3.5% in Fuel Flow
	+1.1% in Life-Cycle Cost

TABLE 24. REGENERATIVE ENGINE MISSION EVALUATION RESULTS - LIGHT TWIN ENGINE HELICOPTER

Change In	Uninstalled	Installed
Takeoff Gross Weight - %	+ .9	+ 2.3
Fuel Burned - %	-23.5	-20.0
Life-Cycle Cost - %*	+10.9	+12.0

*1979 Dollars, Fuel Cost $1/Gallon

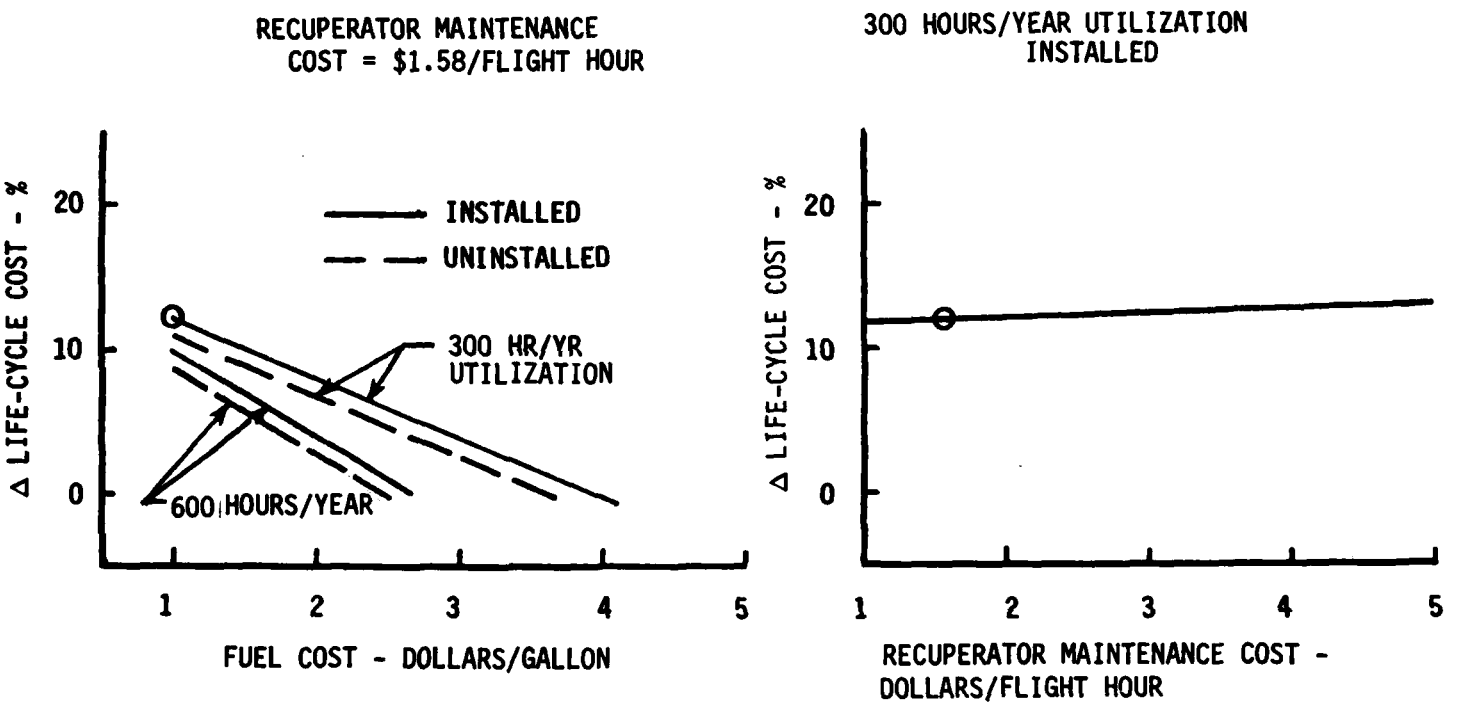

Figure 69. Sensitivity of Life-Cycle Cost to Fuel Cost, Utilization, and Maintenance Cost.

ASSESSMENT OF TECHNICAL RISK AND UNCERTAINTY

The level of basic engine technology used in this study is that which is currently available or under development and suitable for a near term engine demonstrator program. Therefore, development of the 500 shp regenerative turboshaft engine as defined in the Task II preliminary design would involve only the normal risk of a new engine in terms of meeting estimated performance levels, life requirements, or mechanical integrity.

The variable area turbine nozzle is essential to the regenerative engine in order to realize the full potential for part power SFC improvement. Some uncertainty exists in the possible long service performance deterioration or maintenance aspects of the VATN. This uncertainty is not considered to be limiting since General Electric has significant production service experience with compressor variable stator designs and demonstrator engine experience with variable area turbine nozzles.

The recuperator proposed by AiResearch is state of the art and poses little technical risk in terms of meeting performance and weight. The manufacturing processes to be used in recuperator fabrication are also well proven.

An area of uncertainty is in the regenerative engine performance deterioration with time due to recuperator fouling. Reference 3 summarizes results of experimental investigations to date on the fouling effects of turbine exhaust gases on heat exchanger tubes. Heat exchanger fouling is evidenced by increased gas side pressure drop and reduced heat transfer rates. Experimental evidence to date suggests that fouling rates are a function of combustor characteristics (smoke generation), fuel composition, and exhaust gas temperature.

Thus, some heat exchanger performance deterioration with time is expected and represents an area of uncertainty in terms of regenerative engine maintenance costs. There is also some uncertainty of the durability of the regenerator in an aircraft environment because of the thin (7 mils) tubes required to keep weight in line. While this study assumed a maintenance cost penalty associated with the heat exchanger by treating the heat exchanger as a hot frame, there is no firm basis for judging the validity of the magnitude of the assumed penalty.

3. Rogalski, R.D., FOULING EFFECTS OF TURBINE EXHAUST GASES ON HEAT EXCHANGER TUBES FOR HEAT RECOVERY SYSTEMS, SAE Technical Paper 790647, June 1979

CONCLUSIONS

1. For the selected mission, study results indicate that the following cycle parameters provide the best regenerative engine performance.

    a. Cycle P/P = 8 to 10

    b. Cycle Temperature = 2400°F

    c. Recuperator Effectiveness = 70%

    d. Recuperator Total $\Delta P/P$ = 7-1/2%

2. A power turbine VATN can be utilized to minimize regenerative engine low power fuel consumption.

3. The regenerative engine provides a 25% reduction in SFC and a 20% reduction in fuel burned relative to a nonregenerative engine at the same T_{41} when installed in a light twin engine military helicopter.

4. The regenerative engine life-cycle cost penalty is 12% of engine related costs (relative to a nonregenerative engine) at $1/gallon fuel costs (1979 dollars).

5. The regenerative engine life-cycle cost penalty is sensitive to fuel costs and vehicle utilization. The life-cycle cost would equal that of a nonregenerative engine at $4/gallon fuel costs for the current utilization rate of 300 hours/year; at 600 hours/year utilization the breakeven fuel cost would be $2.50/gallon.

6. Technology advancements over the next 10 years are projected to improve the SFC by 7% relative to the selected regenerative cycle of this study. The nonregenerative engine would also improve by 5% on a consistent basis so that the net regenerative cycle advantage would improve by 2%.

RECOMMENDATIONS

Results of this study have shown that the regenerative engine fuel savings benefits are obtained at the expense of a life-cycle cost penalty (current fuel costs). Projected technology advancements should improve the regenerative engine fuel savings potential and continued escalation of fuel costs will provide a more attractive economic picture.

Specific technology advancements that would enhance the regenerative engine benefits are:

1. Basic Engine Technology:

    a. Small compressor and turbine efficiency improvements.

    b. Hot parts materials development for higher cycle temperature.

2. Basic Engine Technology - Unique to Regenerative Cycle:

    a. Power turbine VATN performance improvement.

    b. Exhaust diffuser performance (duct from power turbine to recuperator).

    c. Infrared radiation suppressor integrated with recuperator.

3. Recuperator Technology:

    a. Materials development for higher temperature capability.

    b. Low cost design and manufacturing processes.

Programs in the above area are recommended followed by a regenerative engine demonstrator program that would take into account results from the above technology developments.

REFERENCES

1. McDonald, Colin F., STUDIES OF LIGHTWEIGHT INTEGRAL REGENERATIVE GAS TURBINES FOR HIGH PERFORMANCE. The Garret Corporation, AiResearch Manufacturing Co., USAAVLABS Technical Report 70-39, U.S. Army Aviation Material Laboratories, Fort Eustis, Virginia, August 1970, AD877464.

2. Piscopo, P.F., Lazarick, R.T., and Cyrus, J.D., FUEL CONSERVATION BENEFITS AND CRITICAL TECHNOLOGIES OF RECUPERATIVE AND ADVANCED CONVENTIONAL CYCLE TURBOSHAFT ENGINES, AIAA Technical Paper AlAA-80-0224, January 1980.

3. Rogalski, R.D., FOULING EFFECTS OF TURBINE EXHAUST GASES ON HEAT EXCHANGER TUBES FOR HEAT RECOVERY SYSTEMS, SAE Technical Paper 790647, June 1979.

LIST OF SYMBOLS AND ABBREVIATIONS

SYMBOLS

A	annulus area
C_L/L	tip clearance to blade height ratio
D	tube inside diameter
F_G	gross thrust
g	acceleration due to gravity
J	mechanical equivalent of heat
L	blade height
M	power turbine inlet Mach number
N	rotational speed
P/P	pressure ratio
P_0	ambient pressure
P_2	compressor inlet pressure
P_3	compressor discharge pressure
P_3/P_2	compressor pressure ratio
P_4	high pressure turbine inlet pressure
P_{45}	power turbine inlet pressure
P_8	exhaust nozzle pressure
P_8/P_0	exhaust nozzle pressure ratio
S	tube dimple spacing
T_2	compressor inlet temperature
T_3	compressor discharge temperature
T_{35}	heat exchanger cold side discharge temperature
T_{39}	combustor exit temperature
T_{41}	high-pressure turbine rotor inlet temperature

LIST OF SYMBOLS AND ABBREVIATIONS - (Continued)

SYMBOLS

T_{45}	power turbine inlet temperature
T_5	power turbine exit temperature
T_8	exhaust gas temperature
U_P	pitch line wheel speed
W_A	total engine airflow
W_2	compressor inlet airflow
$W_2\sqrt{\theta}/\delta$	compressor inlet corrected airflow
W_C	cooling airflow
W_F	fuel burned
$W\sqrt{T/P_4}$	high-pressure turbine flow function
$W\sqrt{T/P_{45}}$	power turbine flow function

GREEK SYMBOLS

ϵ	recuperator effectiveness
Δ	change in indicated parameter
ΔH	turbine energy extraction
$\Delta P/P$	pressure loss parameter
δ	P/14.696 or dimple depth
η	adiabatic efficiency
η/η	efficiency ratio
ψ	tube ring dimple parameter
ψ_P	turbine loading parameter

LIST OF SYMBOLS AND ABBREVIATIONS - (Continued)

ABBREVIATIONS

AR	aspect ratio
CDP	compressor discharge pressure
HEX	heat exchanger
HPT	high-pressure turbine
ID	inner diameter
IR	infrared radiation
IRP	intermediate rated power
IPS	inlet particle separator
LCC	life-cycle cost
LP	low pressure
LPT	low-pressure (power) turbine
MC (Max Cont)	maximum continuous power
OD	outer diameter
RNI	Reynolds number index
RPM	shaft rotational speed
SFC	specific fuel consumption
SL	sea level
SLS	sea level static
SM	stall margin
SHP	shaft horsepower
TOGW	takeoff gross weight
VATN	variable area turbine nozzle

6183-80

END

DATE
FILMED

8 1 - 1 1

DTIC